

1 **Transverse energy analysis of**
2 **relativistic heavy ion collisions**
3 **through the use of identified particles**
4 **spectra**

5 A Thesis Presented for the
6 Master of Science
7 Degree
8 The University of Tennessee, Knoxville

9 Biswas Sharma

10 May 2018

11

© by Biswas Sharma, 2018

12

All Rights Reserved.

13 Table of Contents

14	1 Introduction	1
15	2 Theoretical Background	3
16	2.1 Quantum Chromodynamics	3
17	2.2 Phase Transitions	4
18	2.3 Quark-Gluon Plasma	5
19	3 Relativistic Heavy Ion Collisions	7
20	3.1 RHIC and LHC	7
21	3.2 Collision Energy and Geometry	9
22	3.3 Kinematic Variables (will go into Appendix)	10
23	3.4 QGP Evolution	13
24	3.5 Detection of Collision Products	14
25	3.6 Detection of QGP Signatures	15
26	3.6.1 Bjorken Energy Density	15
27	3.6.2 Elliptic Flow	15
28	3.6.3 Direct and Thermal Photons	17
29	3.6.4 Strangeness Enhancement	18
30	3.6.5 Jet Quenching	19
31	3.7 The Beam Energy Scan Program	20
32	4 Measurement of Transverse Energy	21
33	4.1 Definition of Transverse Energy	21

34	4.2	E_T Measurement with Calorimeters	22
35	4.2.1	Calorimeter	22
36	4.2.2	E_T from PHENIX Calorimetry	23
37	4.3	E_T Measurement with Tracking Detectors	24
38	4.3.1	Tracking and Particle Identification	24
39	4.3.2	Calculation of $\frac{dE_T}{d\eta}$ from p_T spectra	25
40	4.3.3	Tracking Detectors in STAR	26
41	5	Data Analysis	28
42	5.0.1	STAR p_T spectra	28
43	5.1	Extrapolation of Spectra	29
44	5.1.1	Boltzmann-Gibbs Blast Wave	30
45	5.1.2	Fitting Spectra to BGBW	30
46	5.2	Calculations from the Spectral Fits	31
47	5.2.1	Calculation of $\frac{dE_T}{dy}$, $\frac{dE_T}{d\eta}$, $\frac{dN_{ch}}{dy}$, and $\frac{dN_{ch}}{d\eta}$	31
48	5.2.2	Corrections for Unidentified Particles and Estimation of Total E_T . .	31
49	5.2.3	Lambdas Centralitiy Adjustments and E_T Interpolations	32
50	5.3	Uncertainties	32
51	6	Results	33
52	7	Conclusion	39
53	8	Future Work	40
54	8.1	Goodness of Fit	40
55	8.2	Bjorken Energy Density Estimate	40
56	8.3	Asymmetric beams	41
57		Bibliography	42
58		Appendices	75

59 List of Tables

<small>60</small>	3.1 Colliding species and associated collision energies at RHIC [24].	10
<small>61</small>	5.1 Isospin states of different identified particles.	31

List of Figures

63	2.1	Schematic of the QCD phase diagram [9].	6
64	3.1	Initial layout of the RHIC.[26].	8
65	3.2	An illustration of a mid-central collision of two nuclei traveling in the z	
66		direction. The X-axis is parallel to the line joining the centers of the two	
67		nuclei at the time of collision [14].	11
68	3.3	An illustration of a collision consisting of participants (solid red) and	
69		spectators (open blue) within the colliding nuclei labeled A and B. t_c denotes	
70		the time of maximum overlap of the two nuclei. The apparent narrowing of	
71		the volumes of the nuclei in the z-direction is due to Lorentz contraction [37].	12
72	3.4	Evolution of the QGP represented in a lightcone diagram. τ_0 denotes the	
73		formation time of the QGP. T_c is the critical temperature of the transition	
74		from the QGP to the hadron gas phase. T_{ch} and T_{fo} stand for the temperatures	
75		at, respectively, chemical freeze-out and thermal freeze-out [14].	13
76	3.5	Minimum-bias Au+Au ($\sqrt{s_{NN}} = 200GeV$) elliptic flow spectra for identified	
77		particles: (a) v_2 vs p_T and (b) v_2 vs KE_T . [4]	16
78	3.6	Minimum-bias Au+Au ($\sqrt{s_{NN}} = 200GeV$) elliptic flow spectra for identified	
79		particles: (a) $\frac{v_2}{n_q}$ vs $\frac{p_T}{n_q}$ and (b) $\frac{v_2}{n_q}$ vs $\frac{KE_T}{n_q}$. [4]	17
80	3.7	Feynman diagram representing the production of photons from quarks and	
81		gluons. (a) and (b) represent annihilation processes, whereas (c) and (d)	
82		represent Compton processes.[39]	18

83	3.8	Illustration of jet quenching. Two jets are produced from each of the hard	
84		scatterings occuring at the locations of the solid dots. Jets originating closer	
85		to the initial surface are more probable to propagate outside the medium, as	
86		shown. Jets opposite to them interact with the medium, losing their energy	
87		and resulting in bow front shock waves.[36]	19
88	4.1	Energy loss distribution in the STAR TPC for primary and secondary	
89		particles. [19].	27
90	5.1	Transverse momentum spectra for π^+ , π^- , K^+ , K^- , p , and \bar{p} at midrapidity	
91		($ y < 0.1$) from 39 GeV Au+Au collisions at RHIC. The fitting curves	
92		on the 0-5% central collision spectra for pions, kaons, and protons/anti-	
93		protons represent, respectively, the Bose-Einstein, m_T -exponential, and	
94		double-exponential functions. [2].	29
95	5.2	Red curve shows the Boltzmann-Gibbs blast wave functional fit on the PRE-	
96		LIMINARY transverse momentum spectrum for lambda particles identified	
97		by the STAR detector for 19.6 GeV Au+Au collisions (10-15% central).	
98		Parameters extracted from the chi-square goodness-of-fit test, as well as other	
99		statistics, are shown in the box on the top right.	31
100	6.1	Parallel coordinates plot for 270 different spectra relating 6 different identified	
101		particles (color-coded) to their respective collision centrality classes, good-fit	
102		parameters, and the transverse energy calculated using said parameters. . . .	33
103	6.2	$(dE_T/d\eta)/0.5N_{part}$ at midrapidity as a function of $\sqrt{s_{NN}}$ for different central-	
104		ities. The curve represents a power-law fit to the 0-5% central data in the	
105		form $y = ax^{2b}$, where x and y are the placeholders for the quantities in the	
106		plot axes. $\chi^2/n.d.f$ for the fit was 1.806, and the good-fit parameters were	
107		$a = 0.4838 \pm 0.0429$ and $b = 0.2005 \pm 0.01466$. The shaded area represents	
108		the uncertainty bounds for the 0-5% central PHENIX data from [3].	34
109	6.3	$(dE_T/d\eta)/(dN_{ch}/d\eta)$ at midrapidity as a function of $\sqrt{s_{NN}}$ for different	
110		centralities.	35

111	6.4	$(dE_T/d\eta)/0.5N_{part}$ at midrapidity as a function of N_{part} for different centralities.	35
112	6.5	$(dE_T/d\eta)/(dN_{ch}/d\eta)$ at midrapidity as a function of N_{part} for different	
113		centralities.	36
114	6.6	$(dE_T/dy)/0.5N_{part}$ at midrapidity as a function of $\sqrt{s_{NN}}$ for different centralities.	36
115	6.7	$(dE_T/dy)/(dN_{ch}/dy)$ at midrapidity as a function of $\sqrt{s_{NN}}$ for different	
116		centralities.	37
117	6.8	$(dE_T/dy)/0.5N_{part}$ at midrapidity as a function of N_{part} for different centralities.	37
118	6.9	$(dE_T/dy)/(dN_{ch}/dy)$ at midrapidity as a function of N_{part} for different	
119		centralities.	38
120	6.10	$\frac{dE_T}{d\eta}/0.5N_{part}$ for 0-5% central collisions at midrapidity as a function of $\sqrt{s_{NN}}$.	
121		The PHENIX data are from [3]. The error bars represent the total statistical	
122		and systematic uncertainties.	38

Chapter 1

Introduction

The Big Bang model is based on observational evidence, such as the cosmic microwave background radiation and the cosmological expansion, and suggests that at the beginning the universe must have been at a state of really high density and temperature. As the universe expanded, it went through several stages of cooling characterized by the formation of matters with different compositions. The matter we mostly observe today exists at temperatures and densities much lower compared to those in the early universe.

The Large Hadron Collider (LHC) at CERN and the Relativistic Heavy Ion Collider (RHIC) at the Brookhaven National Laboratory have the ability to collide heavy nuclei, such as those of gold and uranium, at nearly the speed of light, reaching temperatures of trillions of degrees Celcius. These laboratories have provided evidence of the formation of an exotic state of matter, called the quark-gluon plasma (QGP). It only exists for a brief amount of time after such collisions and instantly freezes out into a plethora of new particles, which carry the signatures we can use to deduct QGP properties. Its properties suggest that it should be similar to the matter that existed within microseconds of the genesis of the universe. It behaves like an almost perfect fluid with a viscosity near 0 [?].

One of the methods to probe the properties of this matter is by analyzing the conversion of the beam-direction energy at the time of collision into transverse energy after the collision. These measurements can be used to estimate the energy density of the QGP. This analysis is generally done by using data from the calorimeters placed around the collision site. In this

thesis, I use the data collected by tracking detectors, instead of the conventional calorimeters, to calculate the transverse energy.

This thesis is structured as follows. chapter 2 touches on the theoretical background associated with the concept of the quark-gluon plasma. In chapter 3, I summarize the experimental concepts pertaining to relativistic heavy-ion collisions and the production and detection of QGP. chapter 4 consists of the formalism of the measurement of transverse energy using calorimeters as well as tracking detectors. It also describes what has been done using calorimeters. chapter 5 describes the data used to perform the analysis in this thesis and notes the relevant details of the analysis. In chapter 6, I present the results and compare them to the ones in literature obtained using a different method. Chapter ??ch:conclusion) concludes the thesis and discusses its implications. Finally, in chapter 8, I present arguments on what can be done in the future using the results of and the software developed for this analysis.

Chapter 2

Theoretical Background

2.1 Quantum Chromodynamics

The strong force is one of the four fundamental interactions in physics. At large scales, it is also known as the residual strong force, and it is responsible for binding the nucleons together to give the nucleus its structure. At smaller scales, it is called the fundamental nuclear force, and it binds the fundamental units of subnuclear matter, the quarks, together to form the nucleons. The force carriers of the interaction are the mesons at the former scale and the gluons at the latter. The electrodynamic interaction between charged particles such as protons and electrons is described by quantum electrodynamics (QED) as mediated by photons; the strong interaction, albeit more complicated, is explained under the framework of quantum chromodynamics (QCD) [22, 32]. The quarks and gluons of QCD are collectively known as partons. Gluons are the gauge bosons of the Yang-Mills theory.

The Yang-Mills theory is a non-Abelian gauge theory. It has a Lagrangian with several degrees of freedom, some of which are redundant and need to be gauged. This is done by a mathematical treatment as prescribed under a gauge theory. [7] The gauge theory associated with the Yang-Mills theory is based on the $SU(N)$ group. It is non-Abelian as represented by the non-commutative transformations. QCD is a gauge theory that describes the application of the $SU(3)$ symmetry transformations on the triplet (what does the tripleness imply?????????) of color charges, namely red, blue, and green. The electroweak interaction,

on the other hand, can be formalized under the gauge group $SU(2) \times U(1)$. Together, they form the $SU(3) \times SU(2) \times U(1)$ gauge theory called the standard model.

One of the ways QCD is different from QED is the confinement of partons. In QED, the fundamental particles are bound together by the Coulomb potential, which diminishes with distance between the charge-carrying particles, as demonstrated by the relation 2.1:

$$V_C \propto \frac{1}{r} \quad (2.1)$$

where V_C is the Coulomb potential, and r is the spatial separation between the particles. This means that bound QED particles can be isolated by increasing their spatial separation. The QCD potential, on the other hand, has an extra linear term in it:

$$V_{QCD} = -\frac{4}{3} \frac{\alpha_S}{r} + kr \quad (2.2)$$

where α_S is the QCD fine-structure constant and k is the strength of the color interaction (1 GeV/fm) [?]. This means that the potential increases linearly with distance at large distances, and so an infinite amount of energy is required to separate quarks. Hence, we never observe isolated quarks and they are said to be confined, not just bound, to form composite structures called hadrons [29]. A quark and an anti-quark forms a meson and that of three quarks forms a baryon. In addition to having a color charge, a quark also carries a flavor. There are six different quarks based on the flavors they carry: up, down, top, bottom, beauty, and strange.

2.2 Phase Transitions

In everyday life, we observe matter existing in four distinct phases: solid, liquid, gas, and plasma. Changes in physical conditions can lead to a transition from one of these phases to another, exemplified by the commonly observed conversion of ice to water. Distinctions among the various phases can be represented in a chart called the phase diagram.

The phase diagram consists of thermodynamic observables such as temperature and density on its axes. Curves in the phase diagram represent boundaries of physical conditions

at which two or more phases of matter can coexist in equilibrium. Crossing a boundary represents an abrupt transition from one phase to another; this abruptness is mathematically characterized by the discontinuity in the change of the derivative of the free energy – a thermodynamic variable – with respect to the physical quantities in the axes. There can also be regions in the diagram representing the ranges of physical conditions in which a smooth phase transition can take place. Christine believes this is only for a first order phase transition.....

One of the main focuses of current experimental and theoretical nuclear physics research is the study of the phase diagram of strongly interacting matter at a range of temperatures and baryon chemical potentials. In experiments involving the collisions of heavy ions at high and low energies, different regions of the phase diagram can be probed by varying the collision energy [3]. For instance, the high-baryon chemical potential regime corresponds to lower beam energies and higher temperatures correspond to higher beam energies. The results of these experiments and model calculations can be used to study the nature of transitions in the QCD phase diagram.

A schematic representing the QCD phase diagram as a function of the temperature (T) and quark chemical potential (μ) is shown in Figure 2.1 [9]. A second-order transition is predicted at low baryon chemical potentials (close to baryon-antibaryon symmetry) and high temperatures reminiscent of the early universe. Methods to study this region of the phase space will be explored in this thesis. At low temperatures and high chemical potentials, loose predictions have been made regarding the existence of exotic phases of high density matter, and programs, such as the Compressed Baryonic Matter experiment at the Facility for Antiproton and Ion Research in Germany, are being designed to study this region of the phase diagram [?].

2.3 Quark-Gluon Plasma

The confinement of quarks into the hadronic phase of QCD matter, as described in section 2.1, has its limitations. At very high densities, when the wave function of a single hadron overlaps with the spatial regions covered by multiple such hadrons, it is impossible to classify

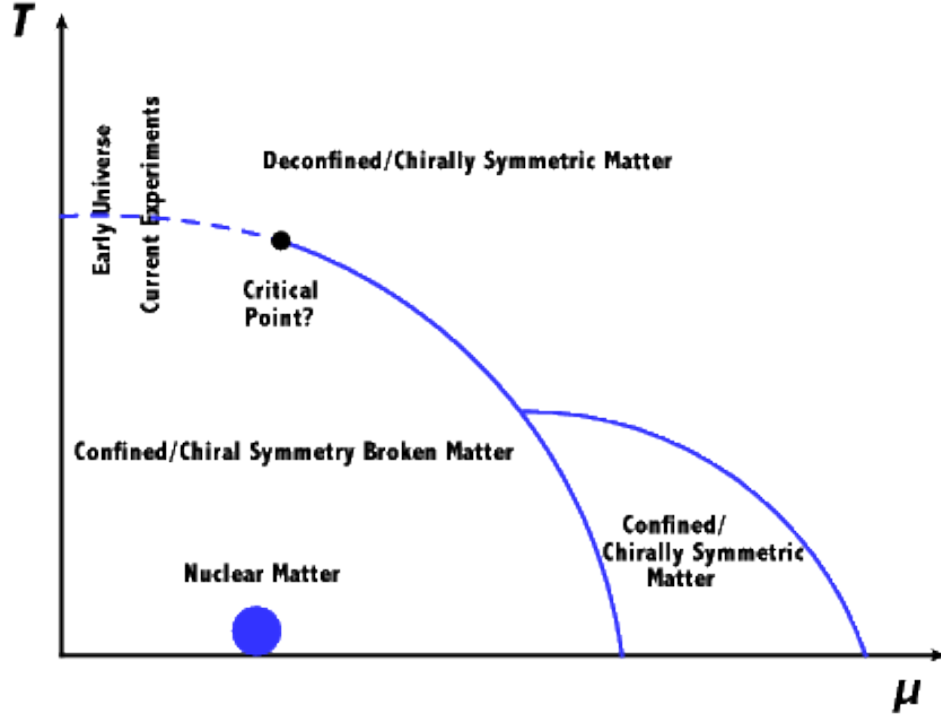


Figure 2.1: Schematic of the QCD phase diagram [9].

228 which pair or triplet of quarks belongs to which meson or baryon. As long as a particular
 229 quark is close enough to the other quarks in the volume, it is deconfined in such a way that it
 230 can freely move anywhere in the volume [29]. QCD predicts such phase transition, at energy
 231 densities above $0.2\text{-}1 \text{ GeV}/\text{fm}^3$ [1] and around a critical temperature of about 160 MeV [?
 232], of strongly interacting matter to a phase with quarks and gluons in thermal and chemical
 233 equilibrium representing the relevant degrees of freedom and behaving like an almost perfect
 234 fluid [12]. This deconfined state of quarks and gluons is termed the quark-gluon plasma
 235 (QGP) in analogy to the quantum electrodynamical plasma phase of matter.

Chapter 3

Relativistic Heavy Ion Collisions

The experimental evidence for the QGP come from the collisions of heavy nuclei. The signatures of such evidence are described in section 3.6. Physicists proposed the existence of such matter since as far back as 1984, when nuclei were accelerated and collided with stationary targets [18]. They were able to agree on a conclusive discovery of this matter during the 2000s, after colliding accelerated nuclei with other such nuclei or smaller species (protons, deuterons) at unprecedented energies and with improved detection schemes [34]. With further increases in collision energies and enhancements in detector technology, modern accelerator facilities provided additional evidence and estimates of some of the properties as well as the dynamics of the evolution of the QGP. The following sections describe two such facilities, the physics of the collisions and what happens after the collisions.

3.1 RHIC and LHC

The Relativistic Heavy Ion Collider (RHIC) is located in Upton, New York in the premises of the Brookhaven National Laboratory (BNL). Its construction started in 1991 and was completed in 1999. Figure 3.1 shows the layout, at the time of construction, of the collider along with the Alternating Gradient Synchrotron (AGS) complex and the locations of the original four detectors: Solenoidal Tracker At RHIC (STAR), Pioneering High Energy Nuclear Interaction eXperiment (PHENIX), Phobos and BRAHMS (Broad RAnge Hadron Magnetic Spectrometers). Phobos, BRAHMS, and PHENIX were decommissioned after the

completion of their science objectives, but STAR is still functional. The AGS was part of BNL before the construction of the RHIC, and its capabilities were augmented with the construction of the AGS Booster in 1991.

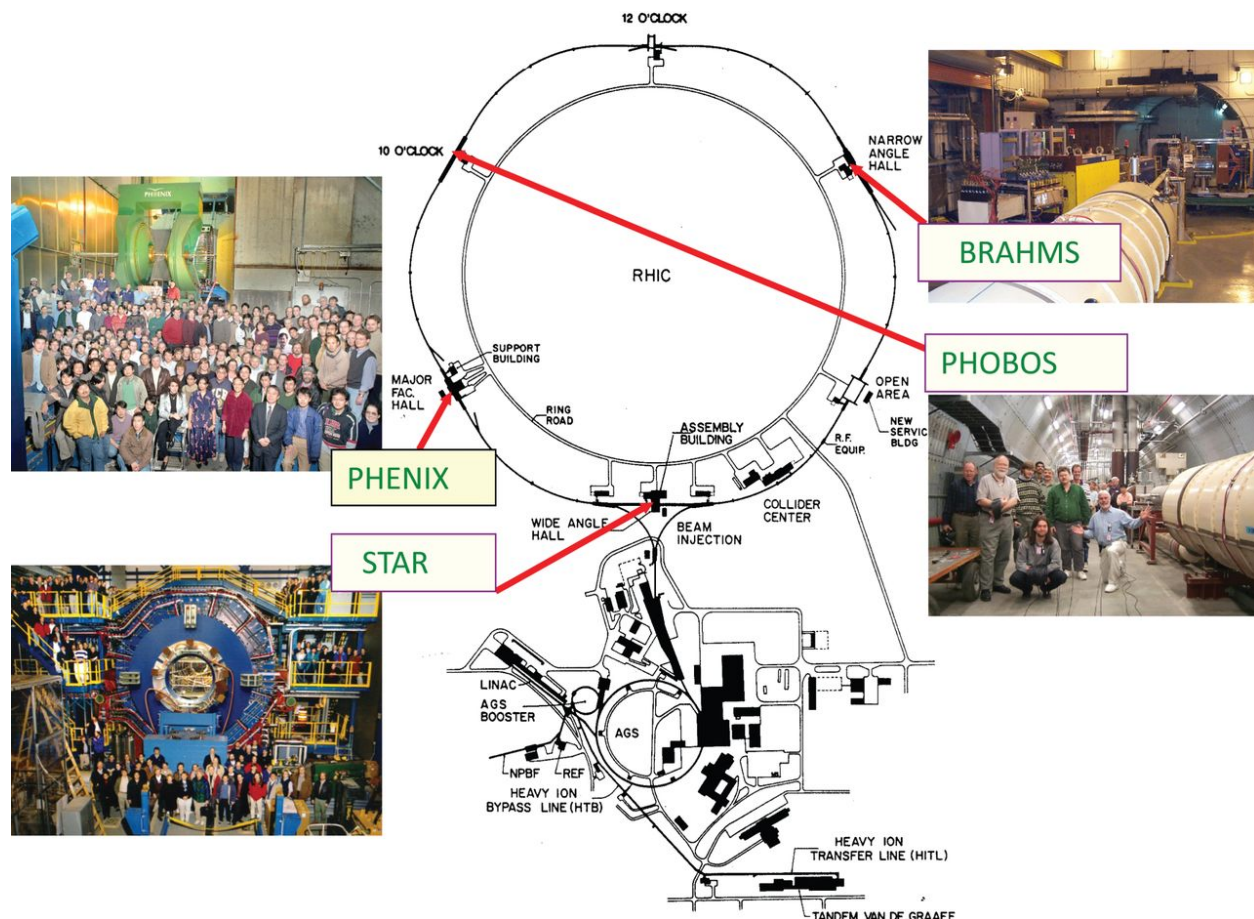


Figure 3.1: Initial layout of the RHIC.[26].

Heavy ion beams in RHIC are created in a series of steps before collision. In case of gold ions, a pulsed sputter source produces negatively charged ions, which are stripped of some of their electrons with a foil on the positive end of the high-voltage Tandem Van de Graaff. The ions are now positively charged and are accelerated to 1MeV/u toward the negative terminal of the Tandem. Upon exiting it, some more stripping takes place. The bending magnets then selectively deliver +32 charge states of the ions to the Booster Synchrotron, which accelerates them to 95MeV/u and strips them to a +77 charge state before injecting them to the AGS. The AGS accelerates them to 10.8 GeV/u and strips them of the remaining two electrons at the exit. The gold ions are then injected through the AGS-to-RHIC Beam Transfer Line to

the two RHIC rings. These rings carry beams moving in opposite directions and intersect at six symmetric locations in the 3.8 km circumference. The original four detectors are located in four of these six locations where the beams undergo head-on collisions.

The Large Hadron Collider (LHC) is located underground (between 45m and 170m) beneath the France-Switzerland border near the city of Geneva. The two rings of the collider were constructed between 1998 and 2008 by the European Organization for Nuclear Research (CERN) in the 26.7 km circular tunnel originally housing CERN's Large Electron-Positron collider. Analogous to the RHIC, the LHC gets its beams prepared by a series of machines in the CERN accelerator complex. The collisions occur at the locations of the four big LHC experiments: Compact Muon Solenoid (CMS), A Toroidal LHC ApparatuS (ATLAS), Large Hadron Collider beauty (LHCb) experiment, and A Large Ion Collider Experiment (ALICE). ALICE is dedicated to the study of heavy-ion collisions [16].

3.2 Collision Energy and Geometry

What happens in the aftermath of a collision depends on how much energy is available at the time of the collision as well as the geometry of the collision. The collision energy is determined by the collider configuration. The geometry of the collision is deduced from the constraints imposed by the static (eg. rest mass) and dynamic (eg. trajectory) properties of the detected products.

In collision experiments, it is convenient to use a reference frame in which the net momentum of the pair of colliding species is zero. This frame is called the center-of-mass frame. In this frame, the total energy of the species in the two beams is a function of the number of nucleons and the center-of-mass energy per nucleon. The collision energy is reported as the center-of-mass energy per nucleon pair, $\sqrt{s_{NN}}$.

RHIC has the unique capability of colliding species at a range of energies spanning almost two orders of magnitude. Table 3.1 lists the collision energies produced so far at RHIC for various collision systems. The LHC boasts the highest amount of collision energy for any collider on earth. It collided species (p+p, p+A, Pb+Pb) at a center of mass energy upto

295 2.76 TeV per nucleon pair at the end of 2010. At the end of 2015, 5.02 TeV Pb+Pb (13 TeV
 296 p+p) collisions were successfully completed [17].

Collision system	$\sqrt{s_{NN}}(GeV)$
p+p	200, 500
d+Au	200
Cu+Cu	62, 200
Au+Au	9, 20, 62, 130, 200

Table 3.1: Colliding species and associated collision energies at RHIC [24].

297 In general, any collision between two nuclei is not perfectly head-on. Some collisions are
 298 close to being head-on and are called central collisions. Some are glancing and are called
 299 peripheral collisions. By convention, 0% is the centrality of a perfectly head-on collision
 300 and 100% is that of the least head-on, i.e., the most peripheral collision. In practice, each
 301 collision event is deducted to belong to a specific centrality bin. For instance, 0-5% would
 302 be the centrality for an identified N_{ch} value which would be the minimum charged particle
 303 multiplicity produced by 5% of the total number of collisions. This identification of the
 304 N_{ch} value is often acheived by using the Glauber model [?]. Figure 3.2 illustrates the
 305 aftermath of a mid-central collision, i.e, a collision in which about half of the volume of each
 306 of the nuclei intersects the other..... add brief discussion of Glauber model and STAR
 307 centrality determination.....

308 The collision of two nuclei can be modeled as collisions of the constituents that make
 309 up the nuclei. The nucleons that take part in the collisions and are called participants.
 310 The rest of the nucleons are known as spectators. Figure 3.3 illustrates the distribution of
 311 participants and spectators in two colliding nuclei. Expectedly, the number of participants
 312 is more in more central collisions.

313 3.3 Kinematic Variables (will go into Appendix)

314 The description of the collision physics and the interpretation of its results are aided by the
 315 construction of variables that undergo simple transformations under a change of reference
 316 frame. Two such variables, rapidity and pseudorapidity, are described in this section.

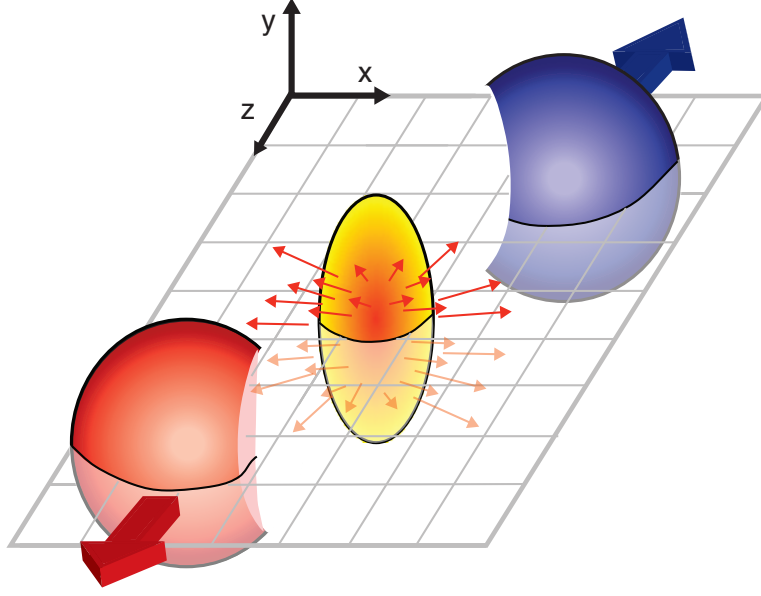


Figure 3.2: An illustration of a mid-central collision of two nuclei traveling in the z direction. The X -axis is parallel to the line joining the centers of the two nuclei at the time of collision [14].

317 The rapidity, y , of a particle is defined as:

$$y \equiv \frac{1}{2} \ln \frac{p_0 + p_z}{p_0 - p_z} \quad (3.1)$$

$$= \frac{1}{2} \ln \frac{E + p_z}{E - p_z}, \quad (3.2)$$

318 where p_0 and p_z are the components of its contravariant four-momentum $p = (p_0, p_x, p_y, p_z)$
 319 with $p_0 = \frac{E}{c}$, E being the relativistic energy of the particle and c , the speed of light, being
 320 equal to 1 in natural units.

321 The rapidity of a particle is used as a relativistic description of its velocity. Unlike the
 322 canonical velocity of a particle, its rapidity transforms simply additively under a Lorentz
 323 boost of the frame of reference. For example, suppose a particle has a rapidity y in
 324 the laboratory frame. Let y' denote its rapidity as measured in a frame that is Lorentz
 325 boosted with a velocity β in the z -direction with respect to the laboratory frame. Then the

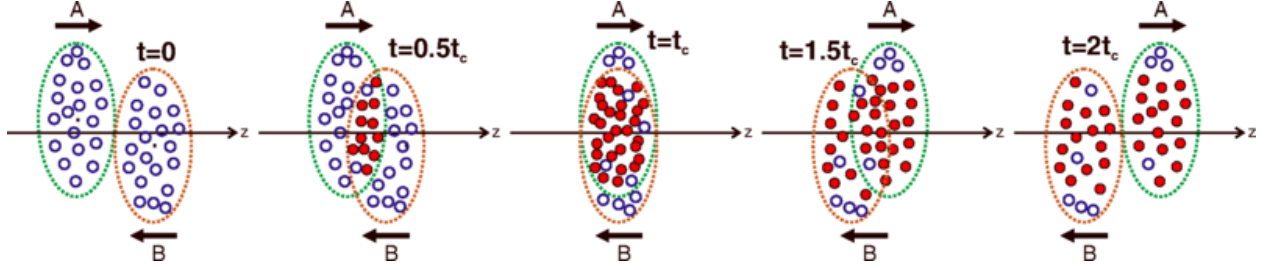


Figure 3.3: An illustration of a collision consisting of participants (solid red) and spectators (open blue) within the colliding nuclei labeled A and B. t_c denotes the time of maximum overlap of the two nuclei. The apparent narrowing of the volumes of the nuclei in the z -direction is due to Lorentz contraction [37].

relationship between the rapidities in the two different frames is simply

$$y' = y - y_\beta \quad (3.3)$$

Here,

$$y_\beta = \frac{1}{2} \ln \frac{1 + \beta}{1 - \beta} \quad (3.4)$$

is the rapidity the particle would have in the laboratory frame if it were moving with a velocity β in the z -direction with respect to the laboratory frame, as can be verified from equation 3.1 with $p_0 = \gamma m$ and $p_z = \gamma \beta m$, γ being the Lorentz factor $\frac{1}{\sqrt{1-\beta^2}}$. [39]

The convenience provided by this construct comes with a cost. As evident from equation 3.1, the calculation of the rapidity of a particle requires the measurement of two different observables associated with it, such as the energy and the z -direction momentum. However, experimental constraints may sometimes only facilitate the measurement of the direction of the detected particle with respect to the beam axis. What's more convenient in such a case is the use of another variable construct called pseudorapidity, η , defined as:

$$\eta \equiv -\ln \tan \frac{\theta}{2}, \quad (3.5)$$

where θ is the angle the particle's momentum vector, \mathbf{p} , makes with the z -direction. The above equation can also be written in terms of the momentum as:

$$\eta = \frac{1}{2} \ln \frac{|\mathbf{p}| + p_z}{|\mathbf{p}| - p_z} \quad (3.6)$$

From equations 3.1 and 3.6, it is evident that $\eta \approx y$ when $|\mathbf{p}| \approx p_0$, i.e., when the momentum is large. The transformation of the particle distribution from the y -space to the η -space is discussed in section 4.3.2.

3.4 QGP Evolution

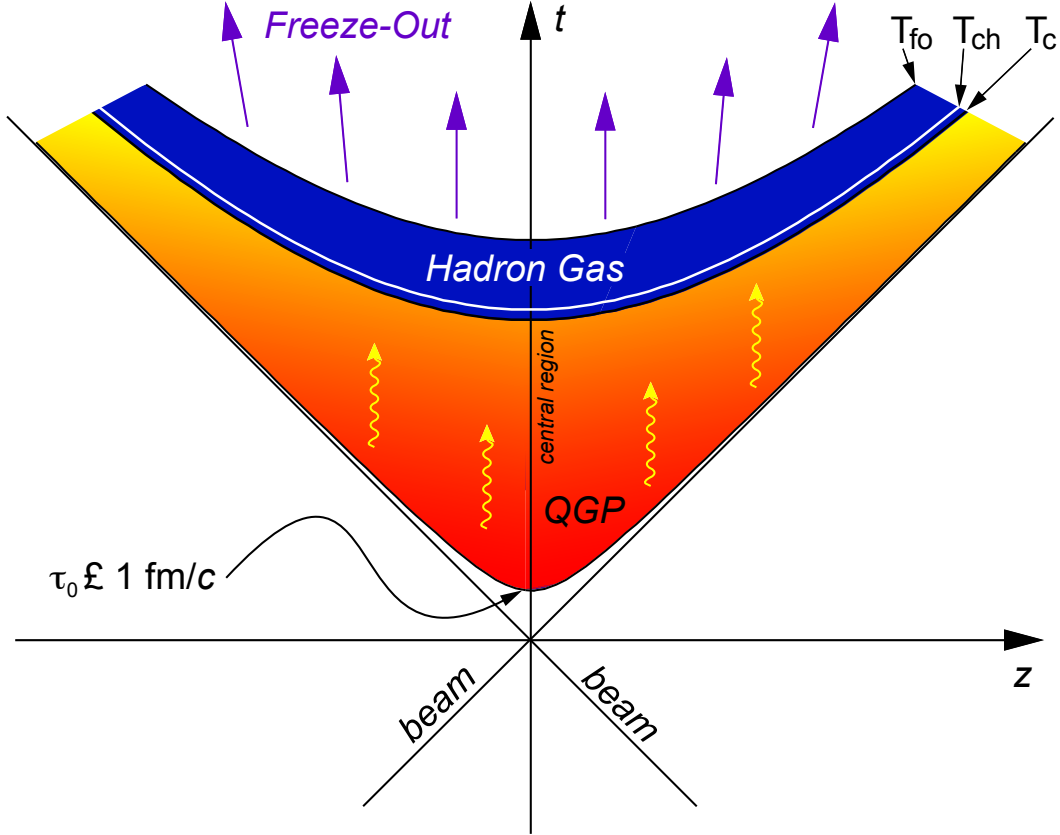


Figure 3.4: Evolution of the QGP represented in a lightcone diagram. τ_0 denotes the formation time of the QGP. T_c is the critical temperature of the transition from the QGP to the hadron gas phase. T_{ch} and T_{fo} stand for the temperatures at, respectively, chemical freeze-out and thermal freeze-out [14].

343 The evolution of the QGP is shown in a lightcone diagram in figure 3.4 [14]. The initial
 344 state of the colliding nuclei is not well known and is the topic of research for upcoming
 345 experiments. During the collision, the participants scatter off of each other while the
 346 spectators keep traveling almost unperturbed in their original direction. The immediate
 347 aftermath of a central collision of heavy ions at RHIC and LHC energies is the formation
 348 of a hot fireball. This fireball evolves in time to form a liquid-like medium of quarks and
 349 gluons. This medium attains a local equilibrium and remains in such a state, depending
 350 on the collision energy, for about 1-10 fm/c. This equilibrium is broken as the liquid
 351 QGP evolves by expanding and cooling to attain a density and temperature at which the
 352 deconfinement of quarks and gluons is lost and they undergo a chemical freeze-out to form a
 353 hadron gas. Collisions between the constituents of this gas become scant as it evolves with
 354 further expansion and cooling, and the hadrons undergo a thermal freeze-out to attain their
 355 final energies and momenta [14].

356 **3.5 Detection of Collision Products**

357 Detectors are placed around the collision site to perform measurements on the final state
 358 particles emitting from the thermal freeze-out of the medium. These measurements typically
 359 include the estimation of the location and time of production of the final states, the type of
 360 particle, and the momentum and energy it carries.

361 Generally, a tracking detector surrounds the collision site, and there are particle identifiers
 362 followed by calorimeters around it. A magnetic field is applied parallel to the beam direction
 363 around the collision site. Due to this orientation of the magnetic field, the spectators traveling
 364 parallel to it move undeflected and the final state charged particles with components of
 365 velocity transverse to the beam axis get deflected around the beam axis with radius given
 366 by

$$r = \frac{p_T}{qB}, \quad (3.7)$$

367 where p_T is the transverse momentum of the particle, q is its electric charge, and B is the
 368 applied magnetic field. Two kinds of detectors most relevant to this thesis, tracking detectors
 369 and calorimeters, are described in chapter 4.

3.6 Detection of QGP Signatures

The existence and properties of the QGP in the aftermath of high-energy heavy-ion collisions can be probed using different techniques relevant to several theoretical characteristics of the medium. No signature can alone be used to claim the production of the QGP, and some of the probes, which should be interpreted together, are described below.

3.6.1 Bjorken Energy Density

In 1983, J.D. Bjorken[11] prescribed a formula to use the final state particles to estimate the initial energy density, ϵ_0 , in a nucleus-nucleus collision. With slight changes in the original formula, the energy density is given by:

$$\epsilon_0 = \frac{1}{\tau_0 A_T} \langle \frac{dE_T}{dy} \rangle, \quad (3.8)$$

where τ_0 is the formation time of QGP equilibration, A_T is the transverse area of the intersection of the two nuclei, and $\langle \frac{dE_T}{dy} \rangle$ is the mean transverse energy per unit rapidity. τ_0 is model-dependent and is normally estimated to be $1 fm/c$. A_T depends on the centrality of the collision and can be estimated using the Glauber models discussed earlier. $\langle \frac{dE_T}{dy} \rangle$ is found from the measurement of the transverse energy carried by the final state particles from the collision and is the central theme of this thesis. Details about it are in the following chapters. The estimate of the initial energy density from Bjorken formula can be compared with the QCD prediction of the critical energy density[1] to check if the results from a collision imply the achievement of the critical physical condition required for the phase transition [21].

3.6.2 Elliptic Flow

The evolution of the medium produced after relativistic heavy ion collisions can be well described under the framework of relativistic hydrodynamics [30, 35]. This description indicates the presence of a collective flow, and hence a liquid-like and thermalized nature, of the constituents that make up the system. The momentum distribution of the final state particles emitted out of the collectively flowing system can be decomposed into its azimuthal

394 Fourier components. The second harmonic coefficient, $\nu_2(y, p_T)$, of this decomposition
 395 characterizes what is known as the elliptic flow [20]. The magnitude of the elliptic flow
 396 from a non-central collision represents the anisotropy in azimuthal momentum space of the
 397 thermalized post-collision system [33]. The elliptic flow of the medium, as a function of
 398 the momentum or the kinetic energy in the transverse direction, points towards quarks,
 399 rather than hadrons, being the relevant degrees of freedom in the QGP. Figure 3.5 shows v_2
 400 as a function of the transverse momentum and the transverse kinetic energy for identified
 401 particles. The spectra scale consistently at lower values of both p_T and KE_T . However,
 402 they branch out at higher values: $p_T \gtrsim 2\text{GeV}/c$ and $KE_T \gtrsim 1\text{GeV}$. Figure 3.6, on the other
 403 hand, is similar to figure 3.5, with the exception that both the axes have quantities that are
 404 normalized by the number of quarks, n_q . In this case, the KE_T spectra strongly exhibits a
 405 scaling which is more comprehensively consistent with the number of quarks than in case of
 406 figure 3.5. This universal quark-number scaling can be interpreted as the degrees of freedom
 of the system being quark-like.[4]

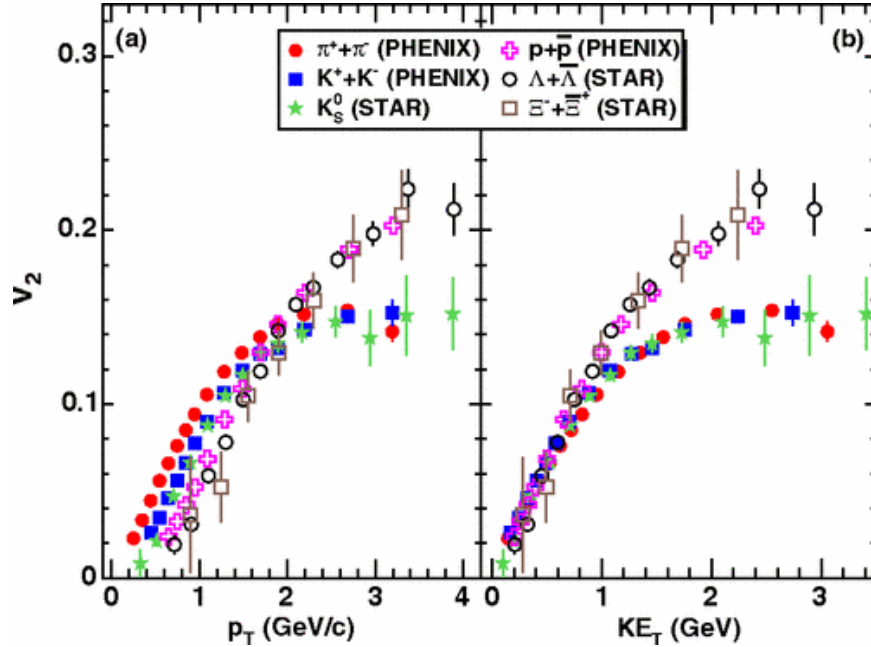


Figure 3.5: Minimum-bias Au+Au ($\sqrt{s_{NN}} = 200\text{GeV}$) elliptic flow spectra for identified particles: (a) v_2 vs p_T and (b) v_2 vs KE_T . [4]

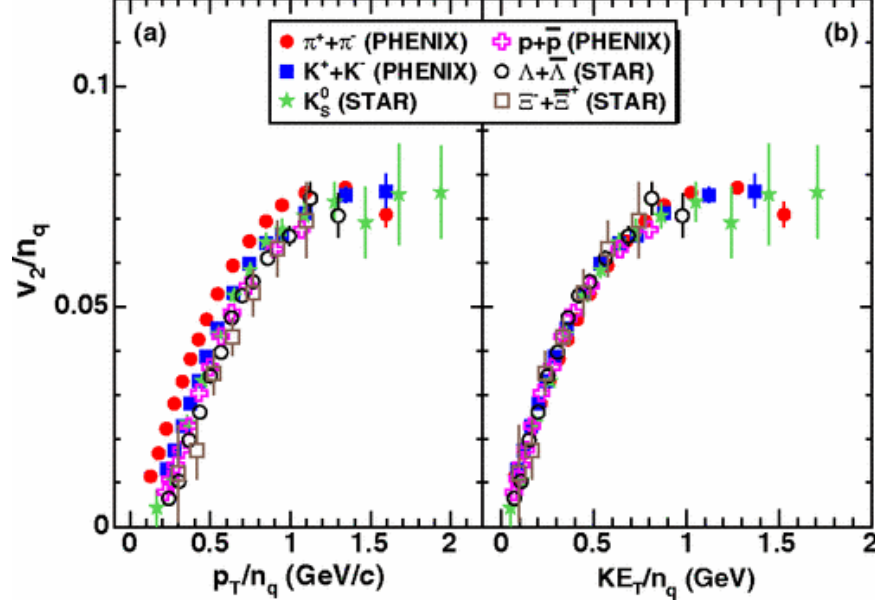


Figure 3.6: Minimum-bias Au+Au ($\sqrt{s_{NN}} = 200\text{GeV}$) elliptic flow spectra for identified particles: (a) $\frac{v_2}{n_q}$ vs $\frac{p_T}{n_q}$ and (b) $\frac{v_2}{n_q}$ vs $\frac{KE_T}{n_q}$. [4]

3.6.3 Direct and Thermal Photons

In the QGP, a quark and an antiquark can annihilate to produce a photon and a gluon. It is also possible for the pair to annihilate and produce two photons, but the probability of this process is smaller than the former by about two orders of magnitude. Furthermore, a quark (or an antiquark) can interact with a gluon to produce an antiquark (or a quark) and a photon, a process analogous to Compton scattering in QED. Just like the leptons described in the previous section, the photons produced in the QGP can only interact with the medium electromagnetically. Therefore, they undergo minimal scattering before being detected, and hence can be used to probe the thermodynamical state of the medium at the time of their creation.[39] Photons can also be produced after hadronization as a result of the scattering of the hadrons within the evolved medium. However, the nature of the p_T distribution is different in this case, and this difference helps distinguish these photons from the direct photons produced by partonic interactions.[38]

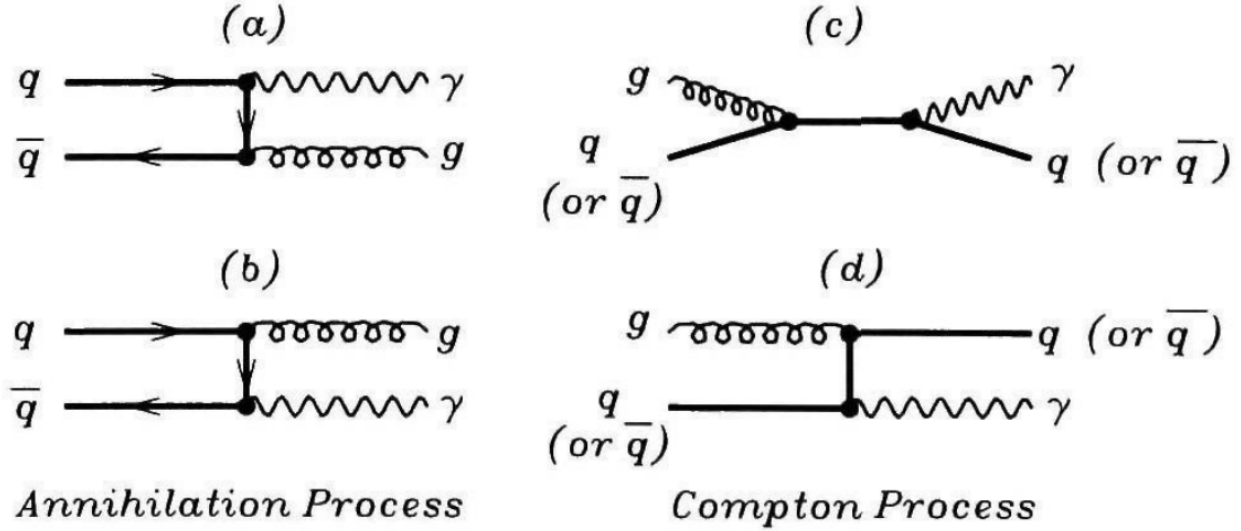


Figure 3.7: Feynman diagram representing the production of photons from quarks and gluons. (a) and (b) represent annihilation processes, whereas (c) and (d) represent Compton processes.[39]

3.6.4 Strangeness Enhancement

One of the implications of the formation of QGP is chiral symmetry restoration. At the energy scale of this phenomenon, strange quarks lose their masses, and hence it is feasible to produce a lot of them. The interacting nuclei carry no net strangeness before colliding, and so a post-collision observation of strange and multi-strange particles would imply the suppression of strange quark mass [15]. Strangeness can also be produced in hadron-hadron collisions. However, it is enhanced in nucleus-nucleus collisions in which a large number of hadrons are produced and are in chemical equilibrium at very high temperatures. The enhancement is exemplified by the ratio of the production of the strange kaons to that of the non-strange pions, which are the most abundant hadrons produced from nucleus-nucleus collisions. Kaon yield increases more rapidly than does pion yield as the temperature increases. This can be shown mathematically by treating the system as a hadron gas in thermal and chemical equilibrium that follows the Bose-Einstein distribution, but it is beyond the scope of this thesis [39]. connect to big picture... why is strangeness enhancement interesting? phase space suppression? chiral symmetry restoration.....?

3.6.5 Jet Quenching

A scattering event in which the participants transfer a large amount of their original momenta is called hard scattering. The products of the scattering are called jets. Ultimately, jets are what are recognized as jets. In heavy-ion collisions, most hard scatterings are the results of two partons from the opposite nuclei scattering off of each other. These partons can lose their momenta by strongly interacting with a medium made of deconfined quarks and gluons. Therefore, the properties of the jets, as carried by the final state hadrons, should be different for collisions that produce the QGP as compared to those that [don't]????????, and hence they can be used as signatures and probes of QGP. Figure 3.8 illustrates the quenching of jets that have to travel long distances in the medium. Formalisms developed to study jet quenching due to radiative and collisional energy losses are detailed in [28].

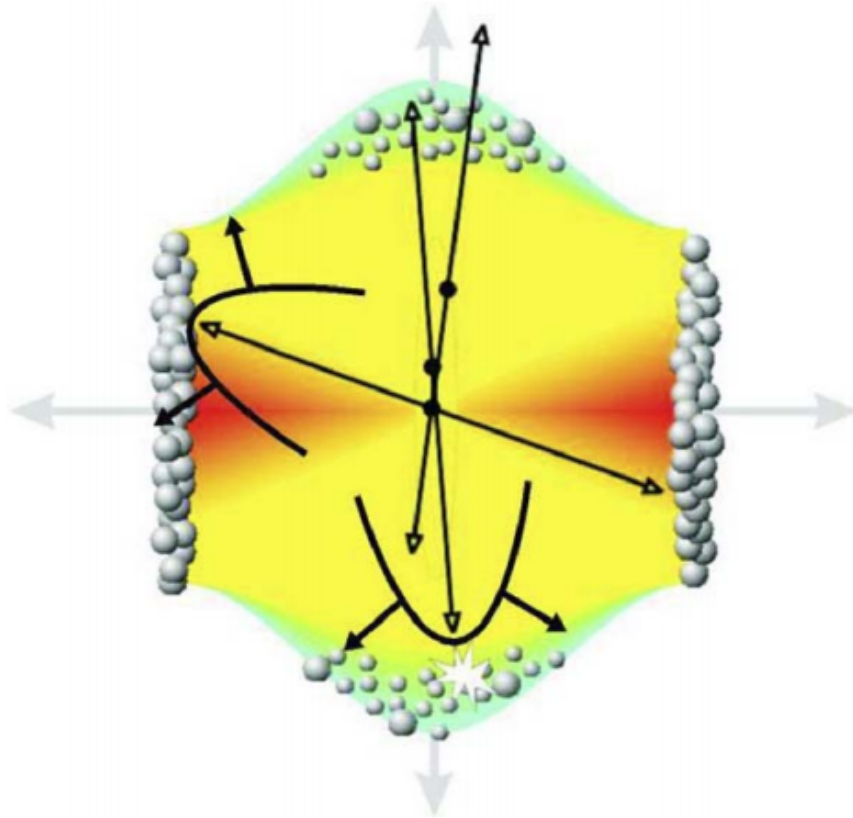


Figure 3.8: Illustration of jet quenching. Two jets are produced from each of the hard scatterings occurring at the locations of the solid dots. Jets originating closer to the initial surface are more probable to propagate outside the medium, as shown. Jets opposite to them interact with the medium, losing their energy and resulting in bow front shock waves.[36]

3.7 The Beam Energy Scan Program

The RHIC, in 2010, started a multi-phase Beam Energy Scan (BES) program to study the QCD phase diagram. Between 2010 and 2011, during the exploratory phase I of the BES program, the collider provided Au+Au collisions at 7.7, 11.5 (not completed in PHENIX), 19.6, 27, and 39 GeV. Together with the data formerly collected by the RHIC at higher collision energies, BES phase I data can scan the interval from 450 MeV to 20 MeV in μ_B space [25, 23]. One of the things that can be studied with the data associated with this region of the phase space is statedly the possibility of a “turn-off of new phenomena already established at higher RHIC energies” (<https://drupal.star.bnl.gov/STAR/starnotes/public/sn0493>). Results corresponding to the high- μ_B region might provide evidence of a first order phase transition, and possibly the critical point [23].

The manifestation of such phenomena would be in terms of the fluctuations or other properties of the post-collision system. One can, for instance, study the scaling of the transverse energy after the collision with the longitudinal energy at the time of the collision, $\sqrt{s_{NN}}$. This can be done in multiple ways using a detector like STAR or PHENIX that is made up of sub-systems such as the Time Of Flight (TOF) detectors, Time Projection Chambers (TPCs)/Time Expansion Chambers, as well as calorimeters. The next chapter describes the measurement of transverse energy using BES data from PHENIX calorimeters. Also, the next chapter and the ones after it contain the procedures and the results of the analysis of the BES data from STAR using the identified particles spectra.

Chapter 4

Measurement of Transverse Energy

This chapter introduces the definitions of transverse energy, ways to measure it using different detectors, and particular examples for the detectors at the RHIC.

4.1 Definition of Transverse Energy

The transverse energy, E_T , from a collision can be defined as the sum of the transverse masses, m_T , of all the particles produced in the collision, i.e.,

$$E_T \equiv \sum_i m_{T,i} \quad (4.1)$$

with

$$m_T \equiv \sqrt{p_T^2 + m^2} \quad (4.2)$$

where m is the rest mass of the particle and p_T is its transverse momentum. Using this definition to calculate the E_T requires perfect identification of all the particles. It has not been possible to do so in experiments, and so a more feasible, operational definition of E_T is used. A commonly accepted definition in case of the feasibility of calorimetric measurements is [5, 12]:

$$E_T = \sum_i E_i \sin \theta_i, \quad (4.3)$$

481

$$\frac{dE_T}{d\eta} = \sin\theta \frac{dE}{d\eta}, \quad (4.4)$$

482 where the index i runs over all the particles going into a fixed solid angle for each event,
 483 θ is the polar angle, i.e, the angle with respect to the beam axis, η is the pseudorapidity
 484 defined as

$$\eta \equiv -\ln \tan \frac{\theta}{2}, \quad (4.5)$$

485 and E_i is the energy deposited in the calorimeter by the i^{th} particle. E_i is considered to be,
 486 by convention [6], the following

$$E_i = \begin{cases} E_i^{tot} - m_0 & \text{for baryons} \\ E_i^{tot} + m_0 & \text{for anti-baryons} \\ E_i^{tot} & \text{otherwise} \end{cases} \quad (4.6)$$

487 where E_i^{tot} is the total energy of the i^{th} particle defined canonically as

$$E^{tot} \equiv \sqrt{p^2 + m_0^2} \quad (4.7)$$

488 and m_0 is the particle's rest mass.

489 E_i given by equation 4.6 is what would be observed by a calorimeter. In order to
 490 account for the portion of the emitted transverse energy not detected or overestimated by
 491 the calorimeters, corrections are made based on simulations.

492 **4.2 E_T Measurement with Calorimeters**

493 **4.2.1 Calorimeter**

494 A calorimeter in a particle or nuclear physics experiment is a device used to measure the
 495 energy carried by a particle by analyzing the signal generated by the shower of particles
 496 produced by the interaction of the incoming particle with the material of the device [? ,
 497 (<http://pdg.lbl.gov/2016/download/rpp-2016-booklet.pdf>)] In theory, a single calorimeter

can be made to measure the energy deposited by different kinds of particles. However, it makes more sense to have two different kinds of calorimeters: one optimized to measure the energy deposited by particles like electrons (or positrons) and photons, called an electromagnetic calorimeter (EMCal), and the other optimized to measure the energy deposited by hadronic particles, called a hadronic calorimeter (HCal). This is because of the difference in the particle showers that these two categories of particles generate. Electrons and photons mostly lose their energies in the calorimeter material via bremsstrahlung, Compton scattering and pair production. They generate particle showers made of electrons and photons which cannot travel much farther into the medium before losing all their energies in a series of interactions producing an avalanche of sequential showers. However, hadrons can interact inelastically with the nucleus generating a shower of hadrons. These secondary hadrons have much larger masses than the secondary electrons in the shower generated by the electrons and photons. This means they are not deflected nearly as much by the electric forces in the material and travel much farther into the calorimeter. For this reason, EMCals are comparably smaller in depth and are placed before the HCals in a detector assembly.

4.2.2 E_T from PHENIX Calorimetry

Adare et al. [3] use electromagnetic calorimetry in PHENIX to analyze the transverse energy corresponding to several different pairs of species colliding at a range of energies. They use the raw transverse energy measured by the EMCal, E_{TEMC} , to obtain the total E_T by making corrections in three different steps. They first scale the data by a constant factor calculated to account for the fiducial acceptance in azimuth and pseudorapidity. The second factor is calculated to adjust for the effects of the calorimeter towers that are disabled. The third factor, k , is computed as follows

$$k = k_{response} \times k_{inflow} \times k_{losses} \quad (4.8)$$

where $k_{response}$ corresponds to hadronic particles only depositing a fraction of their total energy while passing through the EMCal, k_{inflow} is attributable to the energy deposited by particles coming from outside the EMCal's fiducial aperture, and k_{losses} accounts for

the energy not registered in the EMCal due to energy thresholds, edge effects, and more importantly due to the particles that make it into the fiducial aperture but decay into products outside the aperture. Give some sense of what these corrections are... the first two probably have very small systematic uncertainties while the third likely has very large uncertainties.....

4.3 E_T Measurement with Tracking Detectors

Transverse energy analysis can be done using tracking detectors as well if they are able to produce measurements of other physical quantities that implicitly contain information about the transverse energy. Specifically, the charged particle multiplicity distributions with respect to the transverse momenta can be used, with assumptions involving particle ratios and mean p_T , to calculate the particle's transverse energy. Since the corrections related to the tracking detectors are very different from those related to the calorimeters, results from the two different methods can be used to test the assumptions involved in each.

4.3.1 Tracking and Particle Identification

The tracking detectors in experiments such as the STAR (Solenoidal Tracker At RHIC) experiment and ALICE (A Large Ion Collider Experiment) at CERN include Time Projection Chambers (TPCs) and Time-of-Flight (TOF) detectors that can be used to measure the p_T spectra, yields and particle ratios of the identified charged hadrons [27, 2]. The TPCs provide measurements of particle trajectories that can be used to determine the momenta for low-momentum particles. They also provide measurements of their specific energy loss, $\frac{dE}{dx}$, which can be used in combination with the momenta to identify particles using the Bethe-Bloch formula [10]. The particle identification (PID) capabilities of STAR are discussed in section 4.3.3. TOF detectors cover the high-momentum part of the measurements. In ALICE, the combination of the measurements of the TPC with those of the Inner Tracking System (ITS) effectively adds the tracking length, thereby improving the resolution of the measured p_T spectrum. Details about the PID and momentum determination capabilities of the detectors in ALICE can be found in [13].

551 The p_T spectra, reported as $\frac{d^2N}{dydp_T}$ as a function of p_T , can be used to calculate $\frac{dE_T}{d\eta}$ as
 552 formulated in the following section.

553 4.3.2 Calculation of $\frac{dE_T}{d\eta}$ from p_T spectra

554 In relativistic heavy ion collisions, rapidity (y) is defined as follows:

$$y \equiv \frac{1}{2} \ln \frac{E + p_z}{E - p_z}, \quad (4.9)$$

where E is given by equation 4.7 and p_z is the component of the momentum parallel to the beam axis. Pseudorapidity, η , is just y with $m_0 = 0$:

$$\begin{aligned} \eta &= \frac{1}{2} \ln \frac{p + p_z}{p - p_z} \\ &= \frac{1}{2} \ln \frac{1 + \cos \theta}{1 - \cos \theta} \\ &= \frac{1}{2} \ln \frac{2 \cos^2 \frac{\theta}{2}}{2 \sin^2 \frac{\theta}{2}} \end{aligned}$$

$$\therefore \eta = - \ln \left| \tan \frac{\theta}{2} \right| \quad (4.10)$$

555 Note that the absolute value is not necessary for $0 \leq \theta \leq \pi$. Then, taking the exponential
 556 of both sides of the above equation and using Euler's formula, we get:

$$\sin \theta = \frac{1}{\cosh \eta}. \quad (4.11)$$

Hence,

$$\begin{aligned} p &= \frac{p_T}{\sin \theta} \\ &= p_T \cosh \eta, \end{aligned}$$

557 and so we have

$$E_T = E \sin \theta = \frac{\sqrt{p_T^2 \cosh^2 \eta + m_0^2}}{\cosh \eta} \quad (4.12)$$

The Jacobian for the transformation from y -space to η -space is derived to be:

$$\frac{\partial y}{\partial \eta} = \frac{p_T \cosh \eta}{\sqrt{m_0^2 + p_T^2 \cosh^2 \eta}} \quad (4.13)$$

From equations 4.12 and 4.13, we can see that the product of E_T with the Jacobian is equal to p_T . That leads to a formulation of $\frac{dE_T}{d\eta}$ as a function of only η and p_T :

$$\frac{dE_T}{d\eta} = \frac{1}{2a} \int_0^{10 \text{ GeV}/c} \int_{-a}^a p_T \frac{d^2 N}{dy dp_T} d\eta dp_T \quad (4.14)$$

where a and $-a$ are the bounds for η . The estimate for the upper limit of p_T makes sense in accordance with the mean p_T of the spectra being comfortably an order of magnitude less than 10 GeV/c as discussed in chapter 5.

4.3.3 Tracking Detectors in STAR

In the STAR experiment, the TPC is the primary tracking detector. It is 4.2 m long and it cylindrically encloses the accelerator beam pipe from its outside, with an inner diameter of 1 m and an outer diameter of 4 m [24]. It covers a pseudorapidity range of $|y| < 1.8$ in all of azimuth for charged particles. It can identify particles with momenta over 100 MeV/c up to about 1 GeV/c as well as measure their momenta from 100 MeV/c to 30 GeV/c [8]. Figure 4.1 shows the PID capability of the STAR TPC for very high-multiplicity events [19]. Separation of pions from protons is demonstrated up to a little more than 1 GeV/c. At higher momenta, separating particles is more difficult because their energy loss has lower dependence on the rest mass [8]. The TOF system in STAR, with a time resolution of $\lesssim 100$ ps, aids PID at higher momenta. However, at intermediate p_T , between ≈ 2.0 and 4.0 GeV/c, the TPC by itself cannot distinguish between pions and protons and the TOF by itself cannot separate pions from kaons. This problem is resolved by utilizing the fact that the dependence of the particle velocity on p_T – in case of the TPC – is different from that of the energy loss on p_T in case of the TPC; combining the results from the two, hence, makes PID feasible in this p_T range. [31]

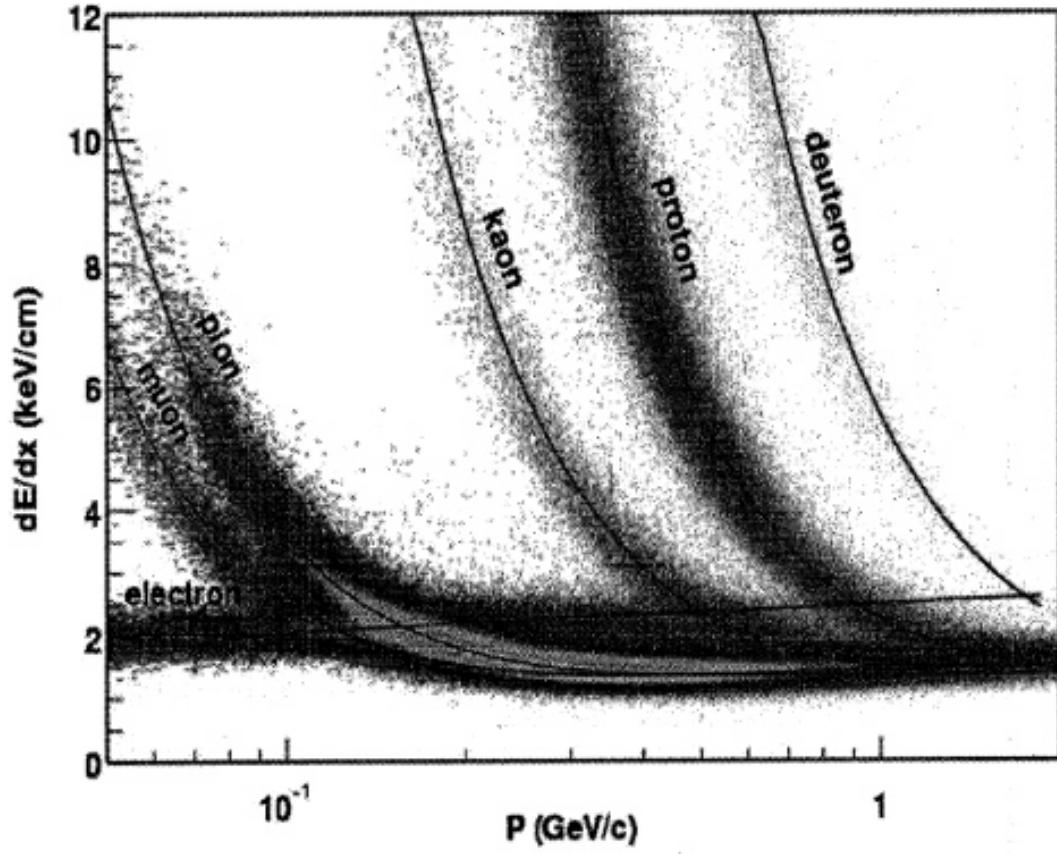


Figure 4.1: Energy loss distribution in the STAR TPC for primary and secondary particles. [19].

Chapter 5

Data Analysis

The analysis of the data involved extrapolating the available spectra and using the results from the fits to calculate the transverse energy for all the available spectra and the particle multiplicity corresponding to charged particles. Details follow.

5.0.1 STAR p_T spectra

This thesis details the method of transverse energy analysis through the use of p_T spectra from the STAR BES data. As described in section 4.3.3, the TPCs and TOF detectors in STAR can identify particles as well as their trajectories and ultimately their multiplicity distributions with respect to the momenta. Adamczyk et al. [2] report the results for the p_T spectra for six different identified hadrons, π^+ , π^- , K^+ , K^- , p , and \bar{p} , from the STAR experiment. The spectra come from Au+Au collisions – at $\sqrt{s_{NN}} = 7.7$, 11.5, and 39 GeV in the year 2010 and at $\sqrt{s_{NN}} = 19.6$ and 27 GeV in 2011 – under the BES Program. Figure 5.1 [2] shows the spectra corresponding to 39 GeV collisions categorized into seven different collision centrality classes. These spectra, and their counterparts for the rest of the energies, were used to calculate an estimate of the total transverse energy per event per particle species. This result was then used to estimate the total transverse energy due to all the collision products.

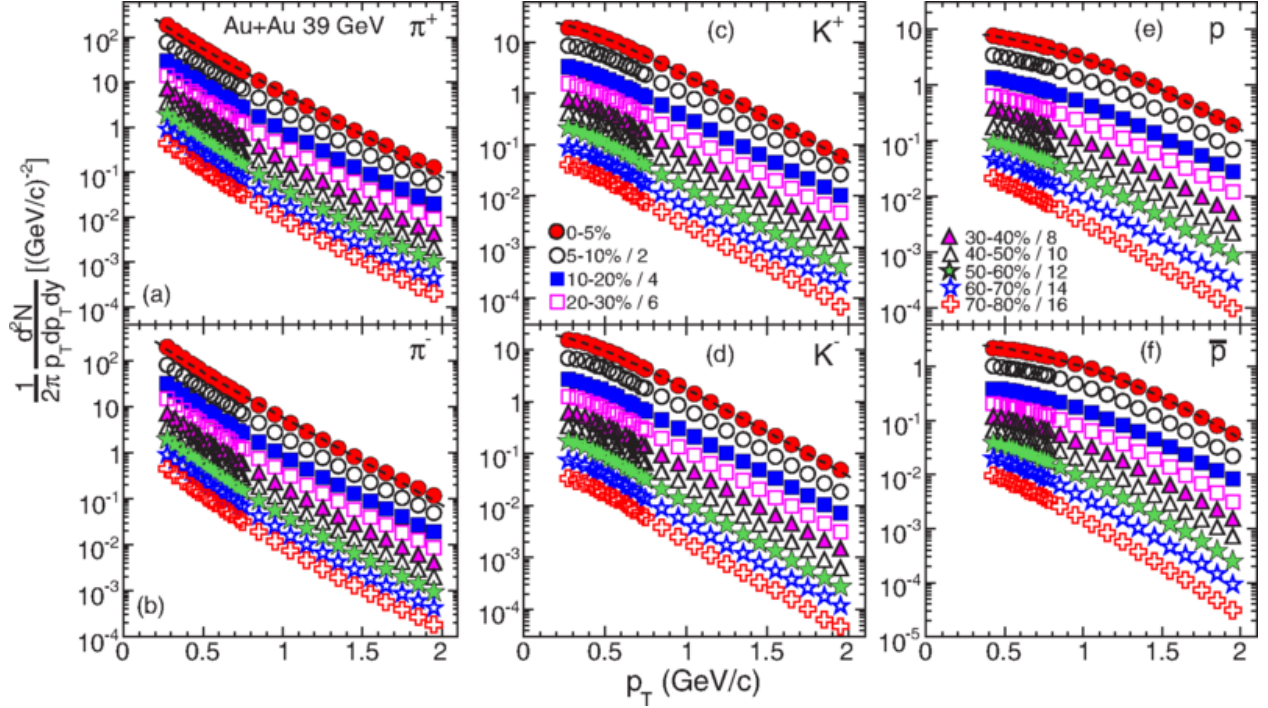


Figure 5.1: Transverse momentum spectra for π^+ , π^- , K^+ , K^- , p , and \bar{p} at midrapidity ($|y| < 0.1$) from 39 GeV Au+Au collisions at RHIC. The fitting curves on the 0-5% central collision spectra for pions, kaons, and protons/anti-protons represent, respectively, the Bose-Einstein, m_T -exponential, and double-exponential functions. [2].

The corrections applied by Adamczyk et al. [2] to the raw data to obtain the spectra and the reported systematic uncertainties in their results are discussed below (under construction)

5.1 Extrapolation of Spectra

The available spectra were limited to a range of transverse momenta ranging from around 0.25 GeV/c to around 2 GeV/c (for pions). To account for the transverse energy corresponding to the momenta for which there was no available data, an extrapolation had to be used. The model used for the extrapolation and the associated statistics are discussed below.

5.1.1 Boltzmann-Gibbs Blast Wave

The blast wave is a common model used in the analysis of the particle spectra.[????] The specific model used in this thesis is the Boltzmann-Gibbs blast wave (BGBW) as represented in equation ?? . It has the parameters mass, temperature, beta, v, and n. I assume that any anomalies in the magnitude of the normalization parameter do not affect the results significantly insomuch as they don't lead to:

- (a) unreasonable relative errors in the extrapolated values of the transverse energy,
- (b) any of the spectral fits having the extrapolated transverse energy more than that calculated from just the available spectra, and
- (c) for the 200 GeV collision samples, at least, the extrapolation at higher p_T being more than that at lower p_T .

$$BGBW \tag{5.1}$$

5.1.2 Fitting Spectra to BGBW

Figure 5.2 presents an example of a Boltzmann-Gibbs Blast Wave (BGBW) fit on one of the individual particle spectra with the goodness-of-fit as well as other statistics and the associated errors. A parallel-coordinates plot is presented in the next chapter in fig. 6.1, which shows the measured centralities, two of the good-fit parameters, and the calculated transverse energies for 270 different particles (lambdas not included).

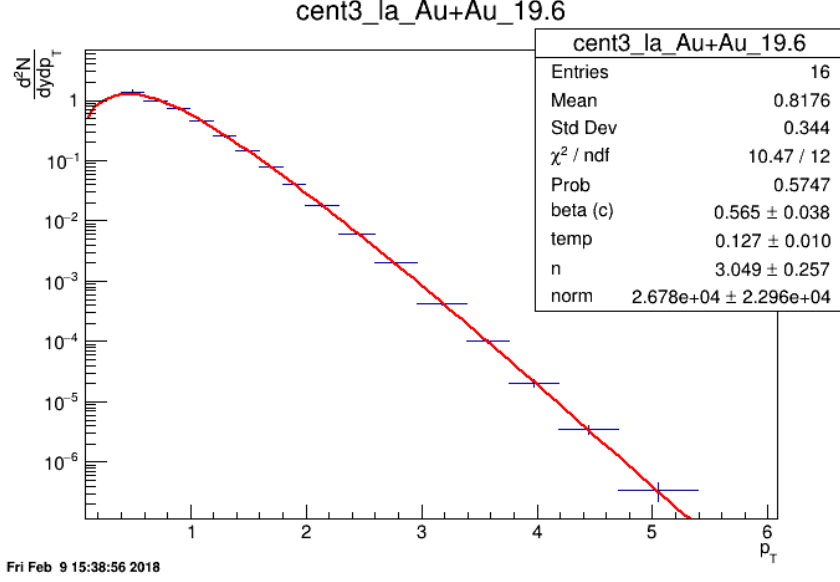


Figure 5.2: Red curve shows the Boltzmann-Gibbs blast wave functional fit on the PRELIMINARY transverse momentum spectrum for lambda particles identified by the STAR detector for 19.6 GeV Au+Au collisions (10-15% central). Parameters extracted from the chi-square goodness-of-fit test, as well as other statistics, are shown in the box on the top right.

5.2 Calculations from the Spectral Fits

5.2.1 Calculation of $\frac{dE_T}{dy}$, $\frac{dE_T}{dn}$, $\frac{dN_{ch}}{dy}$, and $\frac{dN_{ch}}{dn}$

5.2.2 Corrections for Unidentified Particles and Estimation of Total E_T

It is reasonable to assume that, at high energies, there should be roughly the same multiplicity of all the isospin states of a final state particle. Table 5.1 lists the isospin states associated with the pion, the kaon, the proton, and the lambda particles.

Particle	Isospin multiplets
pion	π^+, π^0, π^-
kaon	K^+, K^0, K^-, \bar{K}^0
proton	p, n
lambda	Λ

Table 5.1: Isospin states of different identified particles.

630text content.....

$$E_T = 3E_T^\pi + 4E_T^K + 4E_T^p + 2E_T^\Lambda \quad (5.2)$$

631text content.....

632 **5.2.3 Lambdas Centralitiy Adjustments and E_T Interpolations**

633 The centrality bins corresponding to the lambdas spectra were slightly different from those
634 corresponding to the rest of the particles.....

635 **5.3 Uncertainties**

636 100% correlated point-to-point and uncorrelated between particles..... ?

Chapter 6

Results

Present results and comparisons to Adare et al....

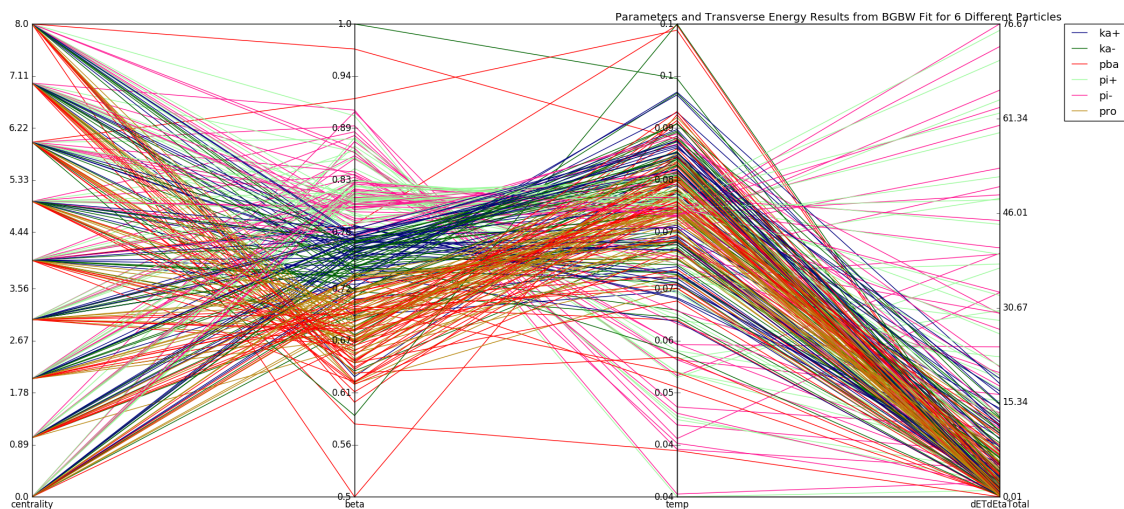


Figure 6.1: Parallel coordinates plot for 270 different spectra relating 6 different identified particles (color-coded) to their respective collision centrality classes, good-fit parameters, and the transverse energy calculated using said parameters.

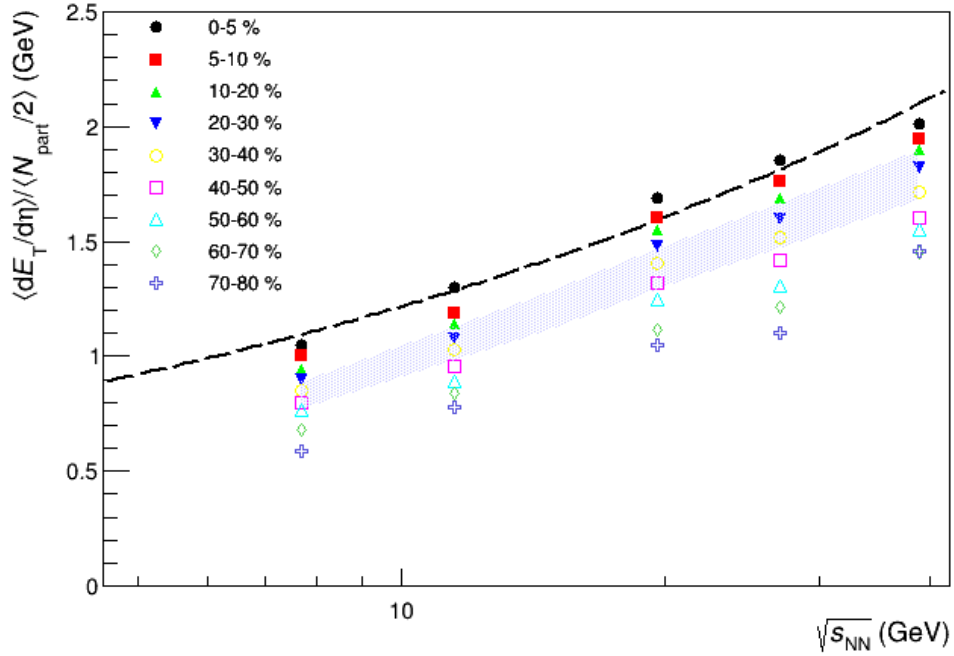


Figure 6.2: $(dE_T/d\eta)/0.5N_{part}$ at midrapidity as a function of $\sqrt{s_{NN}}$ for different centralities. The dashed line represents a power-law fit to the 0-5% central data in the form $y = ax^{2b}$, where x and y are the placeholders for the quantities in the plot axes. $\chi^2/n.d.f$ for the fit was 1.806, and the good-fit parameters were $a = 0.4838 \pm 0.0429$ and $b = 0.2005 \pm 0.01466$. The shaded area represents the uncertainty bounds for the 0-5% central PHENIX data from [3].

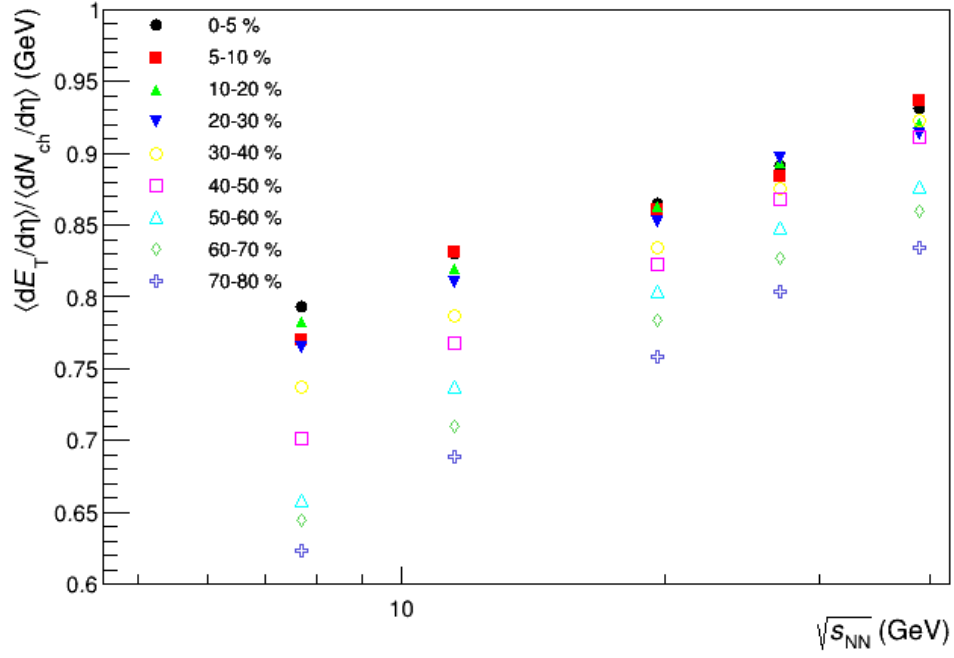


Figure 6.3: $\langle dE_T/d\eta \rangle / \langle dN_{ch}/d\eta \rangle$ at midrapidity as a function of $\sqrt{s_{NN}}$ for different centralities.

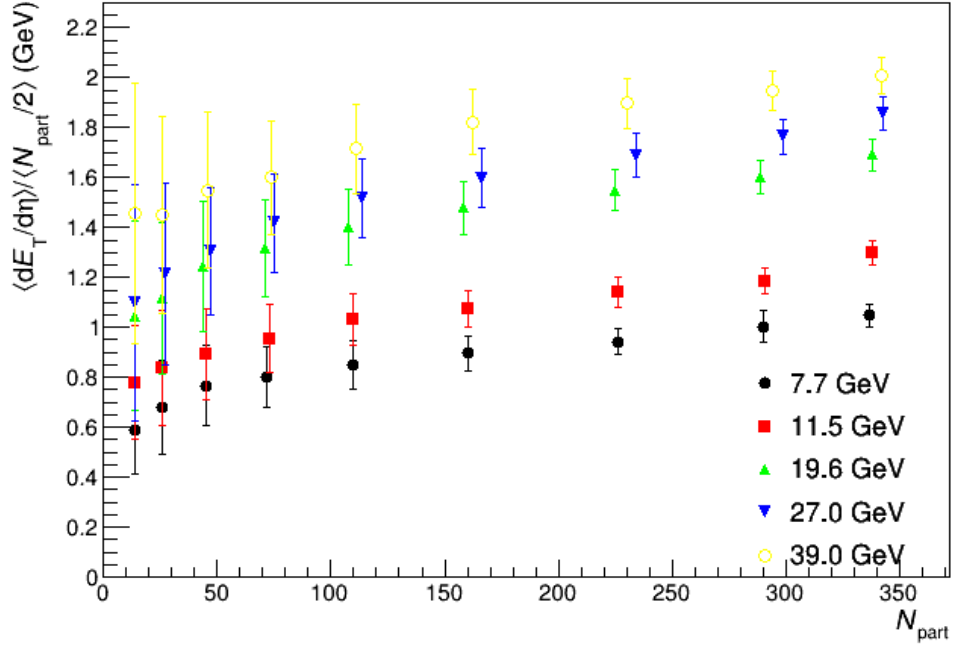


Figure 6.4: $\langle dE_T/d\eta \rangle / 0.5N_{part}$ at midrapidity as a function of N_{part} for different centralities.

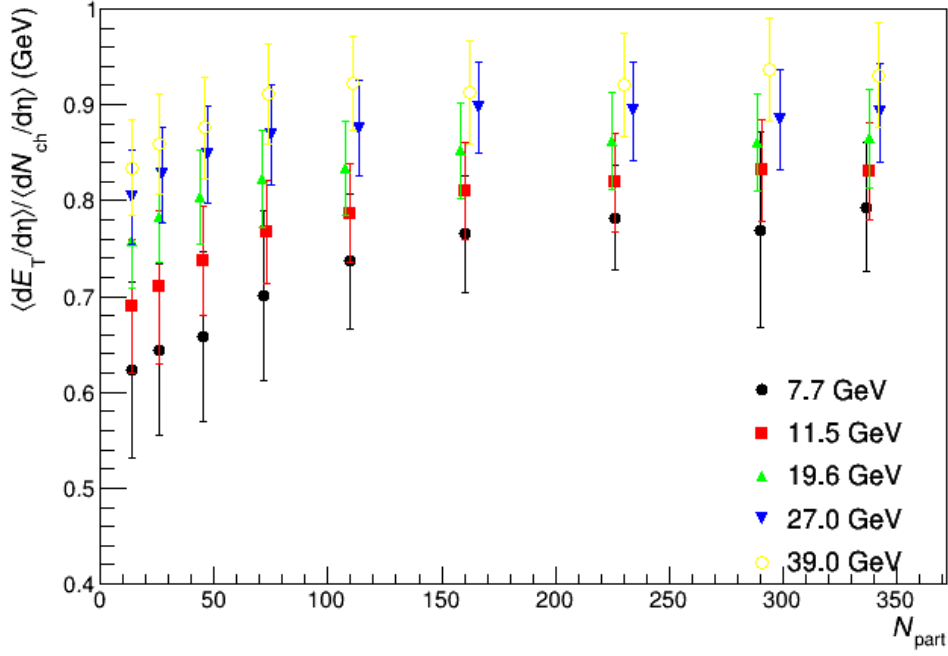


Figure 6.5: $\langle dE_T/d\eta \rangle / \langle dN_{ch}/d\eta \rangle$ at midrapidity as a function of N_{part} for different centralities.

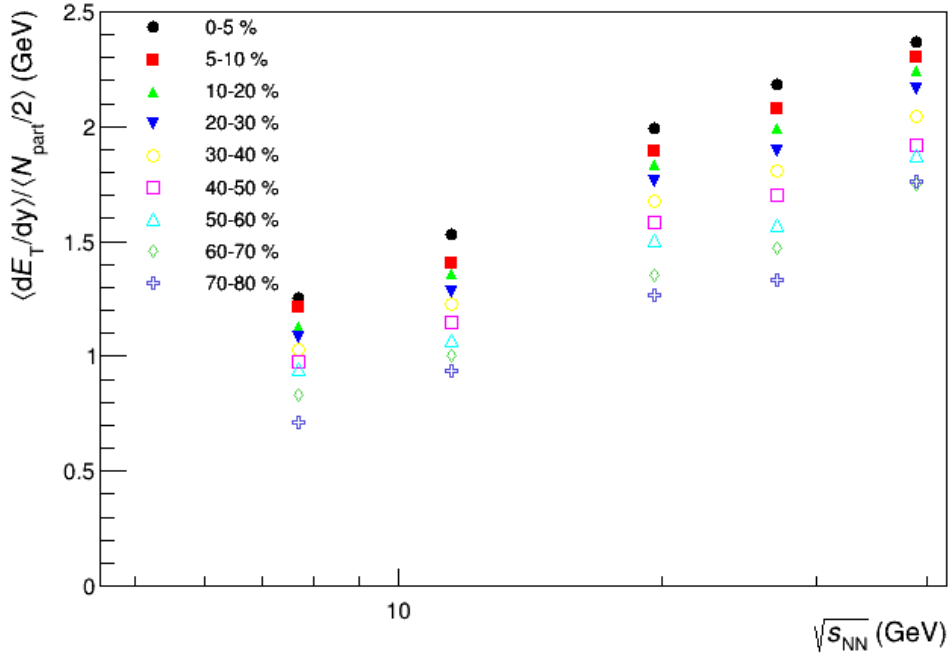


Figure 6.6: $\langle dE_T/dy \rangle / 0.5N_{part}$ at midrapidity as a function of $\sqrt{s_{NN}}$ for different centralities.

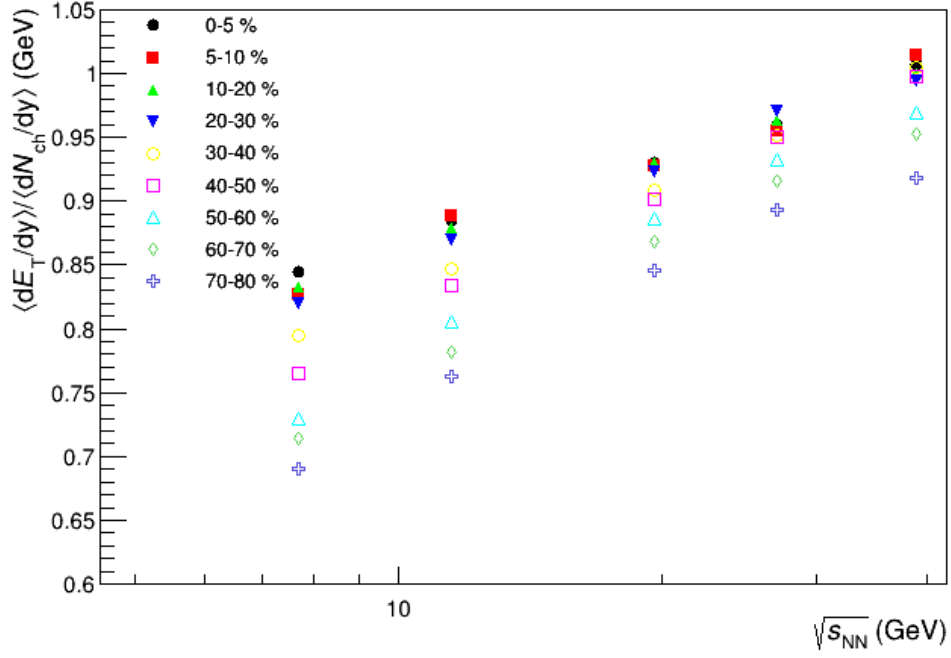


Figure 6.7: $\langle dE_T/dy \rangle / \langle dN_{ch}/dy \rangle$ at midrapidity as a function of $\sqrt{s_{NN}}$ for different centralities.

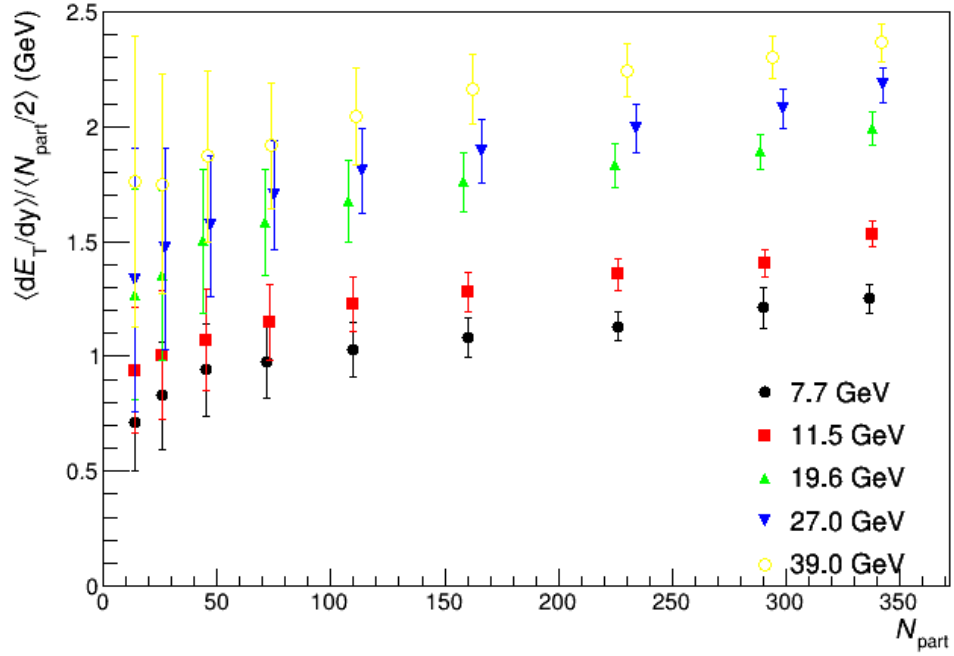


Figure 6.8: $\langle dE_T/dy \rangle / 0.5N_{part}$ at midrapidity as a function of N_{part} for different centralities.

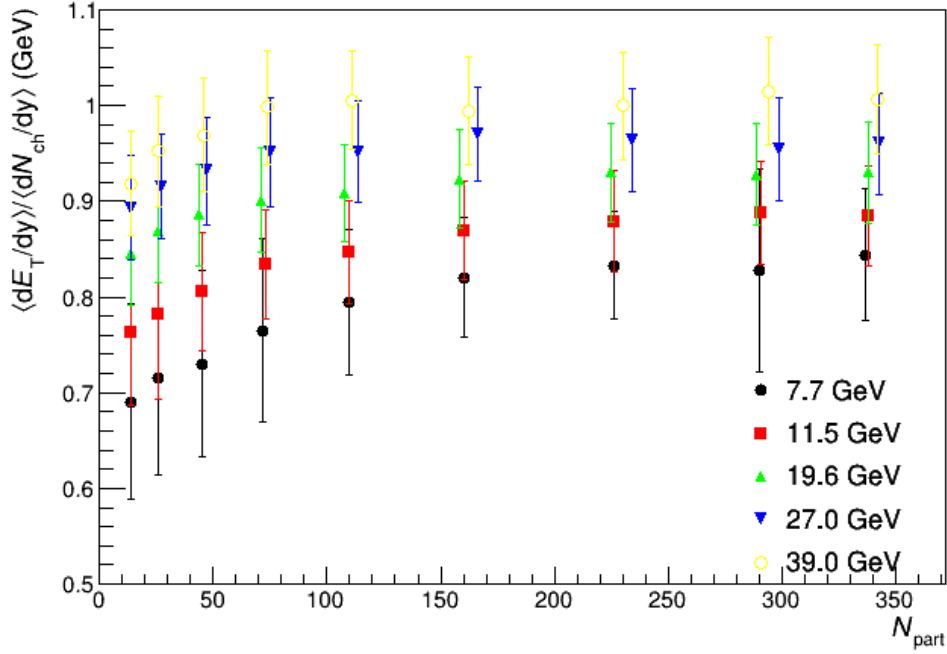


Figure 6.9: $\langle dE_T/dy \rangle / \langle dN_{ch}/dy \rangle$ at midrapidity as a function of N_{part} for different centralities.

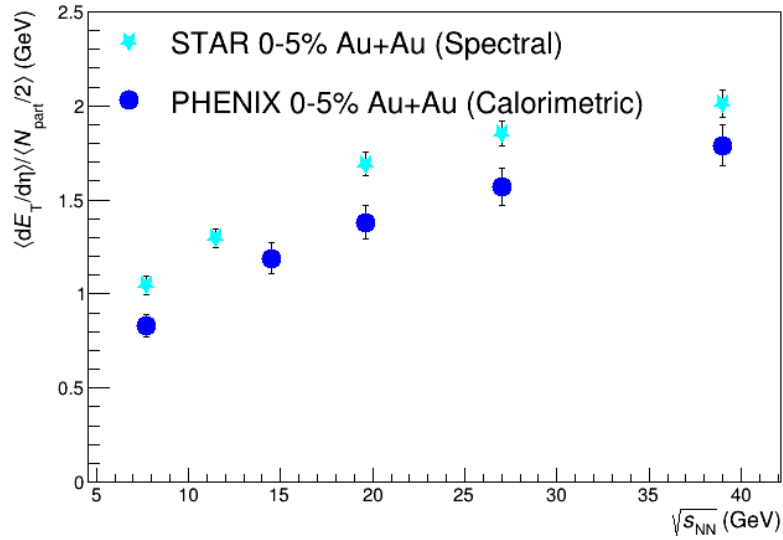


Figure 6.10: $\langle dE_T/d\eta \rangle / 0.5N_{part}$ for 0-5% central collisions at midrapidity as a function of $\sqrt{s_{NN}}$. The PHENIX data are from [3]. The error bars represent the total statistical and systematic uncertainties.

⁶⁴⁰ Chapter 7

⁶⁴¹ Conclusion

⁶⁴² Summary and implications

Chapter 8

Future Work

8.1 Goodness of Fit

A maximum likelihood? fit method can be adopted to compare the results with those using the chi-squared fits.

8.2 Bjorken Energy Density Estimate

Apart from the transverse energy, the calculation of the initial energy density, ϵ , as given by the Bjorken formula in eq. 3.8, requires the estimate of other physical quantities. Adare et al.[3] use the Glauber model to determine A_T , the area of the intersection of the two nuclei in the transverse plane. Since the results in this thesis are cross-checked with those in [3], it would be reasonable to use the same model in the future work pertaining to this thesis. τ_0 , the proper time at the moment of QGP equilibration, also depends on the model of the collision. However, the product of ϵ and τ_0 is often used instead of just ϵ to study how the energy density scales with the collision energy and the number of participants.

657 **8.3 Asymmetric beams**

658 The codes in the repository can be used to analyze more data. In fact, since there is more
659 data available on collisions of asymmetric systems such as d+Au?, we can expect it to be a
660 test to tell if the assumptions? used in this analysis scale to such domains?

Bibliography

662 [1] Adam, J., Adamova, D., Aggarwal, M. M., Aglieri Rinella, G., Agnello, M., Agrawal,
 663 N., Ahammed, Z., Ahmad, S., Ahn, S. U., Aiola, S., Akindinov, A., Alam, S. N., Silva
 664 De Albuquerque, D., Aleksandrov, D., Alessandro, B., Alexandre, D., Alfaro Molina,
 665 J. R., Alici, A., Alkin, A., Millan Almaraz, J. R., Alme, J., Alt, T., Altinpinar, S.,
 666 Altsybeev, I., Alves Garcia Prado, C., Andrei, C., Andronic, A., Anguelov, V., Anticic,
 667 T., Antinori, F., Antonioli, P., Aphecetche, L. B., Appelshaeuser, H., Arcelli, S., Arnaldi,
 668 R., Arnold, O. W., Arsene, I. C., Arslanok, M., Audurier, B., Augustinus, A., Averbek,
 669 R. P., Azmi, M. D., Badala, A., Baek, Y. W., Bagnasco, S., Bailhache, R. M., Bala,
 670 R., Balasubramanian, S., Baldisseri, A., Baral, R. C., Barbano, A. M., Barbera, R.,
 671 Barile, F., Barnafoldi, G. G., Barnby, L. S., Ramillien Barret, V., Bartalini, P., Barth,
 672 K., Bartke, J. G., Bartsch, E., Basile, M., Bastid, N., Basu, S., Bathen, B., Batigne,
 673 G., Batista Camejo, A., Batyunya, B., Batzing, P. C., Bearden, I. G., Beck, H., Bedda,
 674 C., Behera, N. K., Belikov, I., Bellini, F., Bello Martinez, H., Bellwied, R., Belmont Iii,
 675 R. J., Belmont Moreno, E., Belyaev, V., Bencedi, G., Beole, S., Berceanu, I., Bercuci, A.,
 676 Berdnikov, Y., Berenyi, D., Bertens, R. A., Berzano, D., Betev, L., Bhasin, A., Bhat, I. R.,
 677 Bhati, A. K., Bhattacharjee, B., Bhom, J., Bianchi, L., Bianchi, N., Bianchin, C., Bielcik,
 678 J., Bielcikova, J., Bilandzic, A., Biro, G., Biswas, R., Biswas, S., Bjelogric, S., Blair, J. T.,
 679 Blau, D., Blume, C., Bock, F., Bogdanov, A., Boggild, H., Boldizar, L., Bombara, M.,
 680 Book, J. H., Borel, H., Borissov, A., Borri, M., Bossu, F., Botta, E., Bourjau, C., Braun-
 681 Munzinger, P., Bregant, M., Breitner, T. G., Broker, T. A., Browning, T. A., Broz, M.,
 682 Brucken, E. J., Bruna, E., Bruno, G. E., Budnikov, D., Buesching, H., Bufalino, S., Buncic,
 683 P., Busch, O., Buthelezi, E. Z., Bashir Butt, J., Buxton, J. T., Cabala, J., Caffarri, D.,
 684 Cai, X., Caines, H. L., Calero Diaz, L., Caliva, A., Calvo Villar, E., Camerini, P., Carena,
 685 F., Carena, W., Carnesecchi, F., Castillo Castellanos, J. E., Castro, A. J., Casula, E.
 686 A. R., Ceballos Sanchez, C., Cepila, J., Cerello, P., Cerkala, J., Chang, B., Chapeland,
 687 S., Chartier, M., Charvet, J.-L. F., Chattopadhyay, S., Chattopadhyay, S., Chauvin, A.,
 688 Chelnokov, V., Cherney, M. G., Cheshkov, C. V., Cheynis, B., Chibante Barroso, V. M.,
 689 Dobrigkeit Chinellato, D., Cho, S., Chochula, P., Choi, K., Chojnacki, M., Choudhury, S.,
 690 Christakoglou, P., Christensen, C. H., Christiansen, P., Chujo, T., Chung, S.-U., Cicalo,
 691 C., Cifarelli, L., Cindolo, F., Cleymans, J. W. A., Colamaria, F. F., Colella, D., Collu, A.,

692 Colocci, M., Conesa Balbastre, G., Conesa Del Valle, Z., Connors, M. E., Contreras Nuno,
 693 J. G., Cormier, T. M., Corrales Morales, Y., Cortes Maldonado, I., Cortese, P., Cosentino,
 694 M. R., Costa, F., Crochet, P., Cruz Albino, R., Cuautle Flores, E., Cunqueiro Mendez,
 695 L., Dahms, T., Dainese, A., Danisch, M. C., Danu, A., Das, D., Das, I., Das, S., Dash,
 696 A. K., Dash, S., De, S., De Caro, A., De Cataldo, G., De Conti, C., De Cuveland, J.,
 697 De Falco, A., De Gruttola, D., De Marco, N., De Pasquale, S., Deisting, A., Deloff,
 698 A., Denes, E. S., Deplano, C., Dhankher, P., Di Bari, D., Di Mauro, A., Di Nezza,
 699 P., Diaz Corchero, M. A., Dietel, T., Dillenseger, P., Divia, R., Djuvsland, O., Dobrin,
 700 A. F., Domenicis Gimenez, D., Donigus, B., Dordic, O., Drozhzhova, T., Dubey, A. K.,
 701 Dubla, A., Ducroux, L., Dupieux, P., Ehlers Iii, R. J., Elia, D., Endress, E., Engel, H.,
 702 Epple, E., Erasmus, B. E., Erdemir, I., Erhardt, F., Espagnon, B., Estienne, M. D.,
 703 Esumi, S., Eum, J., Evans, D., Evdokimov, S., Eyyubova, G., Fabbietti, L., Fabris, D.,
 704 Faivre, J., Fantoni, A., Fasel, M., Feldkamp, L., Feliciello, A., Feofilov, G., Ferencei, J.,
 705 Fernandez Tellez, A., Gonzalez Ferreira, E., Ferretti, A., Festanti, A., Feuillard, V. J. G.,
 706 Figiel, J., Araujo Silva Figueredo, M., Filchagin, S., Finogeev, D., Fionda, F., Fiore, E. M.,
 707 Fleck, M. G., Floris, M., Foertsch, S. V., Foka, P., Fokin, S., Fragiaco, E., Francescon,
 708 A., Frankenfeld, U. M., Fronze, G. G., Fuchs, U., Furget, C., Furs, A., Fusco Girard, M.,
 709 Gaardhoeje, J. J., Gagliardi, M., Gago Medina, A. M., Gallio, M., Gangadharan, D. R.,
 710 Ganoti, P., Gao, C., Garabatos Cuadrado, J., Garcia-Solis, E. J., Gargiulo, C., Gasik, P. J.,
 711 Gauger, E. F., Germain, M., Gheata, M., Ghosh, P., Ghosh, S. K., Gianotti, P., Giubellino,
 712 P., Giubilato, P., Gladysz-Dziadus, E., Glassel, P., Gomez Coral, D. M., Gomez Ramirez,
 713 A., Sanchez Gonzalez, A., Gonzalez, V., Gonzalez Zamora, P., Gorbunov, S., Gorlich,
 714 L. M., Gotovac, S., Grabski, V., Grachov, O. A., Graczykowski, L. K., Graham, K. L.,
 715 Grelli, A., Grigoras, A. G., Grigoras, C., Grigoryev, V., Grigoryan, A., Grigoryan, S.,
 716 Grynyov, B., Grion, N., Gronefeld, J. M., Grosse-Oetringhaus, J. F., Grosso, R., Guber,
 717 F., Guernane, R., Guerzoni, B., Gulbrandsen, K. H., Gunji, T., Gupta, A., Gupta, R.,
 718 Haake, R., Haaland, O. S., Hadjidakis, C. M., Haiduc, M., Hamagaki, H., Hamar, G.,
 719 Hamon, J. C., Harris, J. W., Harton, A. V., Hatzifotiadou, D., Hayashi, S., Heckel, S. T.,
 720 Hellbar, E., Helstrup, H., Herghelegiu, A. I., Herrera Corral, G. A., Hess, B. A., Hetland,
 721 K. F., Hillemanns, H., Hippolyte, B., Horak, D., Hosokawa, R., Hristov, P. Z., Humanic,

722 T., Hussain, N., Hussain, T., Hutter, D., Hwang, D. S., Ilkaev, R., Inaba, M., Incani,
 723 E., Ippolitov, M., Irfan, M., Ivanov, M., Ivanov, V., Izucheev, V., Jacazio, N., Jacobs,
 724 P. M., Jadhav, M. B., Jadlovská, S., Jadlovsky, J., Jahnke, C., Jakubowska, M. J., Jang,
 725 H. J., Janik, M. A., Pahula Hewage, S., Jena, C., Jena, S., Jimenez Bustamante, R. T.,
 726 Jones, P. G., Jusko, A., Kalinak, P., Kalweit, A. P., Kamin, J. A., Kang, J. H., Kaplin,
 727 V., Kar, S., Karasu Uysal, A., Karavichev, O., Karavicheva, T., Karayan, L., Karpechev,
 728 E., Kebschull, U. W., Keidel, R., Keijndener, D. L., Keil, M., Khan, M. M., Khan, P.,
 729 Khan, S. A., Khanzadeev, A., Kharlov, Y., Kileng, B., Kim, D. W., Kim, D. J., Kim,
 730 D., Kim, H., Kim, J., Kim, M., Kim, S. Y., Kim, T., Kirsch, S., Kisel, I., Kiselev,
 731 S., Kisiel, A. R., Kiss, G., Klay, J. L., Klein, C., Klein, J., Klein-Boesing, C., Klewin,
 732 S., Kluge, A., Knichel, M. L., Knospe, A. G., Kobdaj, C., Kofarago, M., Kollegger, T.,
 733 Kolozhvari, A., Kondratev, V., Kondratyeva, N., Kondratyuk, E., Konevskikh, A., Kopcik,
 734 M., Kostarakis, P., Kour, M., Kouzinopoulos, C., Kovalenko, O., Kovalenko, V., Kowalski,
 735 M., Koyithatta Meethalevedu, G., Kralik, I., Kravcakova, A., Krivda, M., Krizek, F.,
 736 Kryshen, E., Krzewicki, M., Kubera, A. M., Kucera, V., Kuhn, C. C., Kuijer, P. G.,
 737 Kumar, A., Kumar, J., Kumar, L., Kumar, S., Kurashvili, P., Kurepin, A., Kurepin, A.,
 738 Kuryakin, A., Kweon, M. J., Kwon, Y., La Pointe, S. L., La Rocca, P., Ladron De Guevara,
 739 P., Lagana Fernandes, C., Lakomov, I., Langoy, R., Lapidus, K., Lara Martinez, C. E.,
 740 Lardeux, A. X., Lattuca, A., Laudi, E., Lea, R., Leardini, L., Lee, G. R., Lee, S., Lehas, F.,
 741 Lemmon, R. C., Lenti, V., Leogrande, E., Leon Monzon, I., Leon Vargas, H., Leoncino, M.,
 742 Levai, P., Li, S., Li, X., Lien, J. A., Lietava, R., Lindal, S., Lindenstruth, V., Lippmann,
 743 C., Lisa, M. A., Ljunggren, H. M., Lodato, D. F., Lonne, P.-I., Loginov, V., Loizides, C.,
 744 Lopez, X. B., Lopez Torres, E., Lowe, A. J., Luettig, P. J., Lunardon, M., Luparello,
 745 G., Lutz, T. H., Maevskaya, A., Mager, M., Mahajan, S., Mahmood, S. M., Maire,
 746 A., Majka, R. D., Malaev, M., Maldonado Cervantes, I. A., Malinina, L., Mal'Kevich,
 747 D., Malzacher, P., Mamonov, A., Manko, V., Manso, F., Manzari, V., Marchisone, M.,
 748 Mares, J., Margagliotti, G. V., Margotti, A., Margutti, J., Marin, A. M., Markert, C.,
 749 Marquard, M., Martin, N. A., Martin Blanco, J., Martinengo, P., Martinez Hernandez,
 750 M. I., Martinez-Garcia, G., Martinez Pedreira, M., Mas, A. J.-M., Masciocchi, S., Masera,
 751 M., Masoni, A., Mastroserio, A., Matyja, A. T., Mayer, C., Mazer, J. A., Mazzoni,

752 A. M., Mcdonald, D., Meddi, F., Melikyan, Y., Menchaca-Rocha, A. A., Meninno, E.,
 753 Mercado-Perez, J., Meres, M., Miake, Y., Mieskolainen, M. M., Mikhaylov, K., Milano,
 754 L., Milosevic, J., Mischke, A., Mishra, A. N., Miskowiec, D. C., Mitra, J., Mitu, C. M.,
 755 Mohammadi, N., Mohanty, B., Molnar, L., Montano Zetina, L. M., Montes Prado, E.,
 756 Moreira De Godoy, D. A., Perez Moreno, L. A., Moretto, S., Morreale, A., Morsch, A.,
 757 Muccifora, V., Mudnic, E., Muhlheim, D. M., Muhuri, S., Mukherjee, M., Mulligan, J. D.,
 758 Gameiro Munhoz, M., Munzer, R. H., Murakami, H., Murray, S., Musa, L., Musinsky,
 759 J., Naik, B., Nair, R., Nandi, B. K., Nania, R., Nappi, E., Naru, M. U., Ferreira Natal
 760 Da Luz, P. H., Nattrass, C., Rosado Navarro, S., Nayak, K., Nayak, R., Nayak, T. K.,
 761 Nazarenko, S., Nedosekin, A., Nellen, L., Ng, F., Nicassio, M., Niculescu, M., Niedziela,
 762 J., Nielsen, B. S., Nikolaev, S., Nikulin, S., Nikulin, V., Noferini, F., Nomokonov, P.,
 763 Nooren, G., Cabanillas Noris, J. C., Norman, J., Nyanin, A., Nystrand, J. I., Oeschler,
 764 H. O., Oh, S., Oh, S. K., Ohlson, A. E., Okatan, A., Okubo, T., Olah, L., Oleniacz,
 765 J., Oliveira Da Silva, A. C., Oliver, M. H., Onderwaater, J., Oppedisano, C., Orava, R.,
 766 Oravec, M., Ortiz Velasquez, A., Oskarsson, A. N. E., Otwinowski, J. T., Oyama, K.,
 767 Ozdemir, M., Pachmayer, Y. C., Pagano, D., Pagano, P., Paic, G., Pal, S. K., Pan, J.,
 768 Pandey, A. K., Papikyan, V., Pappalardo, G., Pareek, P., Park, W., Parmar, S., Passfeld,
 769 A., Paticchio, V., Patra, R. N., Paul, B., Pei, H., Peitzmann, T., Pereira Da Costa, H.
 770 D. A., Peresunko, D. Y., Perez Lara, C. E., Perez Lezama, E., Peskov, V., Pestov, Y.,
 771 Petracek, V., Petrov, V., Petrovici, M., Petta, C., Piano, S., Pikna, M., Pillot, P., Ozelin
 772 De Lima Pimentel, L., Pinazza, O., Pinsky, L., Piyaathana, D., Ploskon, M. A., Planinic,
 773 M., Pluta, J. M., Pochybova, S., Podesta Lerma, P. L. M., Poghosyan, M., Polishchuk,
 774 B., Poljak, N., Poonsawat, W., Pop, A., Porteboeuf, S. J., Porter, R. J., Pospisil, J.,
 775 Prasad, S. K., Preghenella, R., Prino, F., Pruneau, C. A., Pshenichnov, I., Puccio, M.,
 776 Puddu, G., Pujahari, P. R., Punin, V., Putschke, J. H., Qvigstad, H., Rachevski, A., Raha,
 777 S., Rajput, S., Rak, J., Rakotozafindrabe, A. M., Ramello, L., Rami, F., Raniwala, R.,
 778 Raniwala, S., Rasanen, S. S., Rascanu, B. T., Rathee, D., Read, K. F., Redlich, K., Reed,
 779 R. J., Rehman, A. U., Reichelt, P. S., Reidt, F., Ren, X., Renfordt, R. A. E., Reolon, A. R.,
 780 Reshetin, A., Reygers, K. J., Riabov, V., Ricci, R. A., Richert, T. O. H., Richter, M. R.,
 781 Riedler, P., Riegler, W., Riggi, F., Ristea, C.-L., Rocco, E., Rodriguez Cahuantzi, M.,

782 Rodriguez Manso, A., Roeed, K., Rogochaya, E., Rohr, D. M., Roehrich, D., Ronchetti,
 783 F., Ronflette, L., Rosnet, P., Rossi, A., Roukoutakis, F., Roy, A., Roy, C. S., Roy, P. K.,
 784 Rubio Montero, A. J., Rui, R., Russo, R., Di Ruzza, B., Ryabinkin, E., Ryabov, Y.,
 785 Rybicki, A., Saarinen, S., Sadhu, S., Sadovskiy, S., Safarik, K., Sahlmuller, B., Sahoo, P.,
 786 Sahoo, R., Sahoo, S., Sahu, P. K., Saini, J., Sakai, S., Saleh, M. A., Salzwedel, J. S. N.,
 787 Sambyal, S. S., Samsonov, V., Sandor, L., Sandoval, A., Sano, M., Sarkar, D., Sarkar, N.,
 788 Sarma, P., Scapparone, E., Scarlassara, F., Schiaua, C. C., Schicker, R. M., Schmidt, C. J.,
 789 Schmidt, H. R., Schuchmann, S., Schukraft, J., Schulc, M., Schutz, Y. R., Schwarz, K. E.,
 790 Schweda, K. O., Scioli, G., Scomparin, E., Scott, R. M., Sefcik, M., Seger, J. E., Sekiguchi,
 791 Y., Sekihata, D., Selyuzhenkov, I., Senosi, K., Senyukov, S., Serradilla Rodriguez, E.,
 792 Sevcenco, A., Shabanov, A., Shabetai, A., Shadura, O., Shahoyan, R., Shahzad, M. I.,
 793 Shangaraev, A., Sharma, A., Sharma, M., Sharma, M., Sharma, N., Sheikh, A. I., Shigaki,
 794 K., Shou, Q., Shtejer Diaz, K., Sibiryak, Y., Siddhanta, S., Sielewicz, K. M., Siemiarczuk,
 795 T., Silvermyr, D. O. R., Silvestre, C. M., Simatovic, G., Simonetti, G., Singaraju, R. N.,
 796 Singh, R., Singha, S., Singhal, V., Sinha, B., Sarkar Sinha, T., Sitar, B., Sitta, M., Skaali,
 797 B., Slupecki, M., Smirnov, N., Snellings, R., Snellman, T. W., Song, J., Song, M., Song,
 798 Z., Soramel, F., Sorensen, S. P., Derradi De Souza, R., Sozzi, F., Spacek, M., Spiriti, E.,
 799 Sputowska, I. A., Spyropoulou-Stassinaki, M., Stachel, J., Stan, I., Stankus, P., Stenlund,
 800 E. A., Steyn, G. F., Stiller, J. H., Stocco, D., Strmen, P., Alarcon Do Passo Suaide, A.,
 801 Sugitate, T., Suire, C. P., Suleymanov, M. K. O., Suljic, M., Sultanov, R., Sumbera,
 802 M., Sumowidagdo, S., Szabo, A., Szanto De Toledo, A., Szarka, I., Szczepankiewicz, A.,
 803 Szymanski, M. P., Tabassam, U., Takahashi, J., Tambave, G. J., Tanaka, N., Tarhini,
 804 M., Tariq, M., Tarzila, M.-G., Tauro, A., Tejeda Munoz, G., Telesca, A., Terasaki, K.,
 805 Terrevoli, C., Teyssier, B., Thaeder, J. M., Thakur, D., Thomas, D., Tieulent, R. N.,
 806 Tikhonov, A., Timmins, A. R., Toia, A., Trogolo, S., Trombetta, G., Trubnikov, V.,
 807 Trzaska, W. H., Tsuji, T., Tumkin, A., Turrisi, R., Tveter, T. S., Ullaland, K., Uras, A.,
 808 Usai, G., Utrobicic, A., Vala, M., Valencia Palomo, L., Vallero, S., Van Der Maarel, J.,
 809 Van Hoorne, J. W., Van Leeuwen, M., Vanat, T., Vande Vyvre, P., Varga, D., Diozcora
 810 Vargas Trevino, A., Vargyas, M., Varma, R., Vasileiou, M., Vasiliev, A., Vauthier, A.,
 811 Vazquez Doce, O., Vechernin, V., Veen, A. M., Veldhoen, M., Velure, A., Vercellin, E.,

Vergara Limon, S., Vernet, R., Verweij, M., Vickovic, L., Viinikainen, J. S., Vilakazi, Z.,
Villalobos Baillie, O., Villatoro Tello, A., Vinogradov, A., Vinogradov, L., Vinogradov,
Y., Virgili, T., Vislavicius, V., Viyogi, Y., Vodopyanov, A., Volkl, M. A., Voloshin, K.,
Voloshin, S., Volpe, G., Von Haller, B., Vorobyev, I., Vranic, D., Vrlakova, J., Vulpescu,
B., Wagner, B., Wagner, J., Wang, H., Wang, M., Watanabe, D., Watanabe, Y., Weber,
M., Weber, S. G., Weiser, D. F., Wessels, J. P., Westerhoff, U., Whitehead, A. M.,
Wiechula, J., Wikne, J., Wilk, G. A., Wilkinson, J. J., Williams, C., Windelband, B. S.,
Winn, M. A., Yang, P., Yano, S., Yasin, Z., Yin, Z., Yokoyama, H., Yoo, I.-K., Yoon,
J. H., Yurchenko, V., Yushmanov, I., Zaborowska, A., Zaccolo, V., Zaman, A., Zampolli,
C., Correia Zanolli, H. J., Zaporozhets, S., Zardoshti, N., Zarochentsev, A., Zavada, P.,
Zavvalov, N., Zbroszczyk, H. P., Zgura, S. I., Zhalov, M., Zhang, H., Zhang, X., Zhang,
Y., Chunchui, Z., Zhang, Z., Zhao, C., Zhigareva, N., Zhou, D., Zhou, Y., Zhou, Z.,
Zhu, H., Zhu, J., Zichichi, A., Zimmermann, A., Zimmermann, M. B., Zinovjev, G., and
Zyzak, M. (2016). Measurement of transverse energy at midrapidity in Pb-Pb collisions at
 $\sqrt{s_{NN}} = 2.76$ TeV. *Phys. Rev. C*, 94(CERN-EP-2016-071. CERN-EP-2016-071):034903.
30 p. 30 pages, 14 captioned figures, 2 tables, authors from page 25, published version,
figures at <http://aliceinfo.cern.ch/ArtSubmission/node/2400>. 6, 15

[2] Adamczyk, L., Adkins, J. K., Agakishiev, G., Aggarwal, M. M., Ahammed, Z., Ajitanand,
N. N., Alekseev, I., Anderson, D. M., Aoyama, R., Aparin, A., Arkhipkin, D., Aschenauer,
E. C., Ashraf, M. U., Attri, A., Averichev, G. S., Bai, X., Bairathi, V., Behera, A.,
Bellwied, R., Bhasin, A., Bhati, A. K., Bhattarai, P., Bielcik, J., Bielcikova, J., Bland,
L. C., Bordyuzhin, I. G., Bouchet, J., Brandenburg, J. D., Brandin, A. V., Brown, D.,
Bunzarov, I., Butterworth, J., Caines, H., Calderón de la Barca Sánchez, M., Campbell,
J. M., Cebra, D., Chakaberia, I., Chaloupka, P., Chang, Z., Chankova-Bunzarova, N.,
Chatterjee, A., Chattopadhyay, S., Chen, X., Chen, J. H., Chen, X., Cheng, J., Cherney,
M., Christie, W., Contin, G., Crawford, H. J., Das, S., De Silva, L. C., Debbe, R. R.,
Dedovich, T. G., Deng, J., Derevschikov, A. A., Didenko, L., Dilks, C., Dong, X.,
Drachenberg, J. L., Draper, J. E., Dunkelberger, L. E., Dunlop, J. C., Efimov, L. G.,
Else, N., Engelage, J., Eppley, G., Esha, R., Esumi, S., Evdokimov, O., Ewigleben,

841 J., Eyser, O., Fatemi, R., Fazio, S., Federic, P., Federicova, P., Fedorisin, J., Feng, Z.,
 842 Filip, P., Finch, E., Fisyak, Y., Flores, C. E., Fulek, L., Gagliardi, C. A., Garand, D.,
 843 Geurts, F., Gibson, A., Girard, M., Grosnick, D., Gunarathne, D. S., Guo, Y., Gupta, A.,
 844 Gupta, S., Guryn, W., Hamad, A. I., Hamed, A., Harlenderova, A., Harris, J. W., He, L.,
 845 Heppelmann, S., Heppelmann, S., Hirsch, A., Hoffmann, G. W., Horvat, S., Huang, T.,
 846 Huang, B., Huang, X., Huang, H. Z., Humanic, T. J., Huo, P., Igo, G., Jacobs, W. W.,
 847 Jentsch, A., Jia, J., Jiang, K., Jowzaee, S., Judd, E. G., Kabana, S., Kalinkin, D., Kang,
 848 K., Kauder, K., Ke, H. W., Keane, D., Kechechyan, A., Khan, Z., Kikoła, D. P., Kisel,
 849 I., Kisiel, A., Kochenda, L., Kocmanek, M., Kollegger, T., Kosarzewski, L. K., Kraishan,
 850 A. F., Kravtsov, P., Krueger, K., Kulathunga, N., Kumar, L., Kvapil, J., Kwasizur, J. H.,
 851 Lacey, R., Landgraf, J. M., Landry, K. D., Lauret, J., Lebedev, A., Lednický, R., Lee,
 852 J. H., Li, X., Li, C., Li, W., Li, Y., Lidrych, J., Lin, T., Lisa, M. A., Liu, H., Liu,
 853 P., Liu, Y., Liu, F., Ljubicic, T., Llope, W. J., Lomnitz, M., Longacre, R. S., Luo, S.,
 854 Luo, X., Ma, G. L., Ma, L., Ma, Y. G., Ma, R., Magdy, N., Majka, R., Mallick, D.,
 855 Margetis, S., Markert, C., Matis, H. S., Meehan, K., Mei, J. C., Miller, Z. W., Minaev,
 856 N. G., Mioduszewski, S., Mishra, D., Mizuno, S., Mohanty, B., Mondal, M. M., Morozov,
 857 D. A., Mustafa, M. K., Nasim, M., Nayak, T. K., Nelson, J. M., Nie, M., Nigmatkulov,
 858 G., Niida, T., Nogach, L. V., Nonaka, T., Nurushev, S. B., Odyniec, G., Ogawa, A.,
 859 Oh, K., Okorokov, V. A., Olvitt, D., Page, B. S., Pak, R., Pandit, Y., Panebratsev, Y.,
 860 Pawlik, B., Pei, H., Perkins, C., Pile, P., Pluta, J., Poniatowska, K., Porter, J., Posik,
 861 M., Poskanzer, A. M., Pruthi, N. K., Przybycien, M., Putschke, J., Qiu, H., Quintero, A.,
 862 Ramachandran, S., Ray, R. L., Reed, R., Rehbein, M. J., Ritter, H. G., Roberts, J. B.,
 863 Rogachevskiy, O. V., Romero, J. L., Roth, J. D., Ruan, L., Rusnak, J., Rusnakova, O.,
 864 Sahoo, N. R., Sahu, P. K., Salur, S., Sandweiss, J., Saur, M., Schambach, J., Schmah,
 865 A. M., Schmidke, W. B., Schmitz, N., Schweid, B. R., Seger, J., Sergeeva, M., Seyboth, P.,
 866 Shah, N., Shahaliev, E., Shanmuganathan, P. V., Shao, M., Sharma, A., Sharma, M. K.,
 867 Shen, W. Q., Shi, Z., Shi, S. S., Shou, Q. Y., Sichtermann, E. P., Sikora, R., Simko,
 868 M., Singha, S., Skoby, M. J., Smirnov, N., Smirnov, D., Solyst, W., Song, L., Sorensen,
 869 P., Spinka, H. M., Srivastava, B., Stanislaus, T. D. S., Strikhanov, M., Stringfellow, B.,
 870 Sugiura, T., Sumbera, M., Summa, B., Sun, Y., Sun, X. M., Sun, X., Surrow, B., Svirida,

D. N., Tang, A. H., Tang, Z., Taranenko, A., Tarnowsky, T., Tawfik, A., Thäder, J., Thomas, J. H., Timmins, A. R., Tlusty, D., Todoroki, T., Tokarev, M., Trentalange, S., Tribble, R. E., Tribedy, P., Tripathy, S. K., Trzeciak, B. A., Tsai, O. D., Ullrich, T., Underwood, D. G., Upsal, I., Van Buren, G., van Nieuwenhuizen, G., Vasiliev, A. N., Videbæk, F., Vokal, S., Voloshin, S. A., Vossen, A., Wang, G., Wang, Y., Wang, F., Wang, Y., Webb, J. C., Webb, G., Wen, L., Westfall, G. D., Wieman, H., Wissink, S. W., Witt, R., Wu, Y., Xiao, Z. G., Xie, W., Xie, G., Xu, J., Xu, N., Xu, Q. H., Xu, Y. F., Xu, Z., Yang, Y., Yang, Q., Yang, C., Yang, S., Ye, Z., Ye, Z., Yi, L., Yip, K., Yoo, I.-K., Yu, N., Zbroszczyk, H., Zha, W., Zhang, Z., Zhang, X. P., Zhang, J. B., Zhang, S., Zhang, J., Zhang, Y., Zhang, J., Zhang, S., Zhao, J., Zhong, C., Zhou, L., Zhou, C., Zhu, X., Zhu, Z., and Zyzak, M. (2017). Bulk properties of the medium produced in relativistic heavy-ion collisions from the beam energy scan program. *Phys. Rev. C*, 96:044904. vii, 24, 28, 29

[3] Adare, A., Afanasiev, S., Aidala, C., Ajitanand, N. N., Akiba, Y., Akimoto, R., Al-Bataineh, H., Alexander, J., Alfred, M., Al-Jamel, A., Al-Ta'ani, H., Angerami, A., Aoki, K., Apadula, N., Aphecetche, L., Aramaki, Y., Armendariz, R., Aronson, S. H., Asai, J., Asano, H., Aschenauer, E. C., Atomssa, E. T., Auerbeck, R., Awes, T. C., Azmoun, B., Babintsev, V., Bai, M., Bai, X., Baksay, G., Baksay, L., Baldisseri, A., Bandara, N. S., Bannier, B., Barish, K. N., Barnes, P. D., Bassalleck, B., Basye, A. T., Bathe, S., Batsouli, S., Baublis, V., Bauer, F., Baumann, C., Baumgart, S., Bazilevsky, A., Beaumier, M., Beckman, S., Belikov, S., Belmont, R., Bennett, R., Berdnikov, A., Berdnikov, Y., Bhom, J. H., Bickley, A. A., Bjorndal, M. T., Black, D., Blau, D. S., Boissevain, J. G., Bok, J. S., Borel, H., Boyle, K., Brooks, M. L., Brown, D. S., Bryslawskyj, J., Bucher, D., Buesching, H., Bumazhnov, V., Bunce, G., Burward-Hoy, J. M., Butsyk, S., Campbell, S., Caringi, A., Castera, P., Chai, J.-S., Chang, B. S., Charvet, J.-L., Chen, C.-H., Chernichenko, S., Chi, C. Y., Chiba, J., Chiu, M., Choi, I. J., Choi, J. B., Choi, S., Choudhury, R. K., Christiansen, P., Chujo, T., Chung, P., Churn, A., Chvala, O., Cianciolo, V., Citron, Z., Cleven, C. R., Cobigo, Y., Cole, B. A., Comets, M. P., Conesa del Valle, Z., Connors, M., Constantin, P., Cronin, N., Crossette, N., Csanád, M., Csörgő, T., Dahms,

900 T., Dairaku, S., Danchev, I., Danley, T. W., Das, K., Datta, A., Daugherty, M. S.,
 901 David, G., Dayananda, M. K., Deaton, M. B., DeBlasio, K., Dehmelt, K., Delagrange,
 902 H., Denisov, A., d'Enterria, D., Deshpande, A., Desmond, E. J., Dharmawardane, K. V.,
 903 Dietzsch, O., Ding, L., Dion, A., Diss, P. B., Do, J. H., Donadelli, M., D'Orazio, L.,
 904 Drachenberg, J. L., Drapier, O., Drees, A., Drees, K. A., Dubey, A. K., Durham, J. M.,
 905 Durum, A., Dutta, D., Dzhordzhadze, V., Edwards, S., Efremenko, Y. V., Egdemir, J.,
 906 Ellinghaus, F., Emam, W. S., Engelmores, T., Enokizono, A., En'yo, H., Espagnon, B.,
 907 Esumi, S., Eyser, K. O., Fadem, B., Feege, N., Fields, D. E., Finger, M., Finger, M.,
 908 Fleuret, F., Fokin, S. L., Forestier, B., Fraenkel, Z., Frantz, J. E., Franz, A., Frawley,
 909 A. D., Fujiwara, K., Fukao, Y., Fung, S.-Y., Fusayasu, T., Gadrat, S., Gainey, K., Gal,
 910 C., Gallus, P., Garg, P., Garishvili, A., Garishvili, I., Gastineau, F., Ge, H., Germain, M.,
 911 Giordano, F., Glenn, A., Gong, H., Gong, X., Gonin, M., Gosset, J., Goto, Y., Granier de
 912 Cassagnac, R., Grau, N., Greene, S. V., Grim, G., Grosse Perdekamp, M., Gu, Y., Gunji,
 913 T., Guo, L., Guragain, H., Gustafsson, H.-A., Hachiya, T., Hadj Henni, A., Haegemann,
 914 C., Haggerty, J. S., Hagiwara, M. N., Hahn, K. I., Hamagaki, H., Hamblen, J., Hamilton,
 915 H. F., Han, R., Han, S. Y., Hanks, J., Harada, H., Hartouni, E. P., Haruna, K., Harvey,
 916 M., Hasegawa, S., Haseler, T. O. S., Hashimoto, K., Haslum, E., Hasuko, K., Hayano, R.,
 917 Hayashi, S., He, X., Heffner, M., Hemmick, T. K., Hester, T., Heuser, J. M., Hiejima, H.,
 918 Hill, J. C., Hobbs, R., Hohlmann, M., Hollis, R. S., Holmes, M., Holzmann, W., Homma,
 919 K., Hong, B., Horaguchi, T., Hori, Y., Hornback, D., Hoshino, T., Hotvedt, N., Huang, J.,
 920 Huang, S., Hur, M. G., Ichihara, T., Ichimiya, R., Iinuma, H., Ikeda, Y., Imai, K., Imazu,
 921 Y., Imrek, J., Inaba, M., Inoue, Y., Iordanova, A., Isenhowe, D., Isenhowe, L., Ishihara,
 922 M., Isinhue, A., Isobe, T., Issah, M., Isupov, A., Ivanishchev, D., Iwanaga, Y., Jacak,
 923 B. V., Javani, M., Jeon, S. J., Jezghani, M., Jia, J., Jiang, X., Jin, J., Jinnouchi, O.,
 924 Johnson, B. M., Jones, T., Joo, K. S., Jouan, D., Jumper, D. S., Kajihara, F., Kametani,
 925 S., Kamihara, N., Kamin, J., Kanda, S., Kaneta, M., Kaneti, S., Kang, B. H., Kang, J. H.,
 926 Kang, J. S., Kanou, H., Kapustinsky, J., Karatsu, K., Kasai, M., Kawagishi, T., Kawall,
 927 D., Kawashima, M., Kazantsev, A. V., Kelly, S., Kempel, T., Key, J. A., Khachatryan, V.,
 928 Khandai, P. K., Khanzadeev, A., Kijima, K. M., Kikuchi, J., Kim, A., Kim, B. I., Kim, C.,
 929 Kim, D. H., Kim, D. J., Kim, E., Kim, E.-J., Kim, G. W., Kim, H. J., Kim, K.-B., Kim,

930 M., Kim, Y.-J., Kim, Y. K., Kim, Y.-S., Kimelman, B., Kinney, E., Kiss, A., Kistenev, E.,
 931 Kitamura, R., Kiyomichi, A., Klatsky, J., Klay, J., Klein-Boeing, C., Kleinjan, D., Kline,
 932 P., Koblesky, T., Kochenda, L., Kochetkov, V., Kofarago, M., Komatsu, Y., Komkov,
 933 B., Konno, M., Koster, J., Kotchetkov, D., Kotov, D., Kozlov, A., Král, A., Kravitz, A.,
 934 Krizek, F., Kroon, P. J., Kubart, J., Kunde, G. J., Kurihara, N., Kurita, K., Kurosawa,
 935 M., Kweon, M. J., Kwon, Y., Kyle, G. S., Lacey, R., Lai, Y. S., Lajoie, J. G., Lebedev,
 936 A., Le Bornec, Y., Leckey, S., Lee, B., Lee, D. M., Lee, G. H., Lee, J., Lee, K. B.,
 937 Lee, K. S., Lee, M. K., Lee, S., Lee, S. H., Lee, S. R., Lee, T., Leitch, M. J., Leite, M.
 938 A. L., Leitgab, M., Lenzi, B., Lewis, B., Li, X., Li, X. H., Lichtenwalner, P., Liebing, P.,
 939 Lim, H., Lim, S. H., Linden Levy, L. A., Liška, T., Litvinenko, A., Liu, H., Liu, M. X.,
 940 Love, B., Lynch, D., Maguire, C. F., Makdisi, Y. I., Makek, M., Malakhov, A., Malik,
 941 M. D., Manion, A., Manko, V. I., Mannel, E., Mao, Y., Maruyama, T., Mašek, L., Masui,
 942 H., Masumoto, S., Matathias, F., McCain, M. C., McCumber, M., McGaughey, P. L.,
 943 McGlinchey, D., McKinney, C., Means, N., Meles, A., Mendoza, M., Meredith, B., Miake,
 944 Y., Mibe, T., Midori, J., Mignerey, A. C., Mikeš, P., Miki, K., Miller, T. E., Milov, A.,
 945 Mioduszewski, S., Mishra, D. K., Mishra, G. C., Mishra, M., Mitchell, J. T., Mitrovski,
 946 M., Miyachi, Y., Miyasaka, S., Mizuno, S., Mohanty, A. K., Mohapatra, S., Montuenga,
 947 P., Moon, H. J., Moon, T., Morino, Y., Morreale, A., Morrison, D. P., Moskowitz, M.,
 948 Moss, J. M., Motschwiller, S., Moukhanova, T. V., Mukhopadhyay, D., Murakami, T.,
 949 Murata, J., Mwai, A., Nagae, T., Nagamiya, S., Nagashima, K., Nagata, Y., Nagle, J. L.,
 950 Naglis, M., Nagy, M. I., Nakagawa, I., Nakagomi, H., Nakamiya, Y., Nakamura, K. R.,
 951 Nakamura, T., Nakano, K., Nam, S., Natrass, C., Nederlof, A., Netrakanti, P. K., Newby,
 952 J., Nguyen, M., Nihashi, M., Niida, T., Nishimura, S., Norman, B. E., Nouicer, R., Novák,
 953 T., Novitzky, N., Nukariya, A., Nyanin, A. S., Nystrand, J., Oakley, C., Obayashi, H.,
 954 O'Brien, E., Oda, S. X., Ogilvie, C. A., Ohnishi, H., Oide, H., Ojha, I. D., Oka, M.,
 955 Okada, K., Omiwade, O. O., Onuki, Y., Orjuela Koop, J. D., Osborn, J. D., Oskarsson,
 956 A., Otterlund, I., Ouchida, M., Ozawa, K., Pak, R., Pal, D., Palounek, A. P. T., Pantuev,
 957 V., Papavassiliou, V., Park, B. H., Park, I. H., Park, J., Park, J. S., Park, S., Park, S. K.,
 958 Park, W. J., Pate, S. F., Patel, L., Patel, M., Pei, H., Peng, J.-C., Pereira, H., Perepelitsa,
 959 D. V., Perera, G. D. N., Peresedov, V., Peressounko, D., Perry, J., Petti, R., Pinkenburg,

960 C., Pinson, R., Pisani, R. P., Proissl, M., Purschke, M. L., Purwar, A. K., Qu, H., Rak,
 961 J., Rakotozafindrabe, A., Ramson, B. J., Ravinovich, I., Read, K. F., Rembeczki, S.,
 962 Reuter, M., Reygers, K., Reynolds, D., Riabov, V., Riabov, Y., Richardson, E., Rinn, T.,
 963 Riveli, N., Roach, D., Roche, G., Rolnick, S. D., Romana, A., Rosati, M., Rosen, C. A.,
 964 Rosendahl, S. S. E., Rosnet, P., Rowan, Z., Rubin, J. G., Rukoyatkin, P., Ružička, P.,
 965 Rykov, V. L., Ryu, M. S., Ryu, S. S., Sahlmueller, B., Saito, N., Sakaguchi, T., Sakai, S.,
 966 Sakashita, K., Sakata, H., Sako, H., Samsonov, V., Sano, M., Sano, S., Sarsour, M., Sato,
 967 H. D., Sato, S., Sato, T., Sawada, S., Schaefer, B., Schmoll, B. K., Sedgwick, K., Seele,
 968 J., Seidl, R., Sekiguchi, Y., Semenov, V., Sen, A., Seto, R., Sett, P., Sexton, A., Sharma,
 969 D., Shaver, A., Shea, T. K., Shein, I., Shevel, A., Shibata, T.-A., Shigaki, K., Shimomura,
 970 M., Shohjoh, T., Shoji, K., Shukla, P., Sickles, A., Silva, C. L., Silvermyr, D., Silvestre,
 971 C., Sim, K. S., Singh, B. K., Singh, C. P., Singh, V., Skolnik, M., Skutnik, S., Slunečka,
 972 M., Smith, W. C., Snowball, M., Solano, S., Soldatov, A., Soltz, R. A., Sondheim, W. E.,
 973 Sorensen, S. P., Sourikova, I. V., Staley, F., Stankus, P. W., Steinberg, P., Stenlund, E.,
 974 Stepanov, M., Ster, A., Stoll, S. P., Stone, M. R., Sugitate, T., Suire, C., Sukhanov, A.,
 975 Sullivan, J. P., Sumita, T., Sun, J., Sziklai, J., Tabaru, T., Takagi, S., Takagui, E. M.,
 976 Takahara, A., Taketani, A., Tanabe, R., Tanaka, K. H., Tanaka, Y., Taneja, S., Tanida, K.,
 977 Tannenbaum, M. J., Tarafdar, S., Taranenko, A., Tarján, P., Tennant, E., Themann, H.,
 978 Thomas, D., Thomas, T. L., Tieulent, R., Timilsina, A., Todoroki, T., Togawa, M., Toia,
 979 A., Tojo, J., Tomášek, L., Tomášek, M., Torii, H., Towell, C. L., Towell, R., Towell, R. S.,
 980 Tram, V.-N., Tserruya, I., Tsuchimoto, Y., Tsuji, T., Tuli, S. K., Tydesjö, H., Tyurin,
 981 N., Vale, C., Valle, H., van Hecke, H. W., Vargyas, M., Vazquez-Zambrano, E., Veicht,
 982 A., Velkovska, J., Vértési, R., Vinogradov, A. A., Virius, M., Voas, B., Vossen, A., Vrba,
 983 V., Vznuzdaev, E., Wagner, M., Walker, D., Wang, X. R., Watanabe, D., Watanabe, K.,
 984 Watanabe, Y., Watanabe, Y. S., Wei, F., Wei, R., Wessels, J., Whitaker, S., White, A. S.,
 985 White, S. N., Willis, N., Winter, D., Wolin, S., Woody, C. L., Wright, R. M., Wysocki, M.,
 986 Xia, B., Xie, W., Xue, L., Yalcin, S., Yamaguchi, Y. L., Yamaura, K., Yang, R., Yanovich,
 987 A., Yasin, Z., Ying, J., Yokkaichi, S., Yoo, J. H., Yoon, I., You, Z., Young, G. R., Younus,
 988 I., Yu, H., Yushmanov, I. E., Zajc, W. A., Zaudtke, O., Zelenski, A., Zhang, C., Zhou, S.,

Zimanyi, J., Zolin, L., and Zou, L. (2016). Transverse energy production and charged-particle multiplicity at midrapidity in various systems from $\sqrt{s_{NN}} = 7.7$ to 200 gev. *Phys. Rev. C*, 93:024901. vii, viii, 5, 23, 34, 38, 40

[4] Adare, A., Afanasiev, S., Aidala, C., Ajitanand, N. N., Akiba, Y., Al-Bataineh, H., Alexander, J., Al-Jamel, A., Aoki, K., Aphecetche, L., and et al. (2007). Scaling Properties of Azimuthal Anisotropy in Au+Au and Cu+Cu Collisions at $s_{NN}=200\text{GeV}$. *Physical Review Letters*, 98(16):162301. vi, 16, 17

[5] Adler, S. S., Afanasiev, S., Aidala, C., Ajitanand, N. N., Akiba, Y., Al-Jamel, A., Alexander, J., Aoki, K., Aphecetche, L., Armendariz, R., Aronson, S. H., Auerbeck, R., Awes, T. C., Azmoun, B., Babintsev, V., Baldisseri, A., Barish, K. N., Barnes, P. D., Bassalleck, B., Bathe, S., Batsouli, S., Baublis, V., Bauer, F., Bazilevsky, A., Belikov, S., Bennett, R., Berdnikov, Y., Bjorndal, M. T., Boissevain, J. G., Borel, H., Boyle, K., Brooks, M. L., Brown, D. S., Bruner, N., Bucher, D., Buesching, H., Bumazhnov, V., Bunce, G., Burward-Hoy, J. M., Butsyk, S., Camard, X., Campbell, S., Chai, J.-S., Chand, P., Chang, W. C., Chernichenko, S., Chi, C. Y., Chiba, J., Chiu, M., Choi, I. J., Choudhury, R. K., Chujo, T., Cianciolo, V., Cleven, C. R., Cobigo, Y., Cole, B. A., Comets, M. P., Constantin, P., Csanád, M., Csörgő, T., Cussonneau, J. P., Dahms, T., Das, K., David, G., Deák, F., Delagrange, H., Denisov, A., d'Enterria, D., Deshpande, A., Desmond, E. J., Devismes, A., Dietzsch, O., Dion, A., Drachenberg, J. L., Drapier, O., Drees, A., Dubey, A. K., Durum, A., Dutta, D., Dzhordzhadze, V., Efremenko, Y. V., Egdemir, J., Enokizono, A., En'yo, H., Espagnon, B., Esumi, S., Fields, D. E., Finck, C., Fleuret, F., Fokin, S. L., Forestier, B., Fox, B. D., Fraenkel, Z., Frantz, J. E., Franz, A., Frawley, A. D., Fukao, Y., Fung, S.-Y., Gadrat, S., Gastineau, F., Germain, M., Glenn, A., Gonin, M., Gosset, J., Goto, Y., Granier de Cassagnac, R., Grau, N., Greene, S. V., Grosse Perdekamp, M., Gunji, T., Gustafsson, H.-A., Hachiya, T., Hadj Henni, A., Haggerty, J. S., Hagiwara, M. N., Hamagaki, H., Hansen, A. G., Harada, H., Hartouni, E. P., Haruna, K., Harvey, M., Haslum, E., Hasuko, K., Hayano, R., He, X., Heffner, M., Hemmick, T. K., Heuser, J. M., Hidas, P., Hiejima, H., Hill, J. C., Hobbs, R., Holmes, M., Holzmann, W., Homma, K., Hong, B., Hoover, A., Horaguchi, T., Hur, M. G., Ichihara, T.,

1018 Iinuma, H., Ikonnikov, V. V., Imai, K., Inaba, M., Inuzuka, M., Isenhowe, D., Isenhowe,
 1019 L., Ishihara, M., Isobe, T., Issah, M., Isupov, A., Jacak, B. V., Jia, J., Jin, J., Jinnouchi,
 1020 O., Johnson, B. M., Johnson, S. C., Joo, K. S., Jouan, D., Kajihara, F., Kametani,
 1021 S., Kamihara, N., Kaneta, M., Kang, J. H., Katou, K., Kawabata, T., Kawagishi, T.,
 1022 Kazantsev, A. V., Kelly, S., Khachaturov, B., Khanzadeev, A., Kikuchi, J., Kim, D. J.,
 1023 Kim, E., Kim, E. J., Kim, G.-B., Kim, H. J., Kim, Y.-S., Kinney, E., Kiss, A., Kistenev, E.,
 1024 Kiyomichi, A., Klein-Boesing, C., Kobayashi, H., Kochenda, L., Kochetkov, V., Kohara,
 1025 R., Komkov, B., Konno, M., Kotchetkov, D., Kozlov, A., Kroon, P. J., Kuberg, C. H.,
 1026 Kunde, G. J., Kurihara, N., Kurita, K., Kweon, M. J., Kwon, Y., Kyle, G. S., Lacey, R.,
 1027 Lajoie, J. G., Lebedev, A., Le Bornec, Y., Leckey, S., Lee, D. M., Lee, M. K., Leitch,
 1028 M. J., Leite, M. A. L., Li, X. H., Lim, H., Litvinenko, A., Liu, M. X., Maguire, C. F.,
 1029 Makdisi, Y. I., Malakhov, A., Malik, M. D., Manko, V. I., Mao, Y., Martinez, G., Masui,
 1030 H., Matathias, F., Matsumoto, T., McCain, M. C., McGaughey, P. L., Miake, Y., Miller,
 1031 T. E., Milov, A., Mioduszewski, S., Mishra, G. C., Mitchell, J. T., Mohanty, A. K.,
 1032 Morrison, D. P., Moss, J. M., Moukhanova, T. V., Mukhopadhyay, D., Muniruzzaman,
 1033 M., Murata, J., Nagamiya, S., Nagata, Y., Nagle, J. L., Naglis, M., Nakamura, T., Newby,
 1034 J., Nguyen, M., Norman, B. E., Nyanin, A. S., Nystrand, J., O'Brien, E., Ogilvie, C. A.,
 1035 Ohnishi, H., Ojha, I. D., Okada, K., Omiwade, O. O., Oskarsson, A., Otterlund, I., Oyama,
 1036 K., Ozawa, K., Pal, D., Palounek, A. P. T., Pantuev, V., Papavassiliou, V., Park, J., Park,
 1037 W. J., Pate, S. F., Pei, H., Penev, V., Peng, J.-C., Pereira, H., Peresedov, V., Peressounko,
 1038 D., Pierson, A., Pinkenburg, C., Pisani, R. P., Purschke, M. L., Purwar, A. K., Qu, H.,
 1039 Qualls, J. M., Rak, J., Ravinovich, I., Read, K. F., Reuter, M., Reygers, K., Riabov,
 1040 V., Riabov, Y., Roche, G., Romana, A., Rosati, M., Rosendahl, S. S. E., Rosnet, P.,
 1041 Rukoyatkin, P., Rykov, V. L., Ryu, S. S., Sahlmueller, B., Saito, N., Sakaguchi, T., Sakai,
 1042 S., Samsonov, V., Sanfratello, L., Santo, R., Sarsour, M., Sato, H. D., Sato, S., Sawada,
 1043 S., Schutz, Y., Semenov, V., Seto, R., Sharma, D., Shea, T. K., Shein, I., Shibata, T.-A.,
 1044 Shigaki, K., Shimomura, M., Shohjoh, T., Shoji, K., Sickles, A., Silva, C. L., Silvermyr, D.,
 1045 Sim, K. S., Singh, C. P., Singh, V., Skutnik, S., Smith, W. C., Soldatov, A., Soltz, R. A.,
 1046 Sondheim, W. E., Sorensen, S. P., Sourikova, I. V., Staley, F., Stankus, P. W., Stenlund,
 1047 E., Stepanov, M., Ster, A., Stoll, S. P., Sugitate, T., Suire, C., Sullivan, J. P., Sziklai, J.,

Tabaru, T., Takagi, S., Takagui, E. M., Taketani, A., Tanaka, K. H., Tanaka, Y., Tanida, K., Tannenbaum, M. J., Taranenko, A., Tarján, P., Thomas, T. L., Togawa, M., Tojo, J., Torii, H., Towell, R. S., Tram, V.-N., Tserruya, I., Tsuchimoto, Y., Tuli, S. K., Tydesjö, H., Tyurin, N., Uam, T. J., Vale, C., Valle, H., van Hecke, H. W., Velkovska, J., Velkovsky, M., Vértesi, R., Veszprémi, V., Vinogradov, A. A., Volkov, M. A., Vznuzdaev, E., Wagner, M., Wang, X. R., Watanabe, Y., Wessels, J., White, S. N., Willis, N., Winter, D., Wohn, F. K., Woody, C. L., Wysocki, M., Xie, W., Yanovich, A., Yokkaichi, S., Young, G. R., Younus, I., Yushmanov, I. E., Zajc, W. A., Zaudtke, O., Zhang, C., Zhou, S., Zimányi, J., Zolin, L., and Zong, X. (2014). Transverse-energy distributions at midrapidity in $p + p$, $d + \text{Au}$, and $\text{Au} + \text{Au}$ collisions at $\sqrt{s_{\text{NN}}} = 62.4 \sim 200$ gev and implications for particle-production models. *Phys. Rev. C*, 89:044905. 21

[6] Adler, S. S., Afanasiev, S., Aidala, C., Ajitanand, N. N., Akiba, Y., Alexander, J., Amirikas, R., Aphecetche, L., Aronson, S. H., Auerbeck, R., Awes, T. C., Azmoun, R., Babintsev, V., Baldissieri, A., Barish, K. N., Barnes, P. D., Bassalleck, B., Bathe, S., Batsouli, S., Baublis, V., Bazilevsky, A., Belikov, S., Berdnikov, Y., Bhagavatula, S., Boissevain, J. G., Borel, H., Borenstein, S., Brooks, M. L., Brown, D. S., Bruner, N., Bucher, D., Buesching, H., Bumazhnov, V., Bunce, G., Burward-Hoy, J. M., Butsyk, S., Camard, X., Chai, J.-S., Chand, P., Chang, W. C., Chernichenko, S., Chi, C. Y., Chiba, J., Chiu, M., Choi, I. J., Choi, J., Choudhury, R. K., Chujo, T., Cianciolo, V., Cobigo, Y., Cole, B. A., Constantin, P., d’Enterria, D. G., David, G., Delagrange, H., Denisov, A., Deshpande, A., Desmond, E. J., Dietzsch, O., Drapier, O., Drees, A., Rietz, R. d., Durum, A., Dutta, D., Efremenko, Y. V., Chenawi, K. E., Enokizono, A., En’yo, H., Esumi, S., Ewell, L., Fields, D. E., Fleuret, F., Fokin, S. L., Fox, B. D., Fraenkel, Z., Frantz, J. E., Franz, A., Frawley, A. D., Fung, S.-Y., Garpman, S., Ghosh, T. K., Glenn, A., Gogiberidze, G., Gonin, M., Gosset, J., Goto, Y., Cassagnac, R. G. d., Grau, N., Greene, S. V., Perdekamp, M. G., Guryn, W., Gustafsson, H.-A., Hachiya, T., Haggerty, J. S., Hamagaki, H., Hansen, A. G., Hartouni, E. P., Harvey, M., Hayano, R., He, X., Heffner, M., Hemmick, T. K., Heuser, J. M., Hibino, M., Hill, J. C., Holzmann, W., Homma, K., Hong, B., Hoover, A., Ichihara, T., Ikonnikov, V. V., Imai, K., Isenhower, D., Ishihara,

1077 M., Issah, M., Isupov, A., Jacak, B. V., Jang, W. Y., Jeong, Y., Jia, J., Jinnouchi, O.,
 1078 Johnson, B. M., Johnson, S. C., Joo, K. S., Jouan, D., Kametani, S., Kamihara, N.,
 1079 Kang, J. H., Kapoor, S. S., Katou, K., Kelly, S., Khachaturov, B., Khanzadeev, A.,
 1080 Kikuchi, J., Kim, D. H., Kim, D. J., Kim, D. W., Kim, E., Kim, G.-B., Kim, H. J.,
 1081 Kistenev, E., Kiyomichi, A., Kiyoyama, K., Klein-Boesing, C., Kobayashi, H., Kochenda,
 1082 L., Kochetkov, V., Koehler, D., Kohama, T., Kopytine, M., Kotchetkov, D., Kozlov, A.,
 1083 Kroon, P. J., Kuberg, C. H., Kurita, K., Kuroki, Y., Kweon, M. J., Kwon, Y., Kyle,
 1084 G. S., Lacey, R., Ladygin, V., Lajoie, J. G., Lebedev, A., Leckey, S., Lee, D. M., Lee, S.,
 1085 Leitch, M. J., Li, X. H., Lim, H., Litvinenko, A., Liu, M. X., Liu, Y., Maguire, C. F.,
 1086 Makdisi, Y. I., Malakhov, A., Manko, V. I., Mao, Y., Martinez, G., Marx, M. D., Masui,
 1087 H., Matathias, F., Matsumoto, T., McGaughey, P. L., Melnikov, E., Mendenhall, M.,
 1088 Messer, F., Miake, Y., Milan, J., Miller, T. E., Milov, A., Mioduszewski, S., Mischke,
 1089 R. E., Mishra, G. C., Mitchell, J. T., Mohanty, A. K., Morrison, D. P., Moss, J. M.,
 1090 Mühlbacher, F., Mukhopadhyay, D., Muniruzzaman, M., Murata, J., Nagamiya, S., Nagle,
 1091 J. L., Nakamura, T., Nandi, B. K., Nara, M., Newby, J., Nilsson, P., Nyanin, A. S.,
 1092 Nystrand, J., O'Brien, E., Ogilvie, C. A., Ohnishi, H., Ojha, I. D., Okada, K., Ono, M.,
 1093 Onuchin, V., Oskarsson, A., Otterlund, I., Oyama, K., Ozawa, K., Pal, D., Palounek, A.
 1094 P. T., Pantuev, V. S., Papavassiliou, V., Park, J., Parmar, A., Pate, S. F., Peitzmann,
 1095 T., Peng, J.-C., Peresedov, V., Pinkenburg, C., Pisani, R. P., Plasil, F., Purschke, M. L.,
 1096 Purwar, A. K., Rak, J., Ravinovich, I., Read, K. F., Reuter, M., Reygers, K., Riabov, V.,
 1097 Riabov, Y., Roche, G., Romana, A., Rosati, M., Rosnet, P., Ryu, S. S., Sadler, M. E.,
 1098 Saito, N., Sakaguchi, T., Sakai, M., Sakai, S., Samsonov, V., Sanfratello, L., Santo, R.,
 1099 Sato, H. D., Sato, S., Sawada, S., Schutz, Y., Semenov, V., Seto, R., Shaw, M. R., Shea,
 1100 T. K., Shibata, T.-A., Shigaki, K., Shiina, T., Silva, C. L., Silvermyr, D., Sim, K. S., Singh,
 1101 C. P., Singh, V., Sivertz, M., Soldatov, A., Soltz, R. A., Sondheim, W. E., Sorensen, S. P.,
 1102 Sourikova, I. V., Staley, F., Stankus, P. W., Stenlund, E., Stepanov, M., Ster, A., Stoll,
 1103 S. P., Sugitate, T., Sullivan, J. P., Takagui, E. M., Taketani, A., Tamai, M., Tanaka, K. H.,
 1104 Tanaka, Y., Tanida, K., Tannenbaum, M. J., Tarján, P., Tepe, J. D., Thomas, T. L., Tojo,
 1105 J., Torii, H., Towell, R. S., Tserruya, I., Tsuruoka, H., Tuli, S. K., Tydesjö, H., Tyurin,
 1106 N., Hecke, H. W. v., Velkovska, J., Velkovsky, M., Villatte, L., Vinogradov, A. A., Volkov,

- 1107 M. A., Vznuzdaev, E., Wang, X. R., Watanabe, Y., White, S. N., Wohn, F. K., Woody,
1108 C. L., Xie, W., Yang, Y., Yanovich, A., Yokkaichi, S., Young, G. R., Yushmanov, I. E.,
1109 Zajc, W. A., Zhang, C., Zhou, S., Zhou, S. J., and Zolin, L. (2005). Systematic studies of
1110 the centrality and $\sqrt{s_{NN}}$ dependence of the $de_T/d\eta$ and $dn_{ch}/d\eta$ in heavy ion collisions at
1111 midrapidity. *Phys. Rev. C*, 71:034908. 22
- 1112 [7] Aitchison, I. and Hey, A. (2003). *Gauge Theories in Particle Physics, Volume II: QCD*
1113 *and the Electroweak Theory, Third Edition*. Graduate Student Series in Physics. CRC
1114 Press. 3
- 1115 [8] Anderson, M. et al. (2003). The Star time projection chamber: A Unique tool for studying
1116 high multiplicity events at RHIC. *Nucl. Instrum. Meth.*, A499:659–678. 26
- 1117 [9] Ayala, A. (2016). Hadronic matter at the edge: A survey of some theoretical approaches
1118 to the physics of the qcd phase diagram. *Journal of Physics: Conference Series*,
1119 761(1):012066. vi, 5, 6
- 1120 [10] Bethe, H. A. and Ashkin, J. (1953). Passage of radiations through matter experimental
1121 nuclear physics vol 1 ed e segre. 24
- 1122 [11] Bjorken, J. D. (1983). Highly relativistic nucleus-nucleus collisions: The central rapidity
1123 region. *Phys. Rev. D*, 27:140–151. 15
- 1124 [12] Chatrchyan, S., Khachatryan, V., Sirunyan, A. M., Tumasyan, A., Adam, W., Bergauer,
1125 T., Dragicevic, M., Erö, J., Fabjan, C., Friedl, M., Frühwirth, R., Ghete, V. M., Hammer,
1126 J., Hörmann, N., Hrubec, J., Jeitler, M., Kiesenhofer, W., Knünz, V., Krammer, M., Liko,
1127 D., Mikulec, I., Pernicka, M., Rahbaran, B., Rohringer, C., Rohringer, H., Schöfbeck, R.,
1128 Strauss, J., Taurok, A., Wagner, P., Waltenberger, W., Walzel, G., Widl, E., Wulz, C.-E.,
1129 Mossolov, V., Shumeiko, N., Suarez Gonzalez, J., Bansal, S., Cornelis, T., De Wolf, E. A.,
1130 Janssen, X., Luyckx, S., Maes, T., Mucibello, L., Ochsanu, S., Roland, B., Rougny,
1131 R., Selvaggi, M., Staykova, Z., Van Haevermaet, H., Van Mechelen, P., Van Remortel,
1132 N., Van Spilbeeck, A., Blekman, F., Blyweert, S., D’Hondt, J., Gonzalez Suarez, R.,
1133 Kalogeropoulos, A., Maes, M., Olbrechts, A., Van Doninck, W., Van Mulders, P.,

1134 Van Onsem, G. P., Villella, I., Clerbaux, B., De Lentdecker, G., Dero, V., Gay, A. P. R.,
 1135 Hreus, T., Léonard, A., Marage, P. E., Reis, T., Thomas, L., Vander Velde, C., Vanlaer, P.,
 1136 Wang, J., Adler, V., Beernaert, K., Cimmino, A., Costantini, S., Garcia, G., Grunewald,
 1137 M., Klein, B., Lellouch, J., Marinov, A., McCartin, J., Ocampo Rios, A. A., Ryckbosch, D.,
 1138 Strobbe, N., Thyssen, F., Tytgat, M., Verwilligen, P., Walsh, S., Yazgan, E., Zaganidis,
 1139 N., Basegmez, S., Bruno, G., Castello, R., Ceard, L., Delaere, C., du Pree, T., Favart, D.,
 1140 Forthomme, L., Giammanco, A., Hollar, J., Lemaitre, V., Liao, J., Militaru, O., Nuttens,
 1141 C., Pagano, D., Pin, A., Piotrkowski, K., Schul, N., Vizan Garcia, J. M., Beliy, N.,
 1142 Caeberts, T., Daubie, E., Hammad, G. H., Alves, G. A., Correa Martins Junior, M.,
 1143 De Jesus Damiao, D., Martins, T., Pol, M. E., Souza, M. H. G., Aldá Júnior, W. L.,
 1144 Carvalho, W., Custódio, A., Da Costa, E. M., De Oliveira Martins, C., Fonseca De Souza,
 1145 S., Matos Figueiredo, D., Mundim, L., Nogima, H., Oguri, V., Prado Da Silva, W. L.,
 1146 Santoro, A., Soares Jorge, L., Sznajder, A., Bernardes, C. A., Dias, F. A., Fernandez
 1147 Perez Tomei, T. R., Gregores, E. M., Lagana, C., Marinho, F., Mercadante, P. G., Novaes,
 1148 S. F., Padula, S. S., Genchev, V., Iaydjiev, P., Piperov, S., Rodozov, M., Stoykova, S.,
 1149 Sultanov, G., Tcholakov, V., Trayanov, R., Vutova, M., Dimitrov, A., Hadjiiska, R.,
 1150 Kozhuharov, V., Litov, L., Pavlov, B., Petkov, P., Bian, J. G., Chen, G. M., Chen, H. S.,
 1151 Jiang, C. H., Liang, D., Liang, S., Meng, X., Tao, J., Wang, J., Wang, X., Wang, Z.,
 1152 Xiao, H., Xu, M., Zang, J., Zhang, Z., Asawatangtrakuldee, C., Ban, Y., Guo, S., Guo,
 1153 Y., Li, W., Liu, S., Mao, Y., Qian, S. J., Teng, H., Wang, S., Zhu, B., Zou, W., Avila,
 1154 C., Gomez, J. P., Gomez Moreno, B., Osorio Oliveros, A. F., Sanabria, J. C., Godinovic,
 1155 N., Lelas, D., Plestina, R., Polic, D., Puljak, I., Antunovic, Z., Kovac, M., Brigljevic, V.,
 1156 Duric, S., Kadija, K., Luetic, J., Morovic, S., Attikis, A., Galanti, M., Mavromanolakis,
 1157 G., Mousa, J., Nicolaou, C., Ptochos, F., Razis, P. A., Finger, M., Finger, M., Assran,
 1158 Y., Elgammal, S., Ellithi Kamel, A., Khalil, S., Mahmoud, M. A., Radi, A., Kadastik,
 1159 M., Müntel, M., Raidal, M., Rebane, L., Tiko, A., Azzolini, V., Eerola, P., Fedi, G.,
 1160 Voutilainen, M., Härkönen, J., Heikkinen, A., Karimäki, V., Kinnunen, R., Kortelainen,
 1161 M. J., Lampén, T., Lassila-Perini, K., Lehti, S., Lindén, T., Luukka, P., Mäenpää, T.,
 1162 Peltola, T., Tuominen, E., Tuominiemi, J., Tuovinen, E., Ungaro, D., Wendland, L.,
 1163 Banzuzi, K., Karjalainen, A., Korpela, A., Tuuva, T., Besancon, M., Choudhury, S.,

1164 Dejardin, M., Denegri, D., Fabbro, B., Faure, J. L., Ferri, F., Ganjour, S., Givernaud,
 1165 A., Gras, P., Hamel de Monchenault, G., Jarry, P., Locci, E., Malcles, J., Millischer, L.,
 1166 Nayak, A., Rander, J., Rosowsky, A., Shreyber, I., Titov, M., Baffioni, S., Beaudette,
 1167 F., Benhabib, L., Bianchini, L., Bluj, M., Broutin, C., Busson, P., Charlot, C., Daci,
 1168 N., Dahms, T., Dobrzynski, L., Granier de Cassagnac, R., Haguenaue, M., Miné, P.,
 1169 Mironov, C., Nguyen, M., Ochando, C., Paganini, P., Sabes, D., Salerno, R., Sirois, Y.,
 1170 Veelken, C., Zabi, A., Agram, J.-L., Andrea, J., Bloch, D., Bodin, D., Brom, J.-M.,
 1171 Cardaci, M., Chabert, E. C., Collard, C., Conte, E., Drouhin, F., Ferro, C., Fontaine, J.-
 1172 C., Gelé, D., Goerlach, U., Juillot, P., Le Bihan, A.-C., Van Hove, P., Fassi, F., Mercier,
 1173 D., Beauceron, S., Beaupere, N., Bondu, O., Boudoul, G., Chasserat, J., Chierici, R.,
 1174 Contardo, D., Depasse, P., El Mamouni, H., Fay, J., Gascon, S., Gouzevitch, M., Ille,
 1175 B., Kurca, T., Lethuillier, M., Mirabito, L., Perries, S., Sordini, V., Tosi, S., Tschudi,
 1176 Y., Verdier, P., Viret, S., Tsamalaidze, Z., Anagnostou, G., Beranek, S., Edelhoff, M.,
 1177 Feld, L., Heracleous, N., Hindrichs, O., Jussen, R., Klein, K., Merz, J., Ostapchuk, A.,
 1178 Perieanu, A., Raupach, F., Sammet, J., Schael, S., Sprenger, D., Weber, H., Wittmer,
 1179 B., Zhukov, V., Ata, M., Caudron, J., Dietz-Laursonn, E., Erdmann, M., Güth, A.,
 1180 Hebbeker, T., Heidemann, C., Hoepfner, K., Klingebiel, D., Kreuzer, P., Lingemann,
 1181 J., Magass, C., Merschmeyer, M., Meyer, A., Olschewski, M., Papacz, P., Pieta, H.,
 1182 Reithler, H., Schmitz, S. A., Sonnenschein, L., Steggemann, J., Teyssier, D., Weber, M.,
 1183 Bontenackels, M., Cherepanov, V., Flügge, G., Geenen, H., Geisler, M., Haj Ahmad, W.,
 1184 Hoehle, F., Kargoll, B., Kress, T., Kuessel, Y., Nowack, A., Perchalla, L., Pooth, O.,
 1185 Rennefeld, J., Sauerland, P., Stahl, A., Aldaya Martin, M., Behr, J., Behrenhoff, W.,
 1186 Behrens, U., Bergholz, M., Bethani, A., Borrás, K., Burgmeier, A., Cakir, A., Calligaris,
 1187 L., Campbell, A., Castro, E., Costanza, F., Dammann, D., Diez Pardos, C., Eckerlin, G.,
 1188 Eckstein, D., Flucke, G., Geiser, A., Glushkov, I., Gunnellini, P., Habib, S., Hauk, J.,
 1189 Jung, H., Kasemann, M., Katsas, P., Kleinwort, C., Kluge, H., Knutsson, A., Krämer, M.,
 1190 Krücker, D., Kuznetsova, E., Lange, W., Lohmann, W., Lutz, B., Mankel, R., Marfin, I.,
 1191 Marienfeld, M., Melzer-Pellmann, I.-A., Meyer, A. B., Mnich, J., Mussgiller, A., Naumann-
 1192 Emme, S., Olzem, J., Perrey, H., Petrukhin, A., Pitzl, D., Raspereza, A., Ribeiro Cipriano,
 1193 P. M., Riedl, C., Ron, E., Rosin, M., Salfeld-Nebgen, J., Schmidt, R., Schoerner-Sadenius,

1194 T., Sen, N., Spiridonov, A., Stein, M., Walsh, R., Wissing, C., Autermann, C., Blobel,
 1195 V., Draeger, J., Enderle, H., Erfle, J., Gebbert, U., Görner, M., Hermanns, T., Höing,
 1196 R. S., Kaschube, K., Kaussen, G., Kirschenmann, H., Klanner, R., Lange, J., Mura, B.,
 1197 Nowak, F., Peiffer, T., Pietsch, N., Sander, C., Schettler, H., Schleper, P., Schlieckau, E.,
 1198 Schmidt, A., Schröder, M., Schum, T., Sola, V., Stadie, H., Steinbrück, G., Thomsen,
 1199 J., Vanelderen, L., Barth, C., Berger, J., Chwalek, T., De Boer, W., Dierlamm, A.,
 1200 Feindt, M., Guthoff, M., Hackstein, C., Hartmann, F., Heinrich, M., Held, H., Hoffmann,
 1201 K. H., Honc, S., Katkov, I., Komaragiri, J. R., Lobelle Pardo, P., Martschei, D., Mueller,
 1202 S., Müller, T., Niegel, M., Nürnberg, A., Oberst, O., Oehler, A., Ott, J., Quast, G.,
 1203 Rabbertz, K., Ratnikov, F., Ratnikova, N., Röcker, S., Scheurer, A., Schilling, F.-P.,
 1204 Schott, G., Simonis, H. J., Stober, F. M., Troendle, D., Ulrich, R., Wagner-Kuhr, J.,
 1205 Weiler, T., Zeise, M., Daskalakis, G., Geralis, T., Kesisoglou, S., Kyriakis, A., Loukas,
 1206 D., Manolakos, I., Markou, A., Markou, C., Mavrommatis, C., Ntomari, E., Gouskos, L.,
 1207 Mertzimekis, T. J., Panagiotou, A., Saoulidou, N., Evangelou, I., Foudas, C., Kokkas, P.,
 1208 Manthos, N., Papadopoulos, I., Patras, V., Bencze, G., Hajdu, C., Hidas, P., Horvath, D.,
 1209 Sikler, F., Veszpremi, V., Vesztergombi, G., Beni, N., Czellar, S., Molnar, J., Palinkas, J.,
 1210 Szillasi, Z., Karancsi, J., Raics, P., Trocsanyi, Z. L., Ujvari, B., Beri, S. B., Bhatnagar,
 1211 V., Dhingra, N., Gupta, R., Jindal, M., Kaur, M., Mehta, M. Z., Nishu, N., Saini, L. K.,
 1212 Sharma, A., Singh, J., Ahuja, S., Bhardwaj, A., Choudhary, B. C., Kumar, A., Kumar,
 1213 A., Malhotra, S., Naimuddin, M., Ranjan, K., Sharma, V., Shivpuri, R. K., Banerjee,
 1214 S., Bhattacharya, S., Dutta, S., Gomber, B., Jain, S., Jain, S., Khurana, R., Sarkar,
 1215 S., Sharan, M., Abdulsalam, A., Choudhury, R. K., Dutta, D., Kailas, S., Kumar, V.,
 1216 Mehta, P., Mohanty, A. K., Pant, L. M., Shukla, P., Aziz, T., Ganguly, S., Guchait, M.,
 1217 Maity, M., Majumder, G., Mazumdar, K., Mohanty, G. B., Parida, B., Sudhakar, K.,
 1218 Wickramage, N., Banerjee, S., Dugad, S., Arfaei, H., Bakhshiansohi, H., Etesami, S. M.,
 1219 Fahim, A., Hashemi, M., Hesari, H., Jafari, A., Khakzad, M., Mohammadi Najafabadi,
 1220 M., Paktinat Mehdiabadi, S., Safarzadeh, B., Zeinali, M., Abbrescia, M., Barbone, L.,
 1221 Calabria, C., Chhibra, S. S., Colaleo, A., Creanza, D., De Filippis, N., De Palma, M.,
 1222 Fiore, L., Iaselli, G., Lusito, L., Maggi, G., Maggi, M., Marangelli, B., My, S., Nuzzo,
 1223 S., Pacifico, N., Pompili, A., Pugliese, G., Selvaggi, G., Silvestris, L., Singh, G., Zito,

1224 G., Abbiendi, G., Benvenuti, A. C., Bonacorsi, D., Braibant-Giacomelli, S., Brigliadori,
 1225 L., Capiluppi, P., Castro, A., Cavallo, F. R., Cuffiani, M., Dallavalle, G. M., Fabbri, F.,
 1226 Fanfani, A., Fasanella, D., Giacomelli, P., Grandi, C., Guiducci, L., Marcellini, S., Masetti,
 1227 G., Meneghelli, M., Montanari, A., Navarria, F. L., Odorici, F., Perrotta, A., Primavera,
 1228 F., Rossi, A. M., Rovelli, T., Siroli, G., Travaglini, R., Albergo, S., Cappello, G., Chiorboli,
 1229 M., Costa, S., Potenza, R., Tricomi, A., Tuve, C., Barbagli, G., Ciulli, V., Civinini, C.,
 1230 D'Alessandro, R., Focardi, E., Frosali, S., Gallo, E., Gonzi, S., Meschini, M., Paoletti,
 1231 S., Sguazzoni, G., Tropiano, A., Benussi, L., Bianco, S., Colafranceschi, S., Fabbri, F.,
 1232 Piccolo, D., Fabbricatore, P., Musenich, R., Benaglia, A., De Guio, F., Di Matteo, L.,
 1233 Fiorendi, S., Gennai, S., Ghezzi, A., Malvezzi, S., Manzoni, R. A., Martelli, A., Massironi,
 1234 A., Menasce, D., Moroni, L., Paganoni, M., Pedrini, D., Ragazzi, S., Redaelli, N., Sala,
 1235 S., Tabarelli de Fatis, T., Buontempo, S., Carrillo Montoya, C. A., Cavallo, N., De Cosa,
 1236 A., Dogangun, O., Fabozzi, F., Iorio, A. O. M., Lista, L., Meola, S., Merola, M., Paolucci,
 1237 P., Azzi, P., Bacchetta, N., Bellan, P., Bisello, D., Branca, A., Carlin, R., Checchia, P.,
 1238 Dorigo, T., Dosselli, U., Gasparini, F., Gasparini, U., Gozzelino, A., Kanishchev, K.,
 1239 Lacaprara, S., Lazzizzera, I., Margoni, M., Meneguzzo, A. T., Nespolo, M., Ronchese,
 1240 P., Simonetto, F., Torassa, E., Vanini, S., Zotto, P., Zumerle, G., Gabusi, M., Ratti,
 1241 S. P., Riccardi, C., Torre, P., Vitulo, P., Biasini, M., Bilei, G. M., Fanò, L., Lariccia, P.,
 1242 Lucaroni, A., Mantovani, G., Menichelli, M., Nappi, A., Romeo, F., Saha, A., Santocchia,
 1243 A., Taroni, S., Azzurri, P., Bagliesi, G., Boccali, T., Broccolo, G., Castaldi, R., D'Agnolo,
 1244 R. T., Dell'Orso, R., Fiori, F., Foà, L., Giassi, A., Kraan, A., Ligabue, F., Lomtadze, T.,
 1245 Martini, L., Messineo, A., Palla, F., Rizzi, A., Serban, A. T., Spagnolo, P., Squillacioti, P.,
 1246 Tenchini, R., Tonelli, G., Venturi, A., Verdini, P. G., Barone, L., Cavallari, F., Del Re, D.,
 1247 Diemoz, M., Grassi, M., Longo, E., Meridiani, P., Micheli, F., Nourbakhsh, S., Organtini,
 1248 G., Paramatti, R., Rahatlou, S., Sigamani, M., Soffi, L., Amapane, N., Arcidiacono, R.,
 1249 Argiro, S., Arneodo, M., Biino, C., Cartiglia, N., Costa, M., Demaria, N., Graziano,
 1250 A., Mariotti, C., Maselli, S., Migliore, E., Monaco, V., Musich, M., Obertino, M. M.,
 1251 Pastrone, N., Pelliccioni, M., Potenza, A., Romero, A., Ruspa, M., Sacchi, R., Solano, A.,
 1252 Staiano, A., Vilela Pereira, A., Belforte, S., Candelise, V., Cossutti, F., Della Ricca, G.,
 1253 Gobbo, B., Marone, M., Montanino, D., Penzo, A., Schizzi, A., Heo, S. G., Kim, T. Y.,

1254 Nam, S. K., Chang, S., Kim, D. H., Kim, G. N., Kong, D. J., Park, H., Ro, S. R., Son,
 1255 D. C., Son, T., Kim, J. Y., Kim, Z. J., Song, S., Choi, S., Gyun, D., Hong, B., Jo, M.,
 1256 Kim, H., Kim, T. J., Lee, K. S., Moon, D. H., Park, S. K., Choi, M., Kim, J. H., Park,
 1257 C., Park, I. C., Park, S., Ryu, G., Cho, Y., Choi, Y., Choi, Y. K., Goh, J., Kim, M. S.,
 1258 Kwon, E., Lee, B., Lee, J., Lee, S., Seo, H., Yu, I., Bilinskas, M. J., Grigelionis, I., Janulis,
 1259 M., Juodagalvis, A., Castilla-Valdez, H., De La Cruz-Burelo, E., Heredia-de La Cruz, I.,
 1260 Lopez-Fernandez, R., Magaña Villalba, R., Martínez-Ortega, J., Sánchez-Hernández, A.,
 1261 Villasenor-Cendejas, L. M., Carrillo Moreno, S., Vazquez Valencia, F., Salazar Ibarguen,
 1262 H. A., Casimiro Linares, E., Morelos Pineda, A., Reyes-Santos, M. A., Krofcheck, D.,
 1263 Bell, A. J., Butler, P. H., Doesburg, R., Reucroft, S., Silverwood, H., Ahmad, M.,
 1264 Asghar, M. I., Hoorani, H. R., Khalid, S., Khan, W. A., Khurshid, T., Qazi, S., Shah,
 1265 M. A., Shoaib, M., Bialkowska, H., Boimska, B., Frueboes, T., Gokieli, R., Górski,
 1266 M., Kazana, M., Nawrocki, K., Romanowska-Rybinska, K., Szleper, M., Wrochna, G.,
 1267 Zalewski, P., Brona, G., Bunkowski, K., Cwiok, M., Dominik, W., Doroba, K., Kalinowski,
 1268 A., Konecki, M., Krolikowski, J., Almeida, N., Bargassa, P., David, A., Faccioli, P.,
 1269 Ferreira Parracho, P. G., Gallinaro, M., Seixas, J., Varela, J., Vischia, P., Belotelov,
 1270 I., Bunin, P., Gavrilenko, M., Golutvin, I., Gorbunov, I., Kamenev, A., Karjavin, V.,
 1271 Kozlov, G., Lanev, A., Malakhov, A., Moisenz, P., Palichik, V., Perelygin, V., Shmatov,
 1272 S., Smirnov, V., Volodko, A., Zarubin, A., Evstyukhin, S., Golovtsov, V., Ivanov, Y.,
 1273 Kim, V., Levchenko, P., Murzin, V., Oreshkin, V., Smirnov, I., Sulimov, V., Uvarov,
 1274 L., Vavilov, S., Vorobyev, A., Vorobyev, A., Andreev, Y., Dermenev, A., Gninenko,
 1275 S., Golubev, N., Kirsanov, M., Krasnikov, N., Matveev, V., Pashenkov, A., Tlisov, D.,
 1276 Toropin, A., Epshteyn, V., Erofeeva, M., Gavrilov, V., Kossov, M., Lychkovskaya, N.,
 1277 Popov, V., Safronov, G., Semenov, S., Stolin, V., Vlasov, E., Zhokin, A., Belyaev, A.,
 1278 Boos, E., Ershov, A., Gribushin, A., Klyukhin, V., Kodolova, O., Korotkikh, V., Lokhtin,
 1279 I., Markina, A., Obraztsov, S., Perfilov, M., Petrushanko, S., Popov, A., Sarycheva, L.,
 1280 Savrin, V., Snigirev, A., Vardanyan, I., Andreev, V., Azarkin, M., Dremin, I., Kirakosyan,
 1281 M., Leonidov, A., Mesyats, G., Rusakov, S. V., Vinogradov, A., Azhgirey, I., Bayshev, I.,
 1282 Bitioukov, S., Grishin, V., Kachanov, V., Konstantinov, D., Korablev, A., Krychkin,
 1283 V., Petrov, V., Ryutin, R., Sobol, A., Tourtchanovitch, L., Troshin, S., Tyurin, N.,

1284 Uzunian, A., Volkov, A., Adzic, P., Djordjevic, M., Ekmedzic, M., Krpic, D., Milosevic, J.,
 1285 Aguilar-Benitez, M., Alcaraz Maestre, J., Arce, P., Battilana, C., Calvo, E., Cerrada, M.,
 1286 Chamizo Llatas, M., Colino, N., De La Cruz, B., Delgado Peris, A., Domínguez Vázquez,
 1287 D., Fernandez Bedoya, C., Fernández Ramos, J. P., Ferrando, A., Flix, J., Fouz, M. C.,
 1288 Garcia-Abia, P., Gonzalez Lopez, O., Goy Lopez, S., Hernandez, J. M., Josa, M. I., Merino,
 1289 G., Puerta Pelayo, J., Quintario Olmeda, A., Redondo, I., Romero, L., Santaolalla, J.,
 1290 Soares, M. S., Willmott, C., Albajar, C., Codispoti, G., de Trocóniz, J. F., Brun, H.,
 1291 Cuevas, J., Fernandez Menendez, J., Folgueras, S., Gonzalez Caballero, I., Lloret Iglesias,
 1292 L., Piedra Gomez, J., Brochero Cifuentes, J. A., Cabrillo, I. J., Calderon, A., Chuang,
 1293 S. H., Duarte Campderros, J., Felcini, M., Fernandez, M., Gomez, G., Gonzalez Sanchez,
 1294 J., Jorda, C., Lopez Virto, A., Marco, J., Marco, R., Martinez Rivero, C., Matorras,
 1295 F., Munoz Sanchez, F. J., Rodrigo, T., Rodríguez-Marrero, A. Y., Ruiz-Jimeno, A.,
 1296 Scodellaro, L., Sobron Sanudo, M., Vila, I., Vilar Cortabitarte, R., Abbaneo, D., Auffray,
 1297 E., Auzinger, G., Baillon, P., Ball, A. H., Barney, D., Benitez, J. F., Bernet, C., Bianchi,
 1298 G., Bloch, P., Bocci, A., Bonato, A., Botta, C., Breuker, H., Camporesi, T., Cerminara,
 1299 G., Christiansen, T., Coarasa Perez, J. A., D'Enterria, D., Dabrowski, A., De Roeck,
 1300 A., Di Guida, S., Dobson, M., Dupont-Sagorin, N., Elliott-Peisert, A., Frisch, B., Funk,
 1301 W., Georgiou, G., Giffels, M., Gigi, D., Gill, K., Giordano, D., Giunta, M., Glege, F.,
 1302 Gomez-Reino Garrido, R., Govoni, P., Gowdy, S., Guida, R., Hansen, M., Harris, P.,
 1303 Hartl, C., Harvey, J., Hegner, B., Hinzmann, A., Innocente, V., Janot, P., Kaadze, K.,
 1304 Karavakis, E., Kousouris, K., Lecoq, P., Lee, Y.-J., Lenzi, P., Lourenço, C., Mäki, T.,
 1305 Malberti, M., Malgeri, L., Mannelli, M., Masetti, L., Meijers, F., Mersi, S., Meschi, E.,
 1306 Moser, R., Mozer, M. U., Mulders, M., Musella, P., Nesvold, E., Orimoto, T., Orsini, L.,
 1307 Palencia Cortezon, E., Perez, E., Perrozzi, L., Petrilli, A., Pfeiffer, A., Pierini, M., Pimiä,
 1308 M., Piparo, D., Polese, G., Quertenmont, L., Racz, A., Reece, W., Rodrigues Antunes, J.,
 1309 Rolandi, G., Rommerskirchen, T., Rovelli, C., Rovere, M., Sakulin, H., Santanastasio, F.,
 1310 Schäfer, C., Schwick, C., Segoni, I., Sekmen, S., Sharma, A., Siegrist, P., Silva, P., Simon,
 1311 M., Sphicas, P., Spiga, D., Spiropulu, M., Tsiros, A., Veres, G. I., Vlimant, J. R., Wöhri,
 1312 H. K., Worm, S. D., Zeuner, W. D., Bertl, W., Deiters, K., Erdmann, W., Gabathuler,
 1313 K., Horisberger, R., Ingram, Q., Kaestli, H. C., König, S., Kotlinski, D., Langenegger, U.,

1314 Meier, F., Renker, D., Rohe, T., Sibille, J., Bäni, L., Bortignon, P., Buchmann, M. A.,
 1315 Casal, B., Chanon, N., Deisher, A., Dissertori, G., Dittmar, M., Dünser, M., Eugster, J.,
 1316 Freudenreich, K., Grab, C., Hits, D., Lecomte, P., Lustermann, W., Martinez Ruiz del
 1317 Arbol, P., Mohr, N., Moortgat, F., Nägeli, C., Nef, P., Nessi-Tedaldi, F., Pandolfi, F.,
 1318 Pape, L., Pauss, F., Peruzzi, M., Ronga, F. J., Rossini, M., Sala, L., Sanchez, A. K.,
 1319 Starodumov, A., Stieger, B., Takahashi, M., Tauscher, L., Thea, A., Theofilatos, K.,
 1320 Treille, D., Urscheler, C., Wallny, R., Weber, H. A., Wehrli, L., Aguilo, E., Amsler, C.,
 1321 Chiochia, V., De Visscher, S., Favaro, C., Ivova Rikova, M., Millan Mejias, B., Otiougova,
 1322 P., Robmann, P., Snoek, H., Tupputi, S., Verzetti, M., Chang, Y. H., Chen, K. H., Kuo,
 1323 C. M., Li, S. W., Lin, W., Liu, Z. K., Lu, Y. J., Mekterovic, D., Singh, A. P., Volpe, R., Yu,
 1324 S. S., Bartalini, P., Chang, P., Chang, Y. H., Chang, Y. W., Chao, Y., Chen, K. F., Dietz,
 1325 C., Grundler, U., Hou, W.-S., Hsiung, Y., Kao, K. Y., Lei, Y. J., Lu, R.-S., Majumder, D.,
 1326 Petrakou, E., Shi, X., Shiu, J. G., Tzeng, Y. M., Wan, X., Wang, M., Adiguzel, A., Bakirci,
 1327 M. N., Cerci, S., Dozen, C., Dumanoglu, I., Eskut, E., Girgis, S., Gokbulut, G., Gurpinar,
 1328 E., Hos, I., Kangal, E. E., Karapinar, G., Kayis Topaksu, A., Onengut, G., Ozdemir, K.,
 1329 Ozturk, S., Polatoz, A., Sogut, K., Sunar Cerci, D., Tali, B., Topakli, H., Vergili, L. N.,
 1330 Vergili, M., Akin, I. V., Aliev, T., Bilin, B., Bilmis, S., Deniz, M., Gamsizkan, H., Guler,
 1331 A. M., Ocalan, K., Ozpineci, A., Serin, M., Sever, R., Surat, U. E., Yalvac, M., Yildirim,
 1332 E., Zeyrek, M., Gülmez, E., Isildak, B., Kaya, M., Kaya, O., Ozkorucuklu, S., Sonmez, N.,
 1333 Cankocak, K., Levchuk, L., Bostock, F., Brooke, J. J., Clement, E., Cussans, D., Flacher,
 1334 H., Frazier, R., Goldstein, J., Grimes, M., Heath, G. P., Heath, H. F., Kreczko, L.,
 1335 Metson, S., Newbold, D. M., Nirunpong, K., Poll, A., Senkin, S., Smith, V. J., Williams,
 1336 T., Basso, L., Bell, K. W., Belyaev, A., Brew, C., Brown, R. M., Cockerill, D. J. A.,
 1337 Coughlan, J. A., Harder, K., Harper, S., Jackson, J., Kennedy, B. W., Olaiya, E., Petyt,
 1338 D., Radburn-Smith, B. C., Shepherd-Themistocleous, C. H., Tomalin, I. R., Womersley,
 1339 W. J., Bainbridge, R., Ball, G., Beuselinck, R., Buchmuller, O., Colling, D., Cripps, N.,
 1340 Cutajar, M., Dauncey, P., Davies, G., Della Negra, M., Ferguson, W., Fulcher, J., Futyan,
 1341 D., Gilbert, A., Guneratne Bryer, A., Hall, G., Hatherell, Z., Hays, J., Iles, G., Jarvis,
 1342 M., Karapostoli, G., Lyons, L., Magnan, A.-M., Marrouche, J., Mathias, B., Nandi, R.,
 1343 Nash, J., Nikitenko, A., Papageorgiou, A., Pela, J., Pesaresi, M., Petridis, K., Pioppi,

M., Raymond, D. M., Rogerson, S., Rose, A., Ryan, M. J., Seez, C., Sharp, P., Sparrow, A., Stoye, M., Tapper, A., Vazquez Acosta, M., Virdee, T., Wakefield, S., Wardle, N., Whyntie, T., Chadwick, M., Cole, J. E., Hobson, P. R., Khan, A., Kyberd, P., Leslie, D., Martin, W., Reid, I. D., Symonds, P., Teodorescu, L., Turner, M., Hatakeyama, K., Liu, H., Scarborough, T., Charaf, O., Henderson, C., Rumerio, P., Avetisyan, A., Bose, T., Fantasia, C., Heiste (2012). Measurement of the pseudorapidity and centrality dependence of the transverse energy density in pb-pb collisions at $\sqrt{s_{NN}} = 2.76$ TeV. *Phys. Rev. Lett.*, 109:152303. 6, 21

[13] Collaboration, T. A., Aamodt, K., Quintana, A. A., Achenbach, R., Acounis, S., Adamov, D., Adler, C., Aggarwal, M., Agnese, F., Rinella, G. A., Ahammed, Z., Ahmad, A., Ahmad, N., Ahmad, S., Akindinov, A., Akishin, P., Aleksandrov, D., Alessandro, B., Alfaro, R., Alfarone, G., Alici, A., Alme, J., Alt, T., Altinpinar, S., Amend, W., Andrei, C., Andres, Y., Andronic, A., Anelli, G., Anfreville, M., Angelov, V., Anzo, A., Anson, C., Antici, T., Antonenko, V., Antonczyk, D., Antinori, F., Antinori, S., Antonioli, P., Aphecetche, L., Appelshuser, H., Aprodu, V., Arba, M., Arcelli, S., Argentieri, A., Armesto, N., Arnaldi, R., Arefiev, A., Arsene, I., Asryan, A., Augustinus, A., Awes, T. C., ysto, J., Azmi, M. D., Bablock, S., Badal, A., Badyal, S. K., Baechler, J., Bagnasco, S., Bailhache, R., Bala, R., Baldisseri, A., Baldit, A., Bn, J., Barbera, R., Barberis, P.-L., Barbet, J. M., Barnfoldi, G., Barret, V., Bartke, J., Bartos, D., Basile, M., Basmanov, V., Bastid, N., Batigne, G., Batyunya, B., Baudot, J., Baumann, C., Bearden, I., Becker, B., Belikov, J., Bellwied, R., Belmont-Moreno, E., Belogianni, A., Belyaev, S., Benato, A., Beney, J. L., Benhabib, L., Benotto, F., Beol, S., Berceanu, I., Bercuci, A., Berdermann, E., Berdnikov, Y., Bernard, C., Berny, R., Berst, J. D., Bertelsen, H., Betev, L., Bhasin, A., Baskar, P., Bhati, A., Bianchi, N., Bielik, J., Bielikov, J., Bimbot, L., Blanchard, G., Blanco, F., Blanco, F., Blau, D., Blume, C., Blyth, S., Boccioni, M., Bogdanov, A., Bggild, H., Bogolyubsky, M., Boldizsr, L., Bombara, M., Bombonati, C., Bondila, M., Bonnet, D., Bonvicini, V., Borel, H., Borotto, F., Borshchov, V., Bortoli, Y., Borysov, O., Bose, S., Bosisio, L., Botje, M., Bttger, S., Bourdaud, G., Bourrion, O., Bouvier, S., Braem, A., Braun, M., Braun-Munzinger, P., Bravina, L., Bregant, M., Bruckner, G., Brun, R.,

1373 Bruna, E., Brunasso, O., Bruno, G. E., Bucher, D., Budilov, V., Budnikov, D., Buesching,
 1374 H., Buncic, P., Burns, M., Burachas, S., Busch, O., Bushop, J., Cai, X., Caines, H.,
 1375 Calaon, F., Caldogno, M., Cali, I., Camerini, P., Campagnolo, R., Campbell, M., Cao,
 1376 X., Capitani, G. P., Romeo, G. C., Cardenas-Montes, M., Carduner, H., Carena, F.,
 1377 Carena, W., Cariola, P., Carminati, F., Casado, J., Diaz, A. C., Caselle, M., Castellanos,
 1378 J. C., Castor, J., Catanescu, V., Cattaruzza, E., Cavazza, D., Cerello, P., Ceresa, S.,
 1379 ern, V., Chambert, V., Chapeland, S., Charpy, A., Charrier, D., Chartoire, M., Charvet,
 1380 J. L., Chattopadhyay, S., Chattopadhyay, S., Chepurnov, V., Chernenko, S., Cherney,
 1381 M., Cheshkov, C., Cheynis, B., Chochula, P., Chiavassa, E., Barroso, V. C., Choi, J.,
 1382 Christakoglou, P., Christiansen, P., Christensen, C., Chykalov, O. A., Cicalo, C., Cifarelli-
 1383 Strolin, L., Ciobanu, M., Cindolo, F., Cirstoiu, C., Clausse, O., Cleymans, J., Cobanoglu,
 1384 O., Coffin, J.-P., Coli, S., Colla, A., Colledani, C., Combaret, C., Combet, M., Comets,
 1385 M., Balbastre, G. C., del Valle, Z. C., Contin, G., Contreras, J., Cormier, T., Corsi, F.,
 1386 Cortese, P., Costa, F., Crescio, E., Crochet, P., Cuautle, E., Cussonneau, J., Dahlinger,
 1387 M., Dainese, A., Dalsgaard, H. H., Daniel, L., Das, I., Das, T., Dash, A., Silva, R. D.,
 1388 Davenport, M., Daues, H., Caro, A. D., de Cataldo, G., Cuveland, J. D., Falco, A. D.,
 1389 de Gaspari, M., de Girolamo, P., de Groot, J., Gruttola, D. D., Haas, A. D., Marco, N. D.,
 1390 Pasquale, S. D., Remigis, P. D., de Vaux, D., Decock, G., Delagrange, H., Franco, M. D.,
 1391 Dellacasa, G., Dell'Olio, C., Dell'Olio, D., Deloff, A., Demanov, V., Dnes, E., D'Erasmus,
 1392 G., Derkach, D., Devaux, A., Bari, D. D., Bartolomeo, A. D., Giglio, C. D., Liberto,
 1393 S. D., Mauro, A. D., Nezza, P. D., Dialinas, M., Diaz, L., Valdes, R. D., Dietel, T., Dima,
 1394 R., Ding, H., Dinca, C., Divi, R., Dobretsov, V., Dobrin, A., Doenigus, B., Dobrowolski,
 1395 T., Domnguez, I., Dorn, M., Drouet, S., Dubey, A. E., Ducroux, L., Dumitrache, F.,
 1396 Dumonteil, E., Dupieux, P., Duta, V., Majumdar, A. D., Majumdar, M. D., Dyhre,
 1397 T., Efimov, L., Efremov, A., Elia, D., Emschermann, D., Engster, C., Enokizono, A.,
 1398 Espagnon, B., Estienne, M., Evangelista, A., Evans, D., Evrard, S., Fabjan, C. W.,
 1399 Fabris, D., Faivre, J., Falchieri, D., Fantoni, A., Farano, R., Fearick, R., Fedorov, O.,
 1400 Fekete, V., Felea, D., Feofilov, G., Tllez, A. F., Ferretti, A., Fichera, F., Filchagin, S.,
 1401 Filoni, E., Finck, C., Fini, R., Fiore, E. M., Flierl, D., Floris, M., Fodor, Z., Foka, Y.,
 1402 Fokin, S., Force, P., Formenti, F., Fragiaco, E., Fragiadakis, M., Fraissard, D., Franco,

1403 A., Franco, M., Frankenfeld, U., Fratino, U., Fresneau, S., Frolov, A., Fuchs, U., Fujita, J.,
 1404 Furget, C., Furini, M., Girard, M. F., Gaardhje, J.-J., Gabrielli, A., Gadrat, S., Gagliardi,
 1405 M., Gago, A., Gaido, L., Torreira, A. G., Gallio, M., Gandolfi, E., Ganoti, P., Ganti, M.,
 1406 Garabatos, J., Lopez, A. G., Garizzo, L., Gaudichet, L., Gemme, R., Germain, M., Gheata,
 1407 A., Gheata, M., Ghidini, B., Ghosh, P., Giolu, G., Giraudo, G., Giubellino, P., Glasow,
 1408 R., Glssel, P., Ferreira, E. G., Gutierrez, C. G., Gonzales-Trueba, L. H., Gorbunov, S.,
 1409 Gorbunov, Y., Gos, H., Gosset, J., Gotovac, S., Gottschlag, H., Gottschalk, D., Grabski,
 1410 V., Grassi, T., Gray, H., Grebenyuk, O., Grebieszko, K., Gregory, C., Grigoras, C.,
 1411 Grion, N., Grigoriev, V., Grigoryan, A., Grigoryan, C., Grigoryan, S., Grishuk, Y., Gros,
 1412 P., Grosse-Oetringhaus, J., Grossiord, J.-Y., Grosso, R., Grynyov, B., Guarnaccia, C.,
 1413 Guber, F., Guerin, F., Guernane, R., Guerzoni, M., Guichard, A., Guida, M., Guilloux,
 1414 G., Gulkanyan, H., Gulbrandsen, K., Gunji, T., Gupta, A., Gupta, V., Gustafsson, H.-
 1415 A., Gutbrod, H., Hadjidakis, C., Haiduc, M., Hamar, G., Hamagaki, H., Hamblen, J.,
 1416 Hansen, J. C., Hardy, P., Hatzifotiadou, D., Harris, J. W., Hartig, M., Harutyunyan, A.,
 1417 Hayrapetyan, A., Hasch, D., Hasegan, D., Hehner, J., Heine, N., Heinz, M., Helstrup, H.,
 1418 Herghelegiu, A., Herlant, S., Corral, G. H., Herrmann, N., Hetland, K., Hille, P., Hinke,
 1419 H., Hippolyte, B., Hoch, M., Hoebbel, H., Hoedlmoser, H., Horaguchi, T., Horner, M.,
 1420 Hristov, P., Hivnov, I., Hu, S., Guo, C. H., Humanic, T., Hurtado, A., Hwang, D. S.,
 1421 Ianigro, J. C., Idzik, M., Igolkin, S., Ilkaev, R., Ilkiv, I., Imhoff, M., Innocenti, P. G.,
 1422 Ionescu, E., Ippolitov, M., Irfan, M., Insa, C., Inuzuka, M., Ivan, C., Ivanov, A., Ivanov,
 1423 M., Ivanov, V., Jacobs, P., Jacholkowski, A., Janurov, L., Janik, R., Jasper, M., Jena, C.,
 1424 Jirden, L., Johnson, D. P., Jones, G. T., Jorgensen, C., Jouve, F., Jovanovi, P., Junique,
 1425 A., Jusko, A., Jung, H., Jung, W., Kadija, K., Kamal, A., Kamermans, R., Kapusta, S.,
 1426 Kaidalov, A., Kakoyan, V., Kalcher, S., Kang, E., Kapitan, J., Kaplin, V., Karadzhev, K.,
 1427 Karavichev, O., Karavicheva, T., Karpechev, E., Karpio, K., Kazantsev, A., Kebschull,
 1428 U., Keidel, R., Khan, M. M., Khanzadeev, A., Kharlov, Y., Kikola, D., Kileng, B., Kim,
 1429 D., Kim, D. S., Kim, D. W., Kim, H. N., Kim, J. S., Kim, S., Kinson, J. B., Kiprich, S. K.,
 1430 Kisel, I., Kiselev, S., Kisiel, A., Kiss, T., Kiworra, V., Klay, J., Bsing, C. K., Kliemant, M.,
 1431 Klimov, A., Klovning, A., Kluge, A., Kluit, R., Kniege, S., Kolevatov, R., Kollegger, T.,
 1432 Kolojvari, A., Kondratiev, V., Kornas, E., Koshurnikov, E., Kotov, I., Kour, R., Kowalski,

1433 M., Kox, S., Kozlov, K., Krlik, I., Kramer, F., Kraus, I., Kravkov, A., Krawutschke, T.,
 1434 Krivda, M., Kryshen, E., Kucheriaev, Y., Kugler, A., Kuhn, C., Kuijer, P., Kumar, L.,
 1435 Kumar, N., Kumpumaeki, P., Kurepin, A., Kurepin, A. N., Kushpil, S., Kushpil, V.,
 1436 Kutovsky, M., Kvaerno, H., Kweon, M., Labb, J.-C., Lackner, F., de Guevara, P. L.,
 1437 Lafage, V., Rocca, P. L., Lamont, M., Lara, C., Larsen, D. T., Laurenti, G., Lazzeroni,
 1438 C., Bornec, Y. L., Bris, N. L., Gailliard, C. L., Lebedev, V., Lecoq, J., Lee, K. S., Lee, S. C.,
 1439 Lefvre, F., Legrand, I., Lehmann, T., Leistam, L., Lenoir, P., Lenti, V., Leon, H., Monzon,
 1440 I. L., Lvai, P., Li, Q., Li, X., Librizzi, F., Lietava, R., Lindegaard, N., Lindenstruth, V.,
 1441 Lippmann, C., Lisa, M., Listratenko, O. M., Littel, F., Liu, Y., Lo, J., Lobanov, V.,
 1442 Loginov, V., Noriega, M. L., Lpez-Ramrez, R., Torres, E. L., Lorenzo, P. M., Lvhidden,
 1443 G., Lu, S., Ludolphs, W., Lunardon, M., Luquin, L., Lusso, S., Lutz, J.-R., Luvisetto,
 1444 M., Lyapin, V., Maevskaya, A., Magureanu, C., Mahajan, A., Majahan, S., Mahmoud,
 1445 T., Mairani, A., Mahapatra, D., Makarov, A., Makhlyueva, I., Malek, M., Malkiewicz,
 1446 T., Mal'Kevich, D., Malzacher, P., Mamonov, A., Manea, C., Mangotra, L. K., Maniero,
 1447 D., Manko, V., Manso, F., Manzari, V., Mao, Y., Marcel, A., Marchini, S., Mare, J.,
 1448 Margagliotti, G. V., Margotti, A., Marin, A., Marin, J.-C., Marras, D., Martinengo, P.,
 1449 Martnez, M. I., Martinez-Davalos, A., Garcia, G. M., Martini, S., Chiesa, A. M., Marzocca,
 1450 C., Masciocchi, S., Masera, M., Masetti, M., Maslov, N. I., Masoni, A., Massera, F., Mast,
 1451 M., Mastroserio, A., Matthews, Z. L., Mayer, B., Mazza, G., Mazzaro, M. D., Mazzoni,
 1452 A., Meddi, F., Meleshko, E., Menchaca-Rocha, A., Meneghini, S., Meoni, M., Perez, J. M.,
 1453 Mereu, P., Meunier, O., Miake, Y., Michalon, A., Michinelli, R., Miftakhov, N., Mignone,
 1454 M., Mikhailov, K., Milosevic, J., Minaev, Y., Minafra, F., Mischke, A., Mikowiec, D.,
 1455 Mitsyn, V., Mitu, C., Mohanty, B., Moisa, D., Molnar, L., Mondal, M., Mondal, N.,
 1456 Zetina, L. M., Monteno, M., Morando, M., Morel, M., Moretto, S., Morhardt, T., Morsch,
 1457 A., Moukhanova, T., Mucchi, M., Muccifora, V., Mudnic, E., Miller, H., Miller, W., Munoz,
 1458 J., Mura, D., Musa, L., Muraz, J. F., Musso, A., Nania, R., Nandi, B., Nappi, E., Navach,
 1459 F., Navin, S., Nayak, T., Nazarenko, S., Nazarov, G., Nellen, L., Nendaz, F., Nianine,
 1460 A., Nicassio, M., Nielsen, B. S., Nikolaev, S., Nikolic, V., Nikulin, S., Nikulin, V., Nilsen,
 1461 B., Nitti, M., Noferini, F., Nomokonov, P., Nooren, G., Noto, F., Nouais, D., Nyiri,
 1462 A., Nystrand, J., Odyniec, G., Oeschler, H., Oinonen, M., Oldenburg, M., Oleks, I.,

1463 Olsen, E. K., Onuchin, V., Oppedisano, C., Orsini, F., Ortiz-Velzquez, A., Oskamp, C.,
 1464 Oskarsson, A., Osmic, F., sberman, L., Otterlund, I., Ovrebekk, G., Oyama, K., Pachr,
 1465 M., Pagano, P., Pai, G., Pajares, C., Pal, S., Pal, S., Plla, G., Palmeri, A., Pancaldi,
 1466 G., Panse, R., Pantaleo, A., Pappalardo, G. S., Pastirk, B., Pastore, C., Patarakin, O.,
 1467 Paticchio, V., Patimo, G., Pavlinov, A., Pawlak, T., Peitzmann, T., Pnichot, Y., Pepato,
 1468 A., Pereira, H., Peresunko, D., Perez, C., Griffio, J. P., Perini, D., Perrino, D., Peryt, W.,
 1469 Pesci, A., Peskov, V., Pestov, Y., Peters, A. J., Petrek, V., Petridis, A., Petris, M., Petrov,
 1470 V., Petrov, V., Petrovici, M., Peyr, J., Piano, S., Piccotti, A., Pichot, P., Piemonte, C.,
 1471 Pikna, M., Pilastrini, R., Pillot, P., Pinazza, O., Pini, B., Pinsky, L., Morais, V. P.,
 1472 Pismennaya, V., Piuz, F., Platt, R., Ploskon, M., Plumeri, S., Pluta, J., Pocheptsov,
 1473 T., Podesta, P., Poggio, F., Poghosyan, M., Poghosyan, T., Polk, K., Polichtchouk, B.,
 1474 Polozov, P., Polyakov, V., Pommeresch, B., Pompei, F., Pop, A., Popescu, S., Posa, F.,
 1475 Pospil, V., Potukuchi, B., Pouthas, J., Prasad, S., Preghenella, R., Prino, F., Prodan, L.,
 1476 Prono, G., Protsenko, M. A., Pruneau, C. A., Przybyla, A., Pshenichnov, I., Puddu, G.,
 1477 Pujahari, P., Pulvirenti, A., Punin, A., Punin, V., Putschke, J., Quartieri, J., Quercigh,
 1478 E., Rachevskaya, I., Rachevski, A., Rademakers, A., Radomski, S., Radu, A., Rak, J.,
 1479 Ramello, L., Raniwala, R., Raniwala, S., Rasmussen, O. B., Rasson, J., Razin, V., Read,
 1480 K., Real, J., Redlich, K., Reichling, C., Renard, C., Renault, G., Renfordt, R., Reolon,
 1481 A. R., Reshetin, A., Revol, J.-P., Reygers, K., Ricaud, H., Riccati, L., Ricci, R. A., Richter,
 1482 M., Riedler, P., Rigalleau, L. M., Riggi, F., Riegler, W., Rindel, E., Riso, J., Rivetti, A.,
 1483 Rizzi, M., Rizzi, V., Cahuantzi, M. R., Red, K., Rhrich, D., Romn-Lpez, S., Romanato, M.,
 1484 Romita, R., Ronchetti, F., Rosinsky, P., Rosnet, P., Rossegger, S., Rossi, A., Rostchin,
 1485 V., Rotondo, F., Roukoutakis, F., Rousseau, S., Roy, C., Roy, D., Roy, P., Royer, L.,
 1486 Rubin, G., Rubio, A., Rui, R., Rusanov, I., Russo, G., Ruuskanen, V., Ryabinkin, E.,
 1487 Rybicki, A., Sadovsky, S., afak, K., Sahoo, R., Saini, J., Saiz, P., Salur, S., Sambyal,
 1488 S., Samsonov, V., ndor, L., Sandoval, A., Sann, H., Santiard, J.-C., Santo, R., Santoro,
 1489 R., Sargsyan, G., Saturnini, P., Scapparone, E., Scarlassara, F., Schackert, B., Schiaua,
 1490 C., Schicker, R., Schioler, T., Schippers, J. D., Schmidt, C., Schmidt, H., Schneider, R.,
 1491 Schossmailer, K., Schukraft, J., Schutz, Y., Schwarz, K., Schweda, K., Schyns, E., Scioli,
 1492 G., Scomparin, E., Snow, H., Sedykh, S., Segato, G., Sellitto, S., Semeria, F., Senyukov,

1493 S., Seppnen, H., Serici, S., Serkin, L., Serra, S., Sesselmann, T., Sevcenco, A., Sgura, I.,
 1494 Shabratova, G., Shahoyan, R., Sharkov, E., Sharma, S., Shigaki, K., Shileev, K., Shukla,
 1495 P., Shurygin, A., Shurygina, M., Sibiriak, Y., Siddi, E., Siemiarzczuk, T., Sigward, M. H.,
 1496 Silenzi, A., Silvermyr, D., Silvestri, R., Simili, E., Simion, V., Simon, R., Simonetti, L.,
 1497 Singaraju, R., Singhal, V., Sinha, B., Sinha, T., Siska, M., Sitr, B., Sitta, M., Skaali,
 1498 B., Skowronski, P., Slodkowski, M., Smirnov, N., Smykov, L., Snellings, R., Snoeys, W.,
 1499 Soegaard, C., Soerensen, J., Sokolov, O., Soldatov, A., Soloviev, A., Soltveit, H., Soltz,
 1500 R., Sommer, W., Soos, C., Soramel, F., Sorensen, S., Soyk, D., Spyropoulou-Stassinaki,
 1501 M., Stachel, J., Staley, F., Stan, I., Stavinskiy, A., Steckert, J., Stefanini, G., Stefanek,
 1502 G., Steinbeck, T., Stelzer, H., Stenlund, E., Stocco, D., Stockmeier, M., Stoicea, G.,
 1503 Stolpovsky, P., Strme, P., Stutzmann, J. S., Su, G., Sugitate, T., umbera, M., Suire, C.,
 1504 Susa, T., Kumar, K. S., Swoboda, D., Symons, J., Szarka, I., Szostak, A., Szuba, M.,
 1505 Szymanski, P., Tadel, M., Tagridis, C., Tan, L., Takaki, D. T., Taureg, H., Tauro, A.,
 1506 Tavlet, M., Munoz, G. T., Thder, J., Tieulent, R., Timmer, P., Tolyhy, T., Topilskaya,
 1507 N., de Matos, C. T., Torii, H., Toscano, L., Tosello, F., Tournaire, A., Traczyk, T., Trger,
 1508 G., Tromeur, W., Truesdale, D., Trzaska, W., Tsiledakis, G., Tsilis, E., Tsvetkov, A.,
 1509 Turcato, M., Turrisi, R., Tuveri, M., Tveter, T., Tydesjo, H., Tykarski, L., Tywoniuk, K.,
 1510 Ugolini, E., Ullaland, K., Urbn, J., Urciuoli, G. M., Usai, G. L., Usseglio, M., Vacchi, A.,
 1511 Vala, M., Valiev, F., Vyvre, P. V., Brink, A. V. D., Eijndhoven, N. V., Kolk, N. V. D.,
 1512 van Leeuwen, M., Vannucci, L., Vanzetto, S., Vanuxem, J.-P., Vargas, M. A., Varma,
 1513 R., Vascotto, A., Vasiliev, A., Vassiliou, M., Vasta, P., Vechernin, V., Venaruzzo, M.,
 1514 Vercellin, E., Vergara, S., Verhoeven, W., Veronese, F., Vetlitskiy, I., Vernet, R., Victorov,
 1515 V., Vidak, L., Viesti, G., Vikhlyantsev, O., Vilakazi, Z., Baillie, O. V., Vinogradov, A.,
 1516 Vinogradov, L., Vinogradov, Y., Virgili, T., Viyogi, Y., Vodopianov, A., Volpe, G., Vranic,
 1517 D., Vrlkov, J., Vulpescu, B., Wabnitz, C., Wagner, V., Wallet, L., Wan, R., Wang, Y.,
 1518 Wang, Y., Wheadon, R., Weis, R., Wen, Q., Wessels, J., Westergaard, J., Wiechula, J.,
 1519 Wiesenaecker, A., Wikne, J., Wilk, A., Wilk, G., Williams, C., Willis, N., Windelband, B.,
 1520 Witt, R., Woehri, H., Wyllie, K., Xu, C., Yang, C., Yang, H., Yermia, F., Yin, Z., Yin, Z.,
 1521 Ky, B. Y., Yushmanov, I., Yuting, B., Zabrodin, E., Zagato, S., Zagreev, B., Zaharia, P.,
 1522 Zalite, A., Zampa, G., Zampolli, C., Zanevskiy, Y., Zarochentsev, A., Zaudtke, O., Zvada,

1523 P., Zbroszczyk, H., Zepeda, A., Zeter, V., Zgura, I., Zhalov, M., Zhou, D., Zhou, S., Zhu,
1524 G., Zichichi, A., Zinchenko, A., Zinovjev, G., Zoccarato, Y., Zubarev, A., Zucchini, A.,
1525 and Zuffa, M. (2008). The alice experiment at the cern lhc. *Journal of Instrumentation*,
1526 3(08):S08002. 24

1527 [14] Connors, M., Nattrass, C., Reed, R., and Salur, S. (2017). Review of Jet Measurements
1528 in Heavy Ion Collisions. vi, 11, 13, 14

1529 [15] Elia, D. and the ALICE Collaboration (2013). Strangeness production in alice. *Journal*
1530 *of Physics: Conference Series*, 455(1):012005. 18

1531 [16] Evans, L. and Bryant, P. (2008). Lhc machine. *Journal of Instrumentation*,
1532 3(08):S08001. 9

1533 [17] Foka, P. and Janik, M. A. (2016). An overview of experimental results from ultra-
1534 relativistic heavy-ion collisions at the cern lhc: Bulk properties and dynamical evolution.
1535 *Reviews in Physics*, 1:154 – 171. 10

1536 [18] Gyulassy, M. (2004). The QGP discovered at RHIC. In *Structure and dynamics*
1537 *of elementary matter. Proceedings, NATO Advanced Study Institute, Camyuva-Kemer,*
1538 *Turkey, September 22-October 2, 2003*, pages 159–182. 7

1539 [19] Hilke, H. J. (2010). Time projection chambers. *Reports on Progress in Physics*,
1540 73(11):116201. vii, 26, 27

1541 [20] Huovinen, P., Kolb, P. F., Heinz, U., Ruuskanen, P. V., and Voloshin, S. A. (2001).
1542 Radial and elliptic flow at RHIC: further predictions. *Physics Letters B*, 503:58–64. 16

1543 [21] Jacobs, P. and Wang, X.-N. (2005). Matter in extremis: ultrarelativistic nuclear
1544 collisions at RHIC. *Progress in Particle and Nuclear Physics*, 54:443–534. 15

1545 [22] Kapusta, J. I. (1979). Quantum chromodynamics at high temperature. *Nuclear Physics*
1546 *B*, 148(3):461 – 498. 3

- [23] Luo, X. (2016). Exploring the qcd phase structure with beam energy scan in heavy-ion collisions. *Nuclear Physics A*, 956:75 – 82. The XXV International Conference on Ultrarelativistic Nucleus-Nucleus Collisions: Quark Matter 2015. 20
- [24] Nattrass, C. (2009). System, energy, and flavor dependence of jets through di-hadron correlations in heavy ion collisions. v, 10, 26
- [25] Odyniec, G. (2013). The rhic beam energy scan program in star and what’s next ... *Journal of Physics: Conference Series*, 455(1):012037. 20
- [26] Ozaki, S. and Roser, T. (2015). Relativistic heavy ion collider, its construction and upgrade. *Progress of Theoretical and Experimental Physics*, 2015(3):03A102. vi, 8
- [27] Preghenella, R. (2011). Transverse momentum spectra of identified charged hadrons with the ALICE detector in Pb-Pb collisions at $\sqrt{s_{NN}} = 2.76$ TeV. *PoS, EPS-HEP2011:118*. 24
- [28] Qin, G.-Y. and Wang, X.-N. (2015). Jet quenching in high-energy heavy-ion collisions. *International Journal of Modern Physics E*, 24:1530014–438. 19
- [29] Satz, H. (2006). Colour deconfinement and quarkonium binding. *Journal of Physics G: Nuclear and Particle Physics*, 32(3):R25. 4, 6
- [30] Schenke, B. (2017). Origins of collectivity in small systems. *Nuclear Physics A*, 967:105 – 112. The 26th International Conference on Ultra-relativistic Nucleus-Nucleus Collisions: Quark Matter 2017. 15
- [31] Shao, M., Barannikova, O. Yu., Dong, X., Fisyak, Y., Ruan, L., Sorensen, P., and Xu, Z. (2006). Extensive particle identification with TPC and TOF at the STAR experiment. *Nucl. Instrum. Meth.*, A558:419–429. 26
- [32] Shuryak, E. V. (1988). The qcd vacuum and quark-gluon plasma. *Zeitschrift für Physik C Particles and Fields*, 38(1):141–145. 3
- [33] Snellings, R. (2011). Elliptic flow: a brief review. *New Journal of Physics*, 13(5):055008. 16

- 1573 [34] Stock, R. (2004). Ultra-relativistic nucleus-nucleus collisions. Proceedings, 17th
1574 International Conference, Quark Matter 2004, Oakland, USA, January 11-17, 2004. *J.*
1575 *Phys.*, G30:S633–S648. 7
- 1576 [35] Strickland, M. (2014). Anisotropic hydrodynamics: Motivation and methodology.
1577 *Nuclear Physics A*, 926:92–101. 15
- 1578 [36] Stcker, H. (2005). Collective flow signals the quarkgluon plasma. *Nuclear Physics A*,
1579 750(1):121 – 147. Quark-Gluon Plasma. New Discoveries at RHIC: Case for the Strongly
1580 Interacting Quark-Gluon Plasma. Contributions from the RBRC Workshop held May 14-
1581 15, 2004. vii, 19
- 1582 [37] Vovchenko, V., Anchishkin, D., and Csernai, L. P. (2014). Time dependence of
1583 partition into spectators and participants in relativistic heavy-ion collisions. *Phys. Rev.*
1584 *C*, 90:044907. vi, 12
- 1585 [38] Wilde, M. (2013). Measurement of Direct Photons in pp and Pb-Pb Collisions with
1586 ALICE. *Nucl. Phys.*, A904-905:573c–576c. 17
- 1587 [39] Wong, C.-Y. (1994). *Introduction to high-energy heavy-ion collisions*. World scientific.
1588 vi, 12, 17, 18

Appendices